PRODUCTION OF ENZYME-RESISTANT STARCH

FROM CASSAVA STARCH

Worawikunya Kiatponglarp

A Thesis Submitted in Partial Fulfillment of the Requirements for the

Degree of Master of Science in Food Technology

Suranaree University of Technology

Academic Year 2007

การผลิตแป้งทนต่อการย่อยด้วยเอนไซม์จากแป้งมันสำปะหลัง

นางสาววรวิกัลยา เกียรติ์พงษ์ลาภ

วิทยานิพนธ์นี้สำหรับการศึกษาตามหลักสูตรปริญญาวิทยาศาสตร์มหาบัณฑิต
สาขาวิชาเทคโนโลยีอาหาร
มหาวิทยาลัยเทคโนโลยีสุรนารี
ปีการศึกษา 2550

PRODUCTION OF ENZYME-RESISTANT STARCH

FROM CASSAVA STARCH

Suranaree University of Technology has approved this thesis submitted in partial fulfillment of the requirements for a Master's Degree.

Thesis Examining Committee

_____

(Asst. Prof. Dr. Piyawan Gasaluck)

Chairperson

_____

(Asst. Prof. Dr. Sunanta Tongta)

Member (Thesis Advisor)

_____

(Assoc. Prof. Dr. Klanarong Sriroth)

Member

_____

(Dr. Kuakoon Piyachomkwan)

Member

_____   _____

(Assoc. Prof. Dr. Saowanee Rattanaphani)   (Asst. Prof. Dr. Suwayd Ningsanond)

Vice Rector for Academic Affairs   Dean of Institute of Agricultural Technology

วรวิกัลยา เกียรติ์พงษ์ลาภ : การผลิตแป้งทนต่อการย่อยด้วยเอนไซม์จากแป้งมันสำปะหลัง (PRODUCTION OF ENZYME-RESISTANT STARCH FROM CASSAVA STARCH) อาจารย์ที่ปรึกษา : ผู้ช่วยศาสตราจารย์ ดร. สุนันทา ทองทา , 126 หน้า.

การศึกษาการผลิตแป้งทนต่อการย่อยด้วยเอนไซม์ชนิด 3 จากมันสำปะหลัง (*Manihot esculenta* Crantz) โดยทำการตัดกิ่งแป้งเปียก (ความเข้มข้นร้อยละ 5, 8 และ 10) ด้วยเอนไซม์ พูลลูลาเนส ที่ระดับความเข้มข้นของเอนไซม์ 5, 15 และ 30 พูลลูลาเนสยูนิตต่อกรัมแป้งเป็น ระยะเวลา 0 ถึง 44 ชั่วโมง พบว่า ระดับการย่อยเพิ่มขึ้น เมื่อความเข้มข้นของเอนไซม์และระยะเวลา การย่อยเพิ่มขึ้นในช่วงปริมาณแป้งร้อยละ 5 ถึง 8 โดยระดับการย่อยมีค่าสูงสุดที่ปริมาณแป้งร้อยละ 8 และปริมาณเอนไซม์พูลลูลาเนส 15 และ 30 พูลลูลาเนสยูนิต การตัดกิ่งแป้งร้อยละ 8 ด้วย เอนไซม์พูลลูลาเนส 15 พูลลูลาเนสยูนิต เป็นระยะเวลา 30 นาที ถึง 24 ชั่วโมง ทำให้ระดับการตัด กิ่งเพิ่มขึ้นจากร้อยละ 58.9 ถึงร้อยละ 89.3 และจำนวนสายโซ่เฉลี่ยมีมากขึ้นจาก 22 เป็น 42 สายโซ่ ขณะที่ระดับการพอลิเมอร์ไรเซชันเฉลี่ยลดลงจาก 117 ถึง 61 เมื่อระดับการตัดกิ่งเพิ่มขึ้น โมเลกุลที่ มีมวลโมเลกุลต่ำและโมเลกุลเส้นตรงหลุดออกมามากขึ้น ซึ่งตรวจสอบจากความสามารถในการจับ กับไอโอดีนและความสามารถในการอุ้มน้ำ ในระหว่างการตัดกิ่งโมเลกุลเส้นตรงเกิดการจัดเรียงตัว เป็นโครงสร้างที่เป็นระเบียบ ทำให้แป้งทนต่อการย่อยด้วยเอนไซม์เกิดขึ้นในปริมาณร้อยละ 18.25 ที่ระดับการตัดกิ่งร้อยละ 89.3 การรีโทรเกรดแป้งตัดกิ่งที่อุณหภูมิ 5 องศาเซลเซียสเป็นเวลา 4 วัน ทำให้ปริมาณแป้งทนต่อการย่อยด้วยเอนไซม์เพิ่มขึ้นจากร้อยละ 12.02 ถึง 27.56 ที่ระดับการตัดกิ่ง ร้อยละ 58.9 ถึง 89.3 การศึกษาคุณสมบัติทางผลึกของแป้งทนต่อการย่อยด้วยเอนไซม์ตรวจสอบ โดยเอกซ์-เรย์ดิฟแฟรกชัน พบว่า เมื่อระดับการตัดกิ่งเพิ่มขึ้น ปริมาณผลึกเพิ่มมากขึ้น โดยแป้งตัดกิ่ง แสดงรูปแบบผลึกชนิด C และ C_A แต่แป้งตัดกิ่งที่เกิดการรีโทรเกรดแสดงรูปแบบผลึกชนิด C_B จากสัดส่วนการดูดกลืนแสงของฟูริเออร์ทรานสฟอร์ม อินฟราเรดที่หมายเลขคลื่น 1045 ต่อ 1037 เซนติเมตร$^{-1}$ พบว่า มีค่าเพิ่มขึ้นเมื่อปริมาณผลึกสูงขึ้น อุณหภูมิการหลอมเหลวของแป้งทนต่อการ ย่อยด้วยเอนไซม์จากแป้งตัดกิ่งมีอุณหภูมิในช่วง 50 ถึง 120 องศาเซลเซียส ขณะแป้งตัดกิ่งที่เกิดการ รีโทรเกรดมีอุณหภูมิที่สูงกว่าในช่วง 130 ถึง 150 องศาเซลเซียส ตามลำดับ

การศึกษาการเก็บแป้งตัดกิ่งในสภาวะอุณหภูมิแบบวนรอบต่างๆ กัน เพื่อเพิ่มปริมาณแป้ง ทนต่อการย่อยด้วยเอนไซม์ โดยทำการศึกษาการเก็บในอุณหภูมิแบบวนรอบที่อุณหภูมิการเกิด นิวเคลียสที่ 5 และ 55 องศาเซลเซียส และอุณหภูมิการเติบโตผลึกที่ 80 และ 120 องศาเซลเซียส พบว่า อุณหภูมิการเกิดนิวเคลียสที่ 5 องศาเซลเซียส และอุณหภูมิการเติบโตผลึกที่ 80 องศา เซลเซียส มีผลเชิงบวกกับปริมาณแป้งทนต่อการย่อยด้วยเอนไซม์ ปริมาณผลึก และเอนทาลปีโดย รวม โดยที่การเก็บในอุณหภูมิแบบวนรอบที่ "5 และ 80 องศาเซลเซียส" ทำให้แป้งตัดกิ่งที่ระดับ

การตัดกิ่งร้อยละ 80.6 มีปริมาณแป้งทนต่อการย่อยด้วยเอนไซม์เพิ่มขึ้นถึงร้อยละ 37.83 โครงสร้าง
ทางผลึกของแป้งทนต่อการย่อยด้วยเอนไซม์ที่ระดับการตัดกิ่งสูง (ระดับการตัดกิ่งร้อยละ 80.6 และ
89.3) เมื่อเก็บในอุณหภูมิแบบวนรอบที่ "5 และ 80 องศาเซลเซียส" และ "55 และ 80 องศา
เซลเซียส" แสดงรูปแบบผลึกชนิด B อย่างชัดเจน สำหรับอุณหภูมิการหลอมเหลวของแป้งตัดกิ่งที่
เก็บในอุณหภูมิแบบวนรอบที่ "5 และ 80 องศาเซลเซียส" และ "5 และ 120 องศาเซลเซียส" มี
อุณหภูมิในช่วง 90 ถึง 117 องศาเซลเซียส และ 135 ถึง160 องศาเซลเซียส และพบว่าการเก็บใน
อุณหภูมิแบบวนรอบที่ "55 และ 80 องศาเซลเซียส" และ "55 และ 120 องศาเซลเซียส" อุณหภูมิ
การหลอมเหลวของแป้งตัดกิ่งเพิ่มสูงถึง 110 ถึง 140 องศาเซลเซียส และ 141 ถึง 177 องศา
เซลเซียส นอกจากนี้ แป้งทนต่อการย่อยด้วยเอนไซม์จากการตัดกิ่งและเก็บในอุณหภูมิแบบวนรอบ
แสดงความสามารถในการอุ้มน้ำต่ำ ซึ่งตรวจสอบจากการลดลงของค่าดัชนีการอุ้มน้ำและดัชนีการ
ละลายน้ำ

สาขาวิชาเทคโนโลยีอาหาร   ลายมือชื่อนักศึกษา _____

ปีการศึกษา 2550   ลายมือชื่ออาจารย์ที่ปรึกษา _____

WORAWIKUNYA KIATPONGLARP : PRODUCTION OF ENZYME RESISTANT STARCH FROM CASSAVA STARCH. THESIS ADVISOR : ASST. PROF. SUNANTA TONGTA, Ph.D. 126 PP.

ENZYME-RESISTANT STARCH/DEBRANCHING/RETROGRADATION/ TEMPERATURE CYCLING

Starch from cassava (*Manihot esculenta* Crantz) was investigated for a production of resistant starch type III (RS$_3$). Starch paste (5, 8 and 10%) was debranched by pullulanase at the concentration of 5, 15 and 30 PUN/g of starch for 0-44 h. The degree of hydrolysis (D.H.) increased with increasing enzyme concentration and hydrolysis time at 5 and 8% starch. The maximum D. H. was obtained at 8% starch and 15 and 30 PUN pullulanase. The debranching of 8% starch paste with 15 PUN pullulanase for 0.5-24 h resulted in increasing the degree of debranching (D.B) from 58.9% to 89.3%. The average number of chain (NC̄) also increased from 22 to 42, while the average degree of polymerization (DP$_n$) decreased from 117 to 61. With increasing D.B., the high amount of low molecular weight molecules and linear fragment molecules were liberated, as indicated by iodine binding capacity and water holding capacity. During debranching, linear molecules associated into an ordered structure, resulting in RS formation for 18.25% at the 89.3% D.B. RS content of debranched starch (DBS) at D.B. of 58.9%-89.3% increased from 12.02 to 27.56% as DBS was retrograded at 5°C for 4 days. The crystallinity of RS was monitored using X-ray diffraction. As the D.B. was increased, the relative crystallinity became greater and the crystallites of DBS showed C and C$_A$ polymorph, while C$_B$ polymorph was

observed in retrograded-debranched starch (RDBS). The absorbance ratio of the Fourier transform infrared (FITR) band at 1045 to 1037 cm^{-1} increased with the relative crystallinity. The melting temperature of RS from DBS was in the range of 50-120°C, while that of RDBS was in higher temperature of 130-150°C.

The DBS was subjected to different temperature cycles to improve RS content. The temperature cycling at the nucleation temperature of 5 and 55°C and the propagation temperature of 80 and 120°C was studied. The nucleation temperature at 5°C and propagation temperature at 80°C had a positive effect on RS content, relative crystallinity and total enthalpy. The RS content of DBS at 80.6% D.B increased up to 37.83% after subjecting to the temperature cycling of "5/80°C". The crystallites of RS containing high D.B. (80.6% and 89.3% D.B.) showed a distinct B-type polymorph after temperature cycling at "5/80°C" and "55/80°C". The melting temperatures of DBS were in the range of 90-117 and 135-160°C after subjecting to temperature cycling of "5/80°C" and "5/120°C". Furthermore, the melting temperature increased to 110-140 and 141-117°C at temperature cycling of "55/80°C" and "55/120°C". In addition, RS obtained from debranching and temperature cycling showed low water holding ability as indicated by a decrease in water absorption index and water solubility index.

School of Food Technology   Student's Signature _____

Academic Year 2007   Advisor's Signature _____

ACKNOWLEDGEMENTS

CONTENTS

CONTENTS (Continued)

CONTENTS (Continued)

CONTENTS (Continued)

CONTENTS (Continued)

LIST OF TABLES

LIST OF TABLES (Continued)

LIST OF FIGURES

LIST OF FIGURES (Continued)

LIST OF FIGURES (Continued)

LIST OF ABBREVIATIONS

Å	Angstrom
A_{620}	Absorbance at 620 nm
ANOVA	Analysis of variance
ATR-FTIR	Attenuated total reflectance-Fourier-transform infrared spectroscopy
ATP	Adenosine 5'-triphosphate
°C	Degree celsius
CIR	Cupric ion reduction
$\overline{CL}$	Average chain length
CoA	Coenzyme A
CRD	Completely randomized design
CRYS	Relative crystallinity
db.	Dry basis
D.B.	Degree of debranching
DBS	Debranched starch sample
D.H.	Degree of hydrolysis
DMRT	Duncan's multiple range test
DMSO	Dimethyl sulfoxide
DP	Degree of polymerization
$\overline{DP}_n$	Number-average degree of polymerization
DSC	Differential scanning calorimetry

LIST OF ABBREVIATIONS (Continued)

$\overline{\text{ECL}}$	Average external chain length
g	Gram
h	Hour
ΔH	Enthalpy
ΔH_{T}	Total enthalpy
HDL_1	High-density lipoprotein
HMG	3-hydroxyl-3-methlyglutaryl
HPSEC	High performance size exclusion chromatography
IBC	Iodine binding capacity
$\overline{\text{ICL}}$	Average internal chain length
J	Joule
λ_{max}	Maximum wave length
L	Litter
M	Molar
mM	Millimolar
mL	Milliliter
μL	Microlitter
min	Minute
mg	Milligram
nm	Nanometer
N	Normality
$\overline{\text{NC}}$	Average number of chain
n.d.	Not detected

LIST OF ABBREVIATIONS (Continued)

NPUN	New Pullulanase Unit Novo
PUN	Pullulanase Unit Novo
ppm	Part per million
RCBD	Randomized complete block design
r	Correlation coefficient
r^2	Coefficient of determination
R	Reducing sugar
RDBS	Retrograded-debranched starch sample
RDS	Rapidly digestible starch
rpm	Revolution per minute
RS	Resistant starch
RS_1	Resistant starch type I
RS_2	Resistant starch type II
RS_3	Resistant starch type III
RS_4	Resistant starch type IV
RVA	Rapid visco analyzer
RVU	Rapid visco unit
SCFA	Short chain free fatty acid
SDS	Slowly digestible starch
2θ	Bragg's angle
T	Storage temperature
T_c	Conclusion temperature
T_g	Glass transition temperature

LIST OF ABBREVIATIONS (Continued)

T_m	Melting temperature
T_o	Onset temperature
T_p	Peak temperature
TDF	Total dietary fiber
TS	Total sugar
WAI	Water absorption index
WHC	Water holding capacity
WSI	Water solubility index
w/v	Weight: volume
w/w	Weight: weight
XRD	X-ray diffraction

CHAPTER I

INTRODUCTION

1.1 Introduction

Cassava or tapioca (*Manihot esculenta* Crantz) is an important economic food crop in tropical countries such as Brazil, Nigeria, Indonesia and Thailand. The cassava roots are processed into chips, pellets and starch. The production of cassava root in Thailand was 18 million tons. Ten million tons were converted to starch and the rest to chips and pellets. About 50% of starch was employed locally in food and non-food industries, and the remainder was exported (Food Science and technology Association of Thailand [FAOSTAT], 2001). The commercial value of cassava starch can be improved further by modifying its functional and nutritional characteristic into specialty secondary products. One of them is resistant starch (RS) as a new category of food ingredients. Various studies have demonstrated that resistant starch was a part of dietary fiber, which was defines as the fraction of starch, or the starch product of that starch, that passes through the small intestine into the large intestine (Englyst, Kingman and Cummings, 1992). In intestine, the indigested starch is fermented by gut microflora, producing short chain fatty acids (SCFA), with a high proportion of butyrate. Butyrate stimulated the immunogenicity of cancer cell. As a substrate for colonocytes, it determines the rate of ATP production, and as a signal metabolite, it activates proliferation and differentiation. These effects may lead to the decreased incidence of colon cancer, atherosclerosis, and obesity related complications in

human (Schwiertz, Lehmann, Jacobasch and Blaut 2002; Kim, Chung, Kang, Kim, and Park 2003). Furthermore, various studies demonstrated that consumption of RS can reduce postprandial blood-glucose level and may play a role in providing improved metabolic control in type II diabetes (non-insulin dependent). There also may be benefit for diabetic by lower lipid levels, as well as hypocholesterolemic effect (Haralumpu, 2000).

Resistant starch has been assigned to four categories, base on the nature of starch and its environment in food (Englyst et al., 1992). RS_1 includes physically inaccessible starch for instance in grains, such as in seeds or legumes; RS_2 is granular starch, non-gelatinized sources, such as green banana flour or native potato; RS_3 is indigestible retrograded starch that is formed upon retrogradation after gelatinization; RS_4 is considered to be chemical modified starch, such as hydoxypropyl starch and cross linking starch.

Among these four types, RS_3 seems to be particularly interesting because it preserved its nutritional characteristics when it is added as ingredient to cooked food. RS_3 is produced by gelatinization, which is a disruption of granular structure by heating starch with excess water, and then retrogradation occurs. The formation of RS_3 after hydrothermal treatment is mainly due to an increase interaction between starch polymers. It is generally believed that RS_3 fraction mainly consists of retrograded amylose. Amylose crystallization occurred through chain elongation by double helical formation between amylose molecules. The elongated amylose chain folded and facilitated helix-helix packing by the formation of inner helical hydrogen bond (Eerlingen and Delcour, 1995). However, amylopectin can form RS but it is a slow process and low stability than amylose.

The length of chains influences RS_3 formation significantly. Eerlingen, Deceuninck and Delcour (1993) showed that amylose with low degree of polymerization (DP <100) gave lower RS_3 yield. Nevertheless, Schmidl, Baurelein, Bengs and Jacobasch (2000) reported that chain length of DP 10-20 of synthesized poly 1, 4-α-D-glucan yielded higher RS_3 than that of DP 10-30. The chain length of α-polyglucan with approximately DP 20 was appropriated for high RS formation (Lehmann, Jacobasch and Schmiedl, 2002). Consequently, if the α-1, 6-linked side chains are long enough, it is possible to produce RS_3 from amylopectin rich starch. Cassava starch contained amylopectin with DP 11-20 which were A-chain and small B-chain forming a cluster structure (Piyachomkwan et al., 2000). Therefore, it is likely to be an excellent source for the production of RS_3 as a supplement for a wide range of food. Other factors influencing the RS formation are debranching process, processing temperature, storage condition and presence of low molecular substance such as sugar (Sajilata, Singhal and Kulkarni, 2006). These parameters were of interest in this study.

Resistant starch has been introduced in recent years as functional food ingredients important for human nutrition. RS has also been commercially produced and marketed (Sajilata et al., 2006). Most of RS development method involved gelatinization of starch with more than 40% amylose content, enzymatic debranching of gelatinized starch, deactivation of debranching enzyme and isolation of product either by drying, extrusion and spray dried. The current tend in this research area is the investigation for alternative sources for RS production. Cassava starch is a choice for RS production. Its structure after debranching seems to be suitable for the formation of RS_3. In addition, cassava starch is mainly produced in Thailand. Therefore, the RS

production from cassava starch would be another choice to encourage the cassava manufacturing for food ingredient market.

1.2 Research objectives

The objectives of this research were:

1.2.1 To study the effects of starch concentration, pullulanase concentration and time for optimization of debranching process in order to produce resistant starch.

1.2.2 To study the effect of starch debranching on the structural characteristics of debranched starch.

1.2.3 To study the effects of starch debranching and retrogradation on resistant starch formation.

1.2.4 To study the effect of storage condition with different time-temperature treatment on the improvement of the resistant starch formation.

1.2.5 To characterize physical and thermal properties of RS produced from cassava starch.

1.3 Research hypothesis

The first hypothesis: the high level of debranching would bring up more chains available for chain re-alignment and cross-linking. This would lead to aggregation and development of macromolecule network to form perfectly crystalline structure, thereby leading to the more RS formation. The second hypothesis: time-temperature treatment based on polymer crystallization at nucleation temperature and propagation temperature can increase the RS formation and improved the perfection of RS crystallites. This treatment can produce the thermostable RS_3 from cassava starch.

1.4 Expected results

Result from this research will be more understanding on the formation of RS from varied branch structure of debranched amylopectin and different storage conditions influencing on RS formation. Factor affecting RS formation of cassava starch is important information that is necessary for the RS production. Knowledge gained from this research could be applied to develop a process for RS manufacturing as a new innovative product in Thailand cassava industry.

1.5 References

Eerlingen, R.C., and Delcour, J.A. (1995). Formation, analysis, structure and properties of typeIII enzyme resistant starch. **Journal of Cereal Science** 22: 129-138.

Eerlingen, R.C., Deceuninck, M., and Delcour, J.A. (1993). Enzyme-resistant starch. II. Influence of amylose chain length on resistant starch formation. **Cereal Chemistry** 70 (3): 345-350.

Englyst, H.N., Kingman, S.M., and Cummings, J.H. (1992). Classification and measurement of nutritionally important starch fractions. **European Journal of Clinical Nutrition** 46 (Suppl. 2): 33-50.

Food Science and technology Association of Thailand (2001).

Haralampu, S.G. (2000). Resistant starch-a review of the physical properties and biological impact of RS3. **Carbohydrate Polymers** 41: 285–292.

Kim, W.K., Chung, M.K., Kang, N.E., Kim, M.H., and Park, O.J. (2003). Effect of resistant starch from corn or rice on glucose control, colonic events, and blood lipid concentrations in streptozotocin-induced diabetic rats. **Journal of Nutritional Biochemistry** 14: 166-172.

Lehmann, U., Jacobasch, G., and Schmidiedl, D. (2002). Characterization of resistant starch typeIII from banana (*Musa acuminata*). **Journal of Agricultural and Food Chemistry** 50: 5236-5240.

Piyachomkwan K., et al. (2000). Structural and hydrating properties of cassava (*Manihot esculenta* Crantz) starch from water-stressed crop. In **Proceedings of the 12th Annual meeting of Thai Society for Biotechnology** Kanchanaburi, Thailand: Felix Hotel.

Sajilata, M.G., Singhal, R. S., and Kulkarni, P. R. (2006). Resistant starch-a review. **Comprehensive Reviews in Food Science and Food Safety** 5: 1-17.

Schmidl, D., Baurelein, M., Bengs, H., and Jacobasch, G. (2000). Production of heat-stable, butyrogenic resistant starch. **Carbohydrate Polymers** 43: 183-193.

Schwiertz, A., Lehmann, U., Jacobasch, G., and Blaut, M. (2002). Influence of resistant starch on the SCFA production and cell counts of butyrate-producing Eubacterium spp. in the human intestine. **Journal of Applied Microbiology** 93: 157-162.

CHAPTER II

LITERATURE REVIEWS

2.1 Starch

Starch is main source of energy in the human diet and animal feed. It is the most abundant and universally distributed forms of storage polysaccharide in plants, and occurs as granules in the chloroplast of green leaves and amyloplast of seeds, pulses and tubers (Tester, Karkalas, and Qi, 2004). Starch granule organization is very complicated and depends strongly on the botanical origin. Starch exists naturally in the form of discrete granules within plant cells. The starch granule is mainly composed of a mixture of two polymers: an essential linear polysaccharide called *amylose* and highly branched polysaccharide called *amylopectin*.

2.1.1 Amylose

Amylose is essential a linear chain of $(1\rightarrow4)$-linked α-D-glucopyranosyl units. Many amylose molecules have very few α-D-$(1\rightarrow6)$ branches, may occur once in every 180-320 units, or 0.3-0.5% of the linkages. The average molecular weight of amylose molecule is about 10^6 g/mol and degree of polymerization (DP) of 6000. The chains can easily form single or double helices. The amylose chain gives the molecules a right-handed spiral or helical shape. The inside of the helix contains predominantly hydrogen atom and is lipophilic, while the hydrophilic hydroxyl groups are positioned on the outside of coil (Whistler and BeMiller, 1997).

2.1.2 Amylopectin

Amylopectin is a highly branched polymer and has an average molecular weight range from 10^7 to 5×10^8 g/mol and DP of 2×10^6. This makes it one of the largest polymers in nature. It consists of thousands of short linear chain of $(1\rightarrow4)$-linked α-D-glucopyranosyl units, linked to each other by α-$(1\rightarrow6)$ linkages. The branch point linkages constitute 4-5% of the total linkages (Whistler and BeMiller, 1997). The amylopectin structure is described by a cluster model (Figure 2.1). An amylopectin molecule consists of main chain, called the C chain, which carries the one reducing end-group and numerous branches, in termed A chains and B chains. Short chains (A chains) of DP 12-16 that can form double helices are arranged in clusters. The clusters comprise 80% to 90% of the chain and are linked by longer chains (B chains) that form the other 10% to 20% of the chains. Most B chains extend into 2 (DP about 40) or 3 clusters (DP about 70), but some extend into more clusters (DP about 110) (Thompson, 2000).
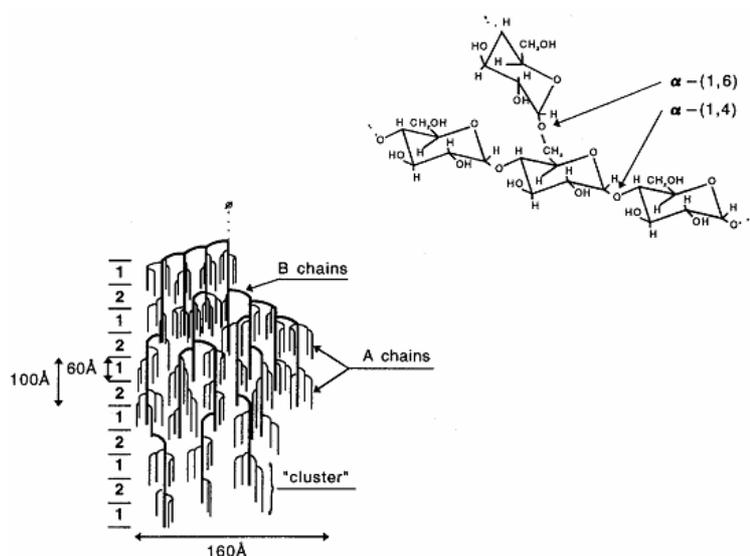
Figure 2.1 Cluster model of amylopectin

Source: Whistler and BeMiller (1997).

2.2 The classification of starch

Starch can be classified as nutritional propose. The classification is based on the extent of digestibility of starch as follows: (Englyst and Hudson, 1996; Englyst and Hudson, 1997)

2.2.1 Rapidly digestible starch

Rapidly digestible starch (RDS) consists mainly of amorphous and dispersed starch. It is digested quickly in the small intestine. In vitro testing, it is hydrolyzed to the constituent glucose molecules in 20 min. RDS is best exemplified by freshly cooked starchy foods, such as mashed potatoes. In this case, starch granules have been gelatinized and are more accessible to enzymatic digestion.

2.2.2 Slowly digestible starch

Slowly digestible starch (SDS) likes RDS, it is expected to be completely digestion in the small intestine but it is digested more slowly than RDS. During in vitro hydrolysis, SDS is converted to glucose between 20 and 110 min. This category consists of physically inaccessible amorphous starch and raw starch with a type A and type C crystalline structure, such as cereals.

2.2.3 Resistant starch

Resistant starch (RS) is a small fraction of starch that was not hydrolyzed after 120 min of in vitro hydrolysis by α-amylase and pullulanase treatment. RS is now defined as that fraction of dietary starch, which escapes digestion in the small intestine. It passes into the large intestine and more or less fermented by gut microflora.

2.3 Definition and classification of resistant starch

European Flair Action Concerted on Resistant Starch (EURESTA) defines RS as the sum of starch and products of starch degradation not absorbed in the small intestine of healthy individuals. It is subdivided into 4 categories regarding the mechanism that prevents its enzymatic digestion (Englyst, Kingman and Cummings, 1992) as follows:

2.3.1 Resistant starch type I

Resistant starch type I (RS_1) represents starch that is resistant because it is physically inaccessible to digestion by entrapment in a non-digestible matrix such as partly milled grains and seeds and in some very dense types of processed starchy food. The microscopic view of the physically inaccessible RS_1 in cell or tissue structure is shows in Figure 2.2. RS_1 is heat stable in most normal cooking operation and enables its use as an ingredient in wide variety of conventional foods.
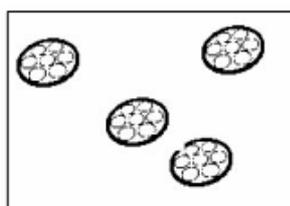
Figure 2.2 Structure of resistant starch type I

Source: Sajilata et al. (2006).

2.3.2 Resistant starch type II

Resistant starch type II (RS_2) represents starch that is a certain granular form and resistant to enzyme digestion. In starch granules, starch is tightly packed in a radical pattern and is relatively dehydrated. This compact structure limits the

accessibility of digestive enzymes and accounts for the resistant nature of RS_2 such as ungelatinized starch. Figure 2.3 shows the RS granule such as raw potato and banana.
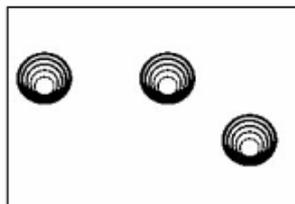
Figure 2.3 Structure of resistant starch type II

Source: Sajilata et al. (2006).

2.3.3 Resistant starch type III

Resistant starch type III (RS_3) represents the most resistant starch fraction and is mainly retrograded starch formed during cooling of gelatinized starch such as cooked and cooled baked potatoes, breakfast cereals. The formation and structure of RS_3 is described in the next section.

2.3.4 Resistant starch type IV

Resistant starch type IV (RS_4) represents the chemical modified starch such as hydroxypropyl starch and cross linking starch.

2.4 Resistant starch type III

Resistant starches are obtained from a variety of sources. The main focus of this research is RS_3 because of its thermal stability. It is stable in most normal cooking processes, enabling it for especially uses as a source of dietary fiber in commercial food applications. To understand RS_3 formation, the principle of RS_3 formation, structure and factor influencing their formation are briefly discussed in this review.

2.4.1 Formation and structure of RS$_3$

RS$_3$ represents retrograded starch. For RS$_3$ formation, the starch granules are disrupted by heating in excess water, commonly known as gelatinization. During starch gelatinization process, the molecular order of the granule is gradually and irreversibly destroyed. The gelatinization temperature is the characteristic of the starch type and depends on the starch source and its amylose content. An amylose is mostly leached out from the granule when it is further heated. Starch granules are disrupted and then partial solubilisation is achieved. Upon cooling, starch undergoes a relative slow re-association process commonly termed retrogradation. During retrogradation, starch molecules re-associate as double helices and can form tightly packed structure stabilized by hydrogen bonding (Eerlingen and Delcour, 1995). The model for double helices are left-handed, parallel stranded helices. The individual strands in the helix contain 6 glucose units per turn in a 2.8 Å repeat (Sajilata, Singhal and Kulkarni, 2006). The association process can be driven further by dehydration. These structures are thermally very stable, and can only be rehydrated at 80 - 150°C, depending upon the extent and nature of the retrogradation.

Retrograded amylose is also known as RS$_3$. Depending on amylose concentrations, amylose upon storage may aggregate or gel. At less than 1.5%, amylose solutions would aggregate and had crystalline double helices of approximately 10 nm interspersed in amorphous regions (Jane and Robyt, 1984). An amylose solution with concentrations higher than 1.5% was stored at room temperature; then, amylose gels were formed. This process occurred in two steps. In the first step, the phase separation occurred resulting in a continuous network of the polymer-rich phase. In the second step, the double helices were formed in the polymer-rich phase

and upon the storage, these helices aggregated to form a three-dimensional crystalline structure. The crystallites were very stable and showed a melting endotherm at 150°C (Eerlingen and Delcour, 1995).

Two possible models of RS_3 formation in aqueous amylose solutions were proposed by Eerlingen, Deceuninck and Delcour (1993): micelle formation and chain folding (lamellar structure).

Micelles were formed by aggregation of a number of different molecules over particular region of the chain in an ordered structure interspersed with amorphous region as illustrate in Figure 2.4. In the case of retrograded amylose, these order regions must be composed of double helices in a hexagonal structure to give a B-type of X-ray diffraction pattern.

Folding of the polymer chain led to two-dimensional structures or lamellar shapes as illustrated in Figure 2.5. Molecular chains arranged a perpendicular orientation to the two-dimensional plane. The regions of the folding were amorphous. The center of the lamella was crystalline. It demonstrated that hydrolysis with amylopectic enzymes could remove these folding regions, and the molecules with short chain were obtained. In the case of retrograded B-type amylose, the crystalline center of the lamella would be composed of double helices ordered in a hexagonal structure.

Mechanism on enzyme action was proposed by Gidley et al. (1995) for B-type polymorph, hexagonal packing of double helices based on the unit cell illustrated in Figure 2.6a. Within individual double helices, each chain contributes three residues to each turn of the helix as illustrated in Figure 2.6b. The turn of the helix above and below was composed of the complementary three residues from each chain (Figure 2.6c).
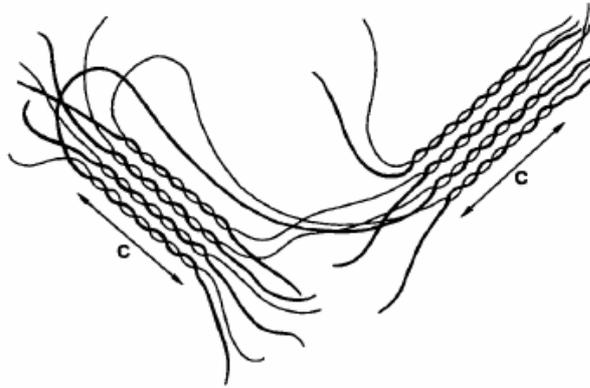
Figure 2.4 Micelle model for the formation of resistant starch in amylose solution. Aggregation occurs over a particular region of the chain in a crystalline structure (C), interspersed with amorphous regions. Different micelles can be linked to each other by the amylose chains.

Source: Eerlingen, Deceuninck and Delcour (1993).
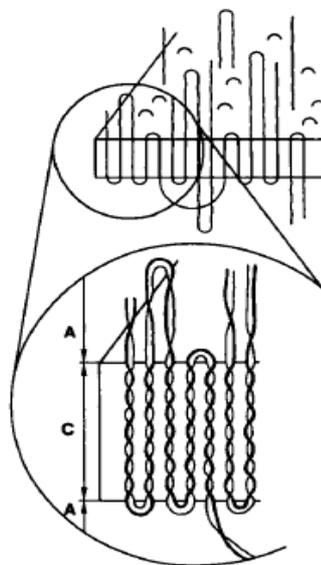
Figure 2.5 Lamella model for the formation of resistant starch in amylose solution. Two-dimensional structures are formed by folding of the polymer chains. The fold zones are amorphous (A). The center of the lamella is crystalline (C).

Source: Eerlingen, Deceuninck and Delcour (1993).

The same position on the double helix was, therefore, occupied by residues six units apart along the primary chain.

Assuming that the primary barrier to enzyme action was a double helical conformation, the limit of enzyme hydrolysis would occur at one end of a helix. If this helix is in an environment similar to helix I in Figure 2.6a, the presence of adjacent helices could be envisaged to direct hydrolysis to glycosidic bonds in the vicinity of the arrow in Figure 2.6a. The same argument can be made concerning enzymatic hydrolysis at the other end of helical segment I. This would entail enzymatic hydrolyses at equivalent geometrical positions, and, therefore, liberation of a single chain containing a multiple of six residues. For helices more peripheral in aggregate structures (Figure 2.6a) two or three glycosidic bonds at each end of the helix might be sterically accessible. This would still lead, on average, to a multiple of six
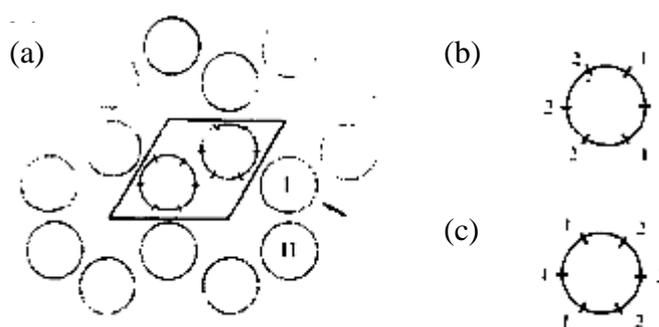
Figure 2.6 (a) Schematic representation of a top view of helix packing in B-type (1→4)-α-D-glucan illustrating both the unit cell and relative positions of glucose residues within each double helix. (b) Contribution of residues from chains 1 and 2 to one turns of a double helix. (c) Contribution of residues from chains 1 and 2 to the turn of a double helix directly above or below that represented in (b).

Source: Gidley et al. (1995)

residues in liberated chains although a broader spread of other adjacent chain lengths would be expected. In the case of both helix types I and II, this proposed mechanism would be predicted to discriminate against the production of chains requiring hydrolysis on opposite sides of the helix segment.

From X-ray diffraction, most of RS_3 shows a B-type crystalline structure. However, an A-type crystalline structure can be obtained if RS is formed in storage of gelatinized starch at high temperature for several hours (Eerlingen, Crombez and Delcour, 1993; Shamai, Peled and Shimoni, 2003). The A-form has a dense structure and only a few water molecules in the monoclinic unit cell, while, the B-form with hexagonal symmetry is more open. Water molecules (36 to 42 molecules per unit cell) in the B-structure are located in fixed positions within a central channel formed by six double helices.

Although RS_3 is often attributed to amylose retrogradation, retrograded amylopectin also reduced enzyme susceptibility as attributed to RS_3. The formation of RS from amylopectin could be ascribed to an increased entanglement of the molecules in the gel network and/or an increased molecular order by the helix formation of the outer short chains (DP 14-20) of amylopectin and by an organization of these helices in a three dimensional (partially crystalline) structure. In general, amylopectin retrogrades very slowly due to the limited dimensions of the chains. The stability of these crystallites is lower than that from amylose. The peak temperature of its melting endotherm was in the range of 55-70°C, depending on the storage condition of starch gel. Therefore, thermally resistant starches, which resist the hydrolysis at 100°C, are not expected to be present in retrograded amylopectin (Rashmi and Urooj, 2003).

2.4.2 Crystallization theory

The above section implies that after retrogradation of starch-water mixture, a partially crystalline polymer system is again obtained. Starch retrogradation can be considered as crystallization in an amorphous matrix. Crystallization is often a three step process that includes 1) nucleation, i.e., formation of critical nuclei; 2) propagation, i.e., growth of crystals from the nuclei formed; 3) maturation, i.e., crystal perfection or continuing slow growth (Roos, 1995b). The rate of crystallization is dependent on temperature (Roos, 1995a). Figure 2.7 shows that the nucleation rate is zero at the melting temperature of crystals (T_m). It increases with increasing the extent of undercooling ($T_m - T$) or decreasing temperature. At temperature below the glass transition temperature (T_g), nucleation rate is negligible, indicating that the system is frozen. The propagation rate is zero at $T < T_g$ because a diffusion of molecule does not occur at such temperature. At higher temperature, diffusion of molecule increases and so does the rate of propagation. At temperature above T_m, the propagation rate is also zero. The maturation rate is dependent on temperature in a similar way to that of the propagation rate.

The overall crystallization rate depends mainly on the nucleation and propagation rates (Figure 2.7). For starch retrogradation, the crystallization mechanism of amylose and amylopectin is thermally reversible above T_g. The rate of crystallization is faster at temperature closed to T_g and the rate approaches a maximum at temperature between T_g and T_m according to polymer crystallization theory (Slade and Levine, 1995). Laine and Roos (1994) studied effect of water content and $T - T_g$ on the extent of crystallization of gelatinized corn starch at low water content and high storage temperatures. Crystallization was found to occur above T_g and the extent of

crystallization increased as the $T - T_g$ increased from 20 to 75°C. It is interesting to notice that the melting temperature of retrograded starch gel was also observed to be dependent on storage temperature. This difference was attributed to the perfection of crystal formed. It was concluded that starch retrogradation was a typical polymer crystallization process that occurred likely to be various extents depending on amount of plasticizer and temperature in relation to T_g and T_m.
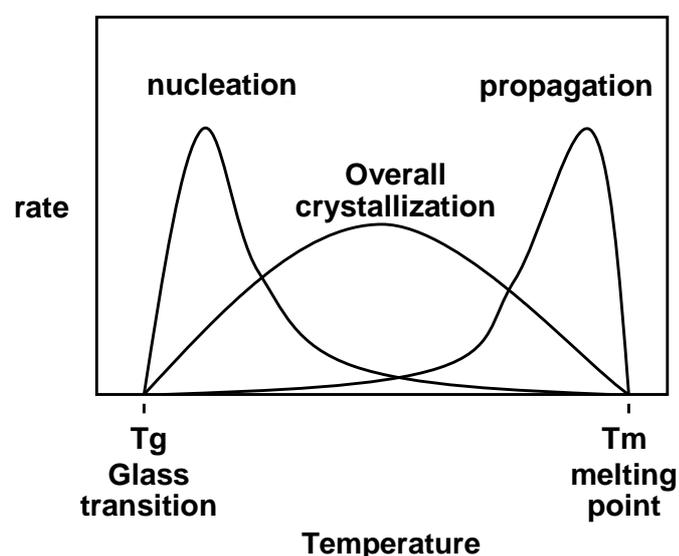
Figure 2.7 Dependence on temperature of the nucleation, propagation and overall crystallization rates of partially crystalline polymers.

Source: Eerlingen, Crombez and Delcour (1993).

2.4.3 Factor influencing the formation of RS_3

Factors that affect on RS formation are molecular ratio of amylose to amylopectin, structures of amylose and amylopectin, storage temperature, storage time, starch concentration, presence and amount of other ingredients (Fennema, 1996). The formation of RS can be considered as the crystallization of amylose in a partially crystalline polymer system which may be influenced by the amorphous environment. Thus, factors affecting the glass transition of the amorphous fraction may also have an

impact on the RS formation. In polymer system, nucleation was favored the temperature far below T_m of the crystal but above T_g, while propagation was favored under far above T_g but well below Tm. The crystallinity of resistant starch fraction increased with storage time of starch gel. A storage at low temperatures and extended periods of time also produced higher RS yields (Eerlingen, Jacobs and Delcour, 1994). When whole corn bread and corn bread crumb were kept at different storage temperature of -20°C, 4°C and 20°C, the highest RS yield was obtained at 4°C and it reached the maximum at the fourth day; then the RS yield decreased thereafter (Niba, 2003). Not only on RS yield, the storage condition also affected on the crystal structure of RS. At the high storage temperature of 95°C and 100°C, RS showed a mixture of A-type with V-type or B-type polymorph when incubated for several hours. At the low temperature of 6°C and 40°C, RS showed B-type polymorph. It was conclude that retrogradation at low temperature led to formation of B-type crystalline structure, whereas retrogradation at high temperature led to formation of mixture of crystalline structure (Eerlingen, Crombez and Delcour, 1993; Shamai et al., 2003).

Amylose content was directly correlated with RS formation. The higher the amylose content, the greater the retrogradation was found. The high amylose starch was more resistant to digestion than amylopectin due to its compact linear structure (Sievert and Pomeranz, 1989). The degree of polymerization (DP) of amylose also affected the formation of RS_3. The RS_3 content became greater with DP from 10 to 100 and remains constant above DP of 100 (Eerlingen, Deceuninck and Delcour, 1993). This finding was supported by Gidley et al. (1995) in that the minimum DP of 10 is necessary to form double helix and the maximum is about 100 glucose units. This indicated why amylopectin was unfavorable on the formation of thermally stable RS.

However, amylopectin debranching was able to improve RS content because the end products of low-molecular weight polymers from debranching could promote the retrogradation. This concept was suggested by Lehmann, Jacobasch, and Schmiedl (2002) in that the debranching of banana starch containing high amylopectin (91.53% in dry matter) with pullulanase could form the RS content up to 51%. In debranched sample, low molecular weight molecules were abundant with high content of DP 6 – 22 in the distribution of DP 6 – 30 of α-1,4-glucan.

The formation of RS is also affected by water content and autoclaving temperature. Sievert and Pomeranz, 1989 found that optimum RS yield was obtained with starch to water ratio of 1:3.5 (w/w). Autoclaving resulted in higher in RS yield. The influence of autoclave time and temperature on RS formation was studied by Sievert and Pomeranz (1989) and Escarpa, Gonzalez, Manas, Garcia-Diz and Saura-Calixto (1996) and Skrabanja, and Kreft (1998). The repeated autoclaving and cooling cycles showed an increase in RS yield in wheat and amylomaize VII starch. The number of cycles was the most pronounced effect on RS. Increasing the number of cycles to 20 could raise RS yield up to 40% (Sievert and Pomeranz, 1989).

The amylose-lipid complexes are able to form in the presence of lipids. With excess lipids, RS yield decreased due to the more formation of lipid-amylose complexes (Czuchajowska et al, 1991). Sugar also has a significant effect on RS yield in starch gel when it contained a high concentration of sugar. In addition, the presence of insoluble and soluble fiber constituents also decreased the RS yield (Escarpa, Gonzalez, Morales and Saura-Calixto, 1997)

2.5 Physiological effect of resistant starch

RS is not a fiber. It can be defined as functional fiber, referring to fiber sources shown to have similar health benefits as dietary fiber. Physiological effects of RS have been proved to be beneficial for health as follows.

2.5.1 Prevention of colonic cancer

RS escapes digestion in the small intestine. It is slowly fermented by the intestine microflora in the large intestine producing a wide range of short-chain fatty acids (SCFA), primarily acetate, propionate and butyrate. SCFA production had a positive impact on bowel health, including epithelial proliferation and lowers colonic pH. The butyrate is a main energy substrate for large intestinal epithelial cells and inhibits the malignant transformation of such cells in vitro. These effects may lead to the decreased incidence of colon cancer, atherosclerosis, and obesity-related complications in human (Haralampu, 2000).

Dramatically changes in fecal pH and bulking as well as greater production of SCFA in the colon of rats fed with RS preparations were reported (Ferguson, Tasman-Jone, Englyst and Harris, 2000). This suggested that RS resembled the effects of soluble dietary fiber. However, when RS was combined with an insoluble dietary fiber such as wheat bran, much higher SCFA, in particular butyrate was observed in the feces.

2.5.2 Hypoglycaemic effects

Foods containing RS moderate the rate of digestion. The slow digestion of RS has implications for its use in controlled glucose release applications. Numerous studies measured glycaemic response in food containing RS, in healthy non-diabetic, non-insulin-dependent diabetes mellitus and hyperinsulinemic subjects. These studies

showed a consistent trend whereby RS had an impact on the glycaemic response, including lower maximum blood-glucose response, lower maximum blood-insulin response, reduced area under the blood-glucose response curve and the blood-insulin response curve. The RS_3-containing bar decreased postprandial blood glucose and might play a role in providing an improved metabolic control in type II diabetes (non-insulin dependent) (Higgins et al., 2004).

2.5.3 Prebiotic potential

RS has been suggested for use in probiotic compositions to promote the growth of beneficial microorganisms such as *bifidobacteria* and *lactobacilli* (David, 1999). Since RS almost entirely passes the small intestine, it can behave as a substrate for growth of the probiotic microorganisms.

2.5.4 Hypocholesterolaemic effects

Hypocholesterolemic effects of RS have been amply proved. In rats, RS diets (25% raw potato) markedly raised the cecal size and the cecal pool of short-chain fatty acids (SCFA), as well as SCFA absorption and lowered plasma cholesterol and triglycerides. Furthermore, there was a lower concentration of cholesterol in all lipoprotein fractions, especially the high-density lipoprotein (HDL_1) and a decreased concentration of triglycerides in the triglyceride-rich lipoprotein fraction (Ranhotra, Gelroth and Leinen, 1997; Kim, Chung, Kang, Kim and Park, 2003). There are two mechanisms involved. The first one is through RS binding bile acids and leading to an increased fecal bile acid excretion. Therefore, less bile acid is recycled. In order to compensate for the excreted bile acid, the liver synthesizes new bile acids from cholesterol and thereby reducing serum cholesterol level. A second mechanism for

lowering serum cholesterol level has been proposed. RS is believed to aid in shifting bile acid pools away from cholic acid to chenodeoxycholic acid. Chenodeoxycholic acid appears to be an inhibitor of 3-hydroxy-3-methylglutaryl (HMG) CoA reductase, a regulatory enzyme necessary for cholesterol biosynthesis (Groff and Gropper, 1999). As HMG CoA reductase activity lowers, the production of cholesterol subsequently decreases therefore resulting in lower serum cholesterol.

2.5.5 Inhibition of fat accumulation

Replacement of 5.4% of total dietary carbohydrates with RS in a meal could significantly increase postprandial lipid oxidation, thereby suggesting a reduction in fat accumulation in a long term (Higgins et al., 2004).

2.5.6 Absorption of minerals

A comparison of intestinal apparent absorption of calcium, phosphorus, iron, and zinc in the presence of either RS or digestible starch was studied. A meal containing 16.4% RS resulted in a greater apparent absorption of calcium and iron as compared with a completely digestible starch (Morais, Feste, Miller and Lifichitz, 1996). Thus, RS could have a positive effect on intestinal calcium and iron absorption.

2.6 Recommendation for resistant starch intake levels

A recommendation for RS intake was approximately 20 g/day to obtain the beneficial health benefit. However, the worldwide dietary intakes of RS are believed to vary considerably. Recommendations for dietary intakes by the World Health Organization (WHO) are 27 to 40 g/day. Dietary intakes of RS in developing countries with high starch consumption rates range from approximately 30 to 40 g/day. Dietary

intakes in India and China were recently estimated at 10 and 18 g/day. The intakes in the Europe are believed to lie between 3 and 6 g/day. Dietary intakes of RS in the United Kingdom are estimated at 2.76 g/day and are believed to range from 5 to 7 g/day in Australia. In Sweden, the daily RS intake is estimated to be 3.2 g. In New Zealand, RS intakes have been approximated to be 8.5 g/day and 5.2 g/day in 15 to18 year old males and females, respectively (Sajilata et al., 2006). Recommended intakes for fiber are also included for children and teenage and present in Table 2.1 (Savlin, 2003).

Table 2.1 Dietary reference intake values for total fiber by life stage

Life stages group	Dietary intake (g/d)	
	Male	Female
1 – 3 years	19	19
4 – 8 years	25	25
9 – 13 years	31	26
14 – 18 years	38	26
19 – 30 years	38	25
31 – 50 years	38	25
51 – 70 years	30	21
Over 70 years	30	21
Pregnancy		28
Lactation		29

Source: Savlin, (2003).

2.7 Functionality and food Application of resistant starch

(www.foodinovation.com/functresist.pdf)

RS is white in color, has a fine particle size and bland flavor. These attributes make it possible to formulate food products with wider often associated with poor taste, texture and mouthfeel. Resistant starch has a low calorific content of 1.6 to 2.8

calories per gram (depending on the grade) and can, therefore, be used to compliment reduced-fat and reduced-sugar formulations. Its physical properties, particularly its low water-holding capacity, provide good handling in processing, as well as crispiness, expansion and improved texture in the end-product.

RS is especially suitable for grain-based, low-moisture and moderate moisture food systems. Many baked goods and cereals are known to provide a source of fiber. Some, such as high-fiber bread and breakfast cereals, are abundant in the marketplace. Others, such as white bread, biscuits and cakes are not normally associated with healthy eating or fiber fortification. However, with process-tolerant-resistant starches, it is now possible to increase the dietary fiber content of these foods. Other foods in which resistant starch applications have been examined include pasta and beverages. Dried pasta products containing up to 15% resistant starch can be made with little or no effect on dough rheology during extrusion. Although the resultant pasta was lighter in colour, a firm texture was obtained in the same cooking time as a control that contained no added fiber.

Resistant starch may also be used in thickened, opaque health drinks where insoluble fiber is desired. Insoluble fiber such as resistant starches generally requires suspension and adds opacity to beverages. Compared with other insoluble fiber, resistant starch imparts a less gritty mouthfeel and masks flavors less.

2.8 Trends in RS$_3$ production

Iyengar, Zaks and Gross (1991) developed a method for produce RS$_3$ that involved the dispersion of high amylomaize starch by cooking an aqueous suspension, incubating at 60 – 120°C, then holding at 4°C. Since the intact amylopectin reduced

the retrogradation rate, the level of RS could be increased by subjecting the retrograded material to enzyme, resulting in a predominately crystalline material with about 92% RS.

A related method for manufacturing RS_3 was described by Chiu, Henley and Altieri (1994) and Henley and Chiu (1995). High amylose starch was used as starting starch. A process of RS production essentially consists of the steps of gelatinizing starch slurry and enzymatic debranching. The alternative of this method was that cooling by extrusion could replace the cooling and heating cycles of dispersion.

Haynes et al. (2000) described the production of thermostable RS_3 with melting point above 140°C. RS is produced using crystal nucleation and propagation temperatures which avoid the substantial production of lower melting amylopectin crystals, lower melting amylose crystals, and lower melting amylose-lipid complexes. The claimed that nucleating temperature was above the melting point of amylopectin crystals and propagating temperature was above the melting point of any amylose-lipid complexes but below the melting point of the enzyme resistant starch. A minimum of one cycle (but preferably four) of nucleation and propagation is required. The first temperature of about 60°C precludes amylopectin crystallization; then at the temperature above amylose lipid complex formation (above 120°C) would remove any amylose lipid complexes formed during nucleation. This method produced a material with up to 35% RS as determined by total dietary (TDF) method.

Kettlitz, Coppin, Roper and Bornet (2000) claimed the production of highly fermentable RS with largely DP 10-35. The starting materials were potato and tapioca maltodextrin. The process steps included enzymatic debranching and retrogradation, drying with spray-drier. The product contained about 55% RS as determined by 37°C

incubation, and had the melting temperature of about 105°C. The advantage of this product is the enhancement of butyrate production, which is thought to contribute to colon health.

Recently, the commercial sources of RS_3 such as CrystaLean® (Opta Food Ingredients, Inc., Bedford, Mass., USA), Novelose®330 (National Starch and Chemical Co., Bridgewater, N.J., USA) and AciStar® (Cerestar Food and Phama Specialties) are available. CrystaLean® is a commercial, highly retrograded RS_3 based on the *ae*-VII hybrid. CrystaLean® containing 41% RS is digested slowly, at approximately haft of the rate of maltodextrin. It is now used in a product for diabetics. Novelose®330 contains 30% TDF, retrograded RS_3 based on the *ae*-VII hybrid of corn. Novelose®330 has a melting temperature of 121.5°C. These products offers very high process tolerance and are therefore suitable for use in a variety of processed food. For AciStar®, it containing 58% RS, made by crystallizing hydrolyzed tapioca starch (maltodextrin).

2.9 References

Chiu, C.-W., Henley, M., and Altieri, P. (1994). Process for making amylase resistant starch from high amylose starch. **US patent# 5,281,276.**

Czuzhajowska, Z., Sievert, D., and Pomeranz, Y. (1991). Enzyme-resistant starch. IV. Effects of complexing lipids. **Cereal Chemistry** 68: 537-542.

David, R.L. (1999). The chemistry of complex carbohydrates. In: S.S. Cho, L. Prosky and M. Dreher (eds.). **Complex carbohydrates in foods**. New York: Marcel Dekker.

Eerlingen, R.C., and Delcour, J.A. (1995). Formation, analysis, structure and properties of typeIII enzyme resistant starch. **Journal of Cereal Science** 22: 129-138.

Eerlingen, R.C., Crombez, M., and Delcour, J.A. (1993). Enzyme-resistant starch. I. Quantitative and qualitative influence of incubation time and temperature of autoclave starch on resistant starch formation. **Cereal Chemistry** 70 (3): 339-344.

Eerlingen, R.C., Deceuninck, M., and Delcour, J.A. (1993). Enzyme-resistant starch. II. Influence of amylose chain length on resistant starch formation. **Cereal Chemistry** 70 (3): 345-350

Eerlingen, R.C., Jacobs, H., and Delcour, J.A. (1994). Enzyme-resistant starch V. effect of retrogradation of waxy maize starch on enzyme susceptibility. **Cereal Chemistry** 71 (4): 351-355.

Englyst, H.N., and Hudson, G.J. (1996). The classification and measurement of dietary carbohydrates. **Food Chemistry** 57(1): 15-21.

Englyst, H.N., and Hudson, G.J. (1997). Starch and health In: P.J. Farazier, Donald A.M. and P. Richmoand (eds.). **Starch: structure and functionality** (pp 8-20). Cambridge, UK: Thomas Graham House.

Englyst, H.N., Kingman, S.M., and Cummings, J.H. (1992). Classification and measurement of nutritionally important starch fractions. **European Journal of Clinical Nutrition** 46 (Suppl. 2): 33-50.

Escarpa, A., Gonzalez, M. C., Morales, M. D., and Saura-Calixto, F. (1997). An approach to the influence of nutrients and other food constituents on resistant starch formation. **Food Chemistry** 60 (4): 527-532.

Escarpa, A., Gonzalez, M.C., Manas, E., Garcia-Diz, L., and Saura-Calixto, F. (1996). Resistant starch formation: standardization of high-pressure autoclave process. **Journal of Agricultural and Food Chemistry** 44: 924-928.

Fennema (1996). Food Chemistry. In R. Owen (eds.). **Carbohydrates** (pp 167- 196). New York: Marcel Dekker.

Ferguson, L.R., Tasman-Jones, C., Englyst, H., and Harris, P.J. (2000). Comparative effects of three resistant starch preparations on transit time and short-chain fatty acid production in rats. **Nutrition Cancer** 36:230-7.

Gidley, M.J., et al. (1995). Molecular order and structure in enzyme-resistant retrograded starch. **Carbohydrate Polymers** 28: 23-31

Groff, J.L. and Gropper, S.J. (1999). **Advance nutritional human metabolism**. California: Delmar.

Haralampu, S.G. (2000). Resistant starch-a review of the physical properties and biological impact of RS$_3$. **Carbohydrate Polymers** 41: 285–292.

Haynes, L., et al. (2000). Process for making enzyme-resistant starch for reduced-calorie flour replacer. **US patent# 6,013,299.**

Henley, M., and Chiu, C.-W. (1995). Amylase resistant starch product form debranched high amylose starch. **US patent# 5,409,542.**

Higgins, J.A., et al. (2004). Resistant starch consumption promotes lipid oxidation **Nutrition and Metabolism** 1: 1-8.

Iyengar, R., Zaks, A., and Gross, A. (1991). Starch-derived, food-grade, insoluble bulking agent. **US patent# 5,051,271.**

Jane, J.L., and Robyt, J.F. (1984). Structure studies of amylose V complexes and retrograded amylose by action of alpha amylases, and a new method for preparing amylodextrins. **Carbohydrate Research** 132: 105-118.

Kettlitz, B.W., Coppin, J.V.J-M, Roper H.W.W., and Bornet, F. (2000). Highly fermentable resistant starch. **US patent# 6,043,229.**

Kim, W.K., Chung, M.K., Kang, N.E., Kim, M.H., and Park, O.J. (2003). Effect of resistant starch from corn or rice on glucose control, colonic events, and blood lipid concentrations in streptozotocin-induced diabetic rats. **Journal of Nutritional Biochemistry** 14: 166–172.

Laine, M.J.K. and Roos, Y.H. (1994). Water plasticization and recrystallization of starch in relation to glass transition. In **Proceeding of poster session. International symposium on the properties of water. Practicum II** (pp 109-112). Maxico: Universidad de las Americas-Puebla.

Lehmann, U., Jacobasch, G., and Schmidiedl, D. (2002). Characterization of resistant starch typeIII from banana (*Musa acuminata*). **Journal of Agricultural and Food Chemistry** 50: 5236-5240.

Morais, M.B., Feste, A., Miller, R.G., and Lifichitz, C.H. (1996). Effect of resistant starch and digestible starch on intestinal absorption of calcium, iron and zinc in infant pigs. **Paediatr Research** 39 (5):872–876.

Niba, L.L. (2003). Effect of storage period and temperature on resistant starch and. beta-glucan content in cornbread. **Food Chemistry** 83(4):493–8.

Ranhotra, G.S., Gelroth, J.A., and Leinen, S.D. (1997). Hypolipidemic effect of resistant starch in hamsters is not dose dependent. **Nutrition Research** 17 (2): 317-323.

Rashmi, S., and Urooj, A. (2003). Effect of processing on nutritionally important starch fractions in rice varieties. **International Journal of Food Sciences and Nutrition** 54: 27-36.

Roos, Y.H. (1995a). Characterization of food polymers using state diagrams. **Journal of Food Engineering** 24: 339-360.

Roos, Y.H. (1995b). **Phase transition in foods**. New York: Academic Press.

Sajilata, M.G., Singhal, R. S., and Kulkarni, P. R. (2006). Resistant starch-a review. **Comprehensive Reviews in Food Science and Food Safety** 5: 1-17.

Shamai, K., Bianco-Peled, H., and Shimoni, E. (2003). Polymorphism of resistant starch type III. **Carbohydrate Polymers** 54: 363-369.

Sievert, D. and Pomeranz, Y. (1989). Enzyme-resistant starch. I. characterization and evaluation by enzymatic, thermoanalytical and microscopic method. **Cereal Chemistry** 66 (4): 342-347.

Skrabanja, V., and Kreft, I. (1998). Resistant starch formation following autoclaving of buckwheat (*Fagopyrum esculentum* Moench) Groats. An in vitro study. **Journal of Agricultural and Food Chemistry** 46: 2020-2023.

Slade, L., and Levine, H. (1995). Water and the glass transition - dependence of the glass transition on composition and chemical structure: special implications for flour functionality in cookie baking. **Journal of Food Engineering** 24: 431-509.

Slavin, J. (2003). Impact of the proposed definition of dietary fiber on nutrient databases. **Journal of Food Composition and Analysis** 16: 287-291.

Tester, R.F, Karkalas, J., and Qi, X. (2004). Starch-composition, fine structure and architecture. **Journal of Cereal Science** 39: 151-165.

Thompson, D.B. (2000). On the non-random nature of amylopectin branching. **Carbohydrate Polymers** 43:223–39.

Whistler, R.L., and BeMiller, J.N. (1997). **Carbohydrate chemistry for food scientists**. Minnesota: Eagan Press.

CHAPTER III

MATERIALS AND METHODS

3.1 Materials

Cassava starch was obtained from Sanguan Wongse Industries Co., Ltd (Nakorn Ratchasima, Thailand). Commercial pullulanase Promozyme D2 (EC 3.2.1.41, from *Bacillus deramificans*, and 1,350 NPUN/g, density 1.36 g/mL) was a gift from Novozymes A/S (Bagsvaerd, Denmark). Amyloglucosidase (EC. 3.2.1.3 from *Aspergillus niger*, 11,500 U/mL), α-amylase (EC 3.2.1.1, type VI-B from porcine pancreas,19.6 U/mg), β-amylase (EC 3.2.1.2, type II-B from barley, 20-80 U/mg), amylose (type II from potato), pullulan from *Aureobasidium* pullulans, glucose oxidase peroxidase reagent (G 3660) and o-dianisidine (D 2679) was purchased from Sigma Chemical Co. (St. Louis Mo., USA). Novelose 330, commercial resistant starch was a gift from National Starch and Chemical Co. (Bridgewater, New Jersey, USA). Other chemicals were of analytical grade.

3.2 Starch Composition

Cassava starch was analyzed for its contents of starch and amylose at Cassava Starch Technology Research Unit (CSTRU/ KAPI; Kasetsart University, Bangkok, Thailand). The content of starch was analyzed by polarimetric method (TIS. 274-2521). The content of amylose was determined by High Performance Size Exclusion Chromatography (HPSEC) using one Ultrahydrogel linear and two Ultrahydrogel 120

columns connected in series according to Govindasamy, Oates and Wong (1992). The content of protein, fat, ash and sulfur dioxide was determined using AOAC methods (AOAC, 1990).

3.3 Starch fractionation

Cassava starch was separated into two fractions, amylose and amylopectin, according to Balagopalan, Padmaja, Nanda, and Moorthy (1988). The aqueous slurry of cassava starch (10% w/v, db.) was prepared. A fifty mL of slurry was mixed with 1 L of 0.157 N NaOH and the mixture was stirred gently until the solution became clears. This stirring was not too vigorous, because it could damage the gel structure of amylopectin. After the solution had become clear, it was stood for 5 min. Then, 200 mL of 5% NaCl was added, and the solution was neutralized to a pH of 7.0 using 1 N HCl. The solution was stood for 12 to 16 h. When the gel was settled and a clear separating division between the gel and supernatant solution became visible. The supernatant was removed.

The settle amylopectin gel was centrifuged at 8,000 rpm, 20°C for 20 min (Hettich Universal 16R, Hettich GmbH, Tuttlingen, Germany). The supernatant was discarded and 100 mL of 1% NaCl was added and stirred gently. The gel was recentrifuged at 3,000 rpm. After further washing with brine solution and recentrifugation, the gel was precipitated in excess absolute ethanol and the residue was air dried at room temperature for overnight.

The amylose in the supernatant was separated from solution by complexing with 1-butanol and stirred gently for 1 h at room temperature. The precipitated amylose-butanol complex was allowed to settle for 2 to 3 h. The amylose complex was

collected by centrifugation at 5,000 rpm for 15 min and the butanol was eradicated on a boiling water bath. The recovered amylose was precipitated in excess absolute ethanol and the residue was air dried at room temperature for overnight.

3.4 Fine structure analysis of cassava starch

3.4.1 Percent of branch linkage, average number of chain and average chain length

Fine structure of amylose and amylopectin were analyzed using the modified method of Hood and Mercier (1978). The polyglucans (25 mg) was dissolved in 1.5 mL of 90% dimethyl sulfoxide (DMSO) and heated in a boiling bath for 20 min in order to complete dissolution. Acetate buffer (3.5 mL, 0.05 M, pH 5.0) and pullulanase (20 μL, 1350 NPUN/mL) were added to polyglucan solution, and the mixtures were incubated at 50°C for 48 h. The enzyme was inactivated by boiling the solution for 20 min. The reducing sugar content was measured using Somogyi's method (Somogyi, 1952) and total sugar content was measured using the phenol-sulfuric acid method (Dubois, Gilles, Hamilton, Rebers and Smith, 1956). Percent of branch linkage was calculated as a following equation:

$$\text{Branch linkage (\%)} = \left[\frac{\text{R of sample after hydrolysis - R of pullulanase}}{\text{TS of sample after hydrolysis - TS of pullulanase}}\right] - \left[\frac{\text{R of sample before hydrolysis}}{\text{TS of sample before hydrolysis}}\right] \times 100$$

The average number of chain ($\overline{\text{NC}}$) and average chain length ($\overline{\text{CL}}_n$) were calculated as follows:

$$\overline{\text{NC}} = \left[\frac{\text{R of sample after hydrolysis - R of pullulanase blank}}{\text{R of sample before hydrolysis}}\right]$$

and

$$\overline{\text{CL}}_n = \left[\frac{\text{TS of sample after hydrolysis - TS of pullulanase blank}}{\text{R of sample after hydrolysis - R of pullulanase blank}} \right]$$

where   R   =   reducing sugar (as mg glucose)

and   TS   =   total sugar (as mg glucose)

3.4.2 β-amylolysis limit, average external chain length and average internal chain length

The analysis procedure was slightly modified from that of Hood and Mercier (1978). The polyglucan solution (1.5 mL, 0.5% w/v in 90% DMSO) was mixed with an acetate buffer solution pH 4.8 (0.3 mL, 0.2 M). β-amylase solution (0.2 mL, 20 units/mL) and deionized water (1.0 mL) were added and mixed, and the solution was incubated at 37°C for 48 h. The reducing sugar content and total sugar content were measured. The percentage of β-amylolysis limit was calculated using a following equation:

$$\beta\text{-amylolysis limit} = \left[\frac{\text{R of sample after hydrolyzed – R of }\beta\text{-amylase blank}}{\text{TS of sample after hydrolyzed – TS of }\beta\text{-amylase blank}} \right] \times 100 \times 1.9$$

where   R   =   reducing sugar (as mg maltose)

and   TS   =   total sugar (as mg glucose)

The β-amylolysis limit was used to calculate the average external chain length ($\overline{\text{ECL}}$) and average internal chain length ($\overline{\text{ICL}}$) according with these equations:

$$\overline{\text{ECL}} = \overline{\text{CL}}_n \times (\% \ \beta\text{-amylolysis limit} / 100) + 2$$

and

$$\overline{\text{ICL}} = \overline{\text{CL}}_n - \overline{\text{ECL}} - 1$$

3.5 RVA analysis

Pasting properties of cassava starch was analyzed using Rapid Visco Analyzer (RVA 4, Newport Science, Australia) using a standard program of number 1. The starch sample was weight for 3.00 g (on 14% moisture basis) in canister. Then, it was put into equipment. The starch suspension was held at 50°C for 1 min with rotation speed of 960 rpm. Later, the sample was heated to 95°C at 12.2°C/min and then held at 95°C for 2.5 min. Subsequently, the sample was cooled to 50°C at 12.2°C/min where it was kept for 2.1 min. A rotation speed of the paddle was 160 rpm for which program. The cooling was performed with water circulated through cooler. Pasting temperature was recorded in °C. Peak viscosity, final viscosity, set back and breakdown were recorded in RVU.

3.6 Pullulanase and alpha-amylase activities assay

The pullulanase activity of Promozyme D2 was evaluated regarding to the analytical method provided by Novozymes A/S (Novo industri A/S, 1983). The 1 PUN (Pullulanase Unit Novo) is defined as the amount of enzyme which hydrolyzes pullulan and liberates reducing carbohydrate with reducing power equivalent to 1 micromol glucose per minute. A 10^4 fold enzymatic dilution in 0.1 M acetate buffer (pH 5.0) was prepared and 0.5 mL of this solution was mixed with 0.5 mL of pullulan solution (0.4% w/w in deionized water). The mixture was incubated at 50°C for 15 min. Then, the reaction was stopped with the addition of 1 mL of Somogyi's copper reagent and reducing sugar content (expressed as glucose) was determined according to Somogyi's method (Somogyi, 1952). For blank, Somogyi's copper reagent was added to the mixture before incubation. The mixtures were measured as mg glucose

using Spectrophotometer at 540 nm (GBC UV/VIS 916, GBC Scientific Equipment Pty, Ltd., Australia). The pullulanase activity was calculated using the definition as described above.

The α-amylase activity was evaluated according to the instruction of Pulluzyme activity (1997). The 1 AU (Amylase Unit) is defined as the amount of enzyme which hydrolyzes amylose and liberates reducing sugar equivalent to 1 micromol glucose per minute. A 0.5 mL of enzyme solution (10^4 fold in 0.1 M acetate buffer, pH 5.0) was mixed with 0.5 mL of amylose solution (1% w/w in deionized water) and incubated at 50°C for 15 min. The reaction was stopped with the addition of 1 mL of Somogyi's copper reagent and reducing sugar content (expressed as glucose) was determined according to Somogyi's method. For blank, Somogyi's copper reagent was added to the mixture before incubation. The α-amylase activity was calculated using the definition as described above.

3.7 Starch concentration and pullulanase concentration for debranching cassava starch

Cassava starch solution (20% w/w) was gelatinized in a shaking water bath at 85°C with continuous shaking for 15 min (Ratex, SWB 20 shaking water bath, Ratek Instruments Pty., Ltd., Australia) and autoclaved at 105°C for 30 min (Sanyo Labo autoclave MLS 3020, Sanyo Electric Co., Ltd., Japan) in order to completely gelatinization. The starch gel was suspended with 0.1 M acetate buffer pH 5.0 to obtain the gel of 5, 8 and 10% starch (w/w). The gel was cooled to 50°C and then pullulanase at different concentration (5, 15 and 30 PUN/g of starch) was added to achieve a substrate:enzyme ratio of 20:1 by weight. The suspension was incubated in a

shaking water bath at 50°C with continuous shaking for 44 h. The sampling was conducted 1.5, 3, 6, 12, 24 and 44 h. A sample was mixed with DMSO and then heated at 85°C for 30 min, to stop enzymatic activity. The sample was cool to room temperature. The reducing sugar content and total sugar content were measured. The hydrolysis extent of cassava starch by pullulanase was evaluated in terms of a degree of hydrolysis (D.H.), which was calculated from the following equation:

$$\text{D.H. (\%)} = \left[\frac{\text{R of sample after hydrolysis - R of pullulanase - R of sample before hydrolysis}}{\text{TS of sample - TS of pullulanase}} \right] \times 100$$

where   R   =   reducing sugar (as mg glucose)

and   TS   =   total sugar (as mg glucose)

3.8 Starch debranching and structural characterization of debranched cassava starch

3.8.1 Starch debranching

Cassava starch was debranched regarding the starch concentration of 8% w/w and enzyme concentration of 15 PUN/g of starch, which were examined previously. Cassava starch gel was prepared as described in the previous section. The gel was hydrolyzed in a shaking water bath at 50°C with continuous shaking, where the debranching time was varied of 30 min, 1, 2, 3, 5, 7, 13, 16 and 24 h. At each specific time, the enzymatic reaction was stopped by heating the hydrolysate product at 85°C for 30 min. The sample was divided into 3 parts. First part was mixed with DMSO and then reducing sugar and total sugar were determined for the study on the

fine structure of debranched starch. Second and third part was studied on iodine binding capacity and water holding capacity respectively.

3.8.2 Fine structure analysis of debranched cassava starch

The debranching extent of cassava starch by pullulanase was evaluated in terms of a degree of debranching (D.B.), which was calculated as follows:

$$\text{D.B. (\%)} = \left[\frac{\text{R of sample after hydrolysis} - \text{R of raw starch}}{\text{R of completely debranched} - \text{R of raw starch}} \right] \times 100$$

The number-average degrees of polymerization ($\overline{\text{DP}}_n$) and average number of chain ($\overline{\text{NC}}$) of debranched starch were calculated as follows:

$$\overline{\text{DP}}_n = \left[\frac{\text{TS of sample after hydrolysis} - \text{TS of pullulanase}}{\text{R of sample after hydrolysis} - \text{R of pullulanase}} \right]$$

and

$$\overline{\text{NC}} = \left[\frac{\text{R of sample after hydrolysis} - \text{R of pullulanase blank}}{\text{R of sample before hydrolysis}} \right]$$

where   R   =   reducing sugar (as mg glucose)

and   TS   =   total sugar (as mg glucose)

3.8.3 β-amylolysis limit of debranched cassava starch

The β-amylolysis limit of debranched starch was evaluated in order to investigate if starch was completely debranched. The analysis procedure was slightly modified from that of Hood and Mercier (1978). The debranched starch suspension (1.5 mL) was mixed with an acetate buffer solution pH 4.8 (0.3 mL; 0.2 M). β-amylase solution (0.2 ml; 20 units/mL) and deionized water (1.0 mL) were added and mixed,

and the solution was incubated at 37°C for 48 h. The reducing sugar and total sugar content of the β-amylolysis product were measured. The % β-amylolysis limit was calculated as the equation in 3.4.2 section.

3.9 Iodine binding capacity of debranched starch

Iodine binding capacity (IBC) was determined using modified Knutson method (1986). The debranched starch suspension was diluted with 90% DMSO and placed in a boiling bath for 20 min. Then, 50 μL of this solution was reacted with 0.6 mM iodine solution in DMSO for 30 min. The reaction product of debranched starch-iodine was measured using spectrophotometer (GBC UV/VIS 916, GBC Scientific Equipment Pty., Ltd., Australia) at 620 nm.

The absorbance of amylose, cassava starch and debranched starch was measured from 400 to 700 nm at 1 nm interval to obtain spectra. For each absorbance spectrum, the maximum absorbance wavelength (λ_{max}) was determined.

3.10 Water holding capacity of debranched starch

The debranched starch suspension was weighed and placed in 1 mL of centrifuge tubes. The tubes were refrigerated at 5°C for 24 h, and then centrifuged at 10,000 rpm for 15 min at 5°C (Hettich Universal 16R, Hettich GmbH, Tuttlingen, Germany). The aqueous phase was removed and the precipitate was weighted. The water holding capacity (WHC) was determined as follows:

$$\text{WHC} = \left[\frac{\text{weight of precipitate (g)}}{\text{weight of total sample (g)}} \right] \times 100$$

3.11 Preparation of resistant starch from cassava starch with starch debranching and retrogradation process

Cassava starch solution (20% w/w) was gelatinized using a shaking water bath at 85°C for 15 min with continuous shaking (Ratex SWB 20, Ratek Instruments PTY., LTD., Australia) and then autoclaved at 105°C for 30 min (Sanyo Labo autoclave MLS 3020, Sanyo Electric Co., Ltd., Japan). The starch gel was suspended with 0.1 M acetate buffer pH 5.0 to obtain the gel of 8% starch (w/w). The gel was cooled to 50°C and the pullulanase concentration of 15 PUN/g of starch was added to obtain a substrate: enzyme ratio of 20:1 by weight. The suspension was incubated with continuous shaking at 50°C for 0, 0.5, 2, 5 and 24 h (at specific degree of debranching which was selected from previous study). The sample was taken out at various time and heat at 85°C for 30 min to stop enzyme reaction. The samples were divided into 2 parts. The first part was the debranched starch sample (DBS) and the second one was cooled down and stored at 5°C for 4 days in refrigerator (Mitsubishi MR-F 36M, Mitsubishi Electric Automation, Japan). The latter part was the retrograded-debranched starch sample (RDBS). Both DBS and RDBS were frozen with liquid nitrogen and then lyophilized using a freeze dryer (Heto FD 8, Heto-Holten A/S, Denmark). All dried DBS and RDBS samples were ground in a blender to reduce and then they were sifted to obtain the particle size of 75-105 micron. The treatment was conducted in duplicate for all debranched sample.

3.12 Temperature cycles treatment

The debranched starch at debranching time of 0, 0.5, 2, 5 and 24 h (at a specific degree of debranching) was prepared as described in the previous section. After

stopping enzyme reaction, the debranched starch suspension was incubated at a specific time and temperature condition. The temperature conditions were chosen from temperature which favored crystal nucleation and propagation. The temperature of 5°C and 55°C were studied to favor nucleation and the temperatures of 80°C and 120°C were investigated to promote propagation. The debranched starch was then subjected to four cycles of nucleation and propagation as follows:

On the first cycle, the debranched starch was aged at the nucleation temperature of 5°C in a refrigerator (Mitsubishi MR-F 36M, Mitsubishi Electric Automation, Japan) or 55°C in convection hot air oven (Memmert ULE 700 AO, Memmert GmbH, Schwabach, Germany) for 3 h, followed by aging at the propagation temperature of 80°C or 120°C in convection hot air oven for 3 h.

On the second cycle, the nucleation temperature of 5°C or 55°C for 18 h, followed by the propagation temperature of 80°C or 120°C for 3 h.

On the third cycle, the nucleation temperature was 5°C or 55°C for 18 h, followed by the propagation temperature of 80°C or 120°C for 3 h.

On the fourth cycle, the nucleation temperature was 5°C or 55°C for 3 h, followed by the propagation temperature of 80°C or 120°C for 1.5 h.

After temperature cycling, the samples were cooled at 5°C or 55°C for 1.5 h The samples were frozen with liquid nitrogen and then lyophilized using a freeze dryer (Heto FD 8, Heto-Holten A/S, Denmark). All dried samples were ground in a blender to reduce and then they were sifted to obtain the particle size of 75-105 micron. The temperature cycling treatment was conducted in duplicate for all debranched sample

3.13 Determination of resistant Starch

Resistant starch content was determined according to McCleary and Monaghan, (2002). A sample of 100 mg was weighed into a 50 mL centrifuge tube and 4 mL of 1.0 M sodium maleate buffer (pH 6.0) containing pancreatic α-amylase (10 mg/mL) and amyloglucosidase (3 U/mL) was added, tighten the cap and mixed. The tube was covered with paraffin film and placed horizontally in a shaking water bath (Ratex SWB 20, Ratek Instruments Pty. Ltd., Australia). The solution was incubated at 37°C with continuous shaking for 16 h. Then, the solution was added with 4 mL of 99% ethanol to precipitate the starch and then the solution was centrifuged at 3000 rpm for 10 min (Eppendorf centrifuge 5810 R, Eppendorf AG, Hamburg, Germany). The supernatant was decanted and the residue was rinse twice with 8 mL of 50% ethanol, followed by the centrifugation at 3,000 rpm for 10 min. The residue was re-suspended with 2 mL of 2 M potassium hydroxide in an ice bath with stirring for 20 min. The 1.2 M Sodium acetate buffer pH 3.8 (8 mL) was added, and then followed by 0.1 mL of amyloglucosidase (3300 U/mL). The sample was mixed and incubated at 50°C with continuous shaking for 30 min (Ratex SWB 20, Ratek Instruments Pty. Ltd., Australia). The sample was diluted with water and then centrifuged at 3,000 rpm for 10 min. The liberated glucose was determined by glucose oxidase assay following the procedure of Bergmeyer and Bernt (1974). The diluted sample was treated with 2 mL of glucose oxidase peroxidase solution with o-dianisidine reagent. The mixture was incubated at 37°C for 30 min and the reaction was stopped with 2 mL of 12 N sulfuric acid. The absorbance was measured against a reagent blank using spectrophotometer (GBC UV/VIS 916, GBC Scientific Equipment Pty., Ltd., Australia) at 540 nm.

The resistant starch content was calculated as follows:

$$\text{RS content (g/ 100 g sample)} = \Delta E \times (F/W) \times DF \times (162/180) \times 100$$

where, ΔE =   absorbance of sample at 540 nm read against a reagent blank

F   =   conversion from absorbance to milligram of glucose

W   =   sample weight (dry weight)

DF   =   dilution factor

and, 162/180 =   factor to convert from free glucose, as determined, to an hydroglucose as occurring in starch

3.14 Water absorption index and water solubility index

Water absorption index (WAI) and water solubility index (WSI) were measured according with a modified method of Schoch (1964). The powder sample (0.4 g dry basis) was mixed with 40 mL of water in a centrifuge tube and mixed with vortex. After heating for 30 min in a water bath at 30ºC, the solution was centrifuge at 3,000 g for 10 min. The WAI and WSI were determined as follows:

$$\text{WAI} = \left[\frac{\text{weight of sediment (g)}}{\text{weight of dry sample solid (g)}} \right]$$

and

$$\text{WSI} = \left[\frac{\text{weight of dissolved solid in supernatant (g)}}{\text{weight of dry sample solid in the original sample(g)}} \right] \times 100$$

3.15 X-ray diffraction

X-ray powder diffraction (XRD) analysis was performed using X-ray diffractometer (Bruker D5005, Bruker GmbH, Germany) using 1.54 Å Cu K_α radiation.

Powder Samples with moisture content of 7-10% were packed tightly in a cell. The samples were exposed to the X-ray beam with X-ray generator running at 40 kV and 40mA. The scanning regions of Bragg's angle (2θ) were 3 - 30°. The other operation conditions were as follows: Step interval of 0.02, scan rate of 2.5^o/min, divergence slit of 0.25^o, anti-scattering of 0.25^o and speed rotation of 30 rpm.

The relative degree of crystallinity of sample was quantitatively estimated according to Hermans and Weidinger (1961). The area over diffractogram was integrated using EVA Diffract plus#1 software (Bruker GmbH, Germany). The ratio of diffraction peak area to total area was referred to the relative degree of crystallinity.

3.16 Fourier transform infrared spectroscopy

The absorbance fourier transform infra-red (FTIR) spectra were acquired using a Spectrum GX FTIR spectrometer (Perkin Elmer Inc., Boston, MA, USA) equipped with a deuterated triglycine sulphate (DTGS) detector using a horizontal attenuated total reflectance (ATR) accessory with a ZnSe crystal at an angle of incidence of 45° (Perkin Elmer Inc., Boston, MA,USA). The powder samples with moisture content of 7-10% were measured directly after pressing the sample on the crystal. The spectra were obtained at the resolution of 4 cm^{-1}. The 32 scans were averaged for each measurement. The measurement was acquired against an empty cell as background in the region of 4000-800 cm^{-1}. The Spectrum was baseline corrected in the region of 1200 - 800 cm^{-1} and then deconvoluted using an enhancement factor of 2.0. The measurement intensity was performed on the deconvoluted spectra by recording the height of absorbance bands from a baseline. According to (Van Soest, Tournois, de Wit and Vliegenthart, 1995), the peak height ratio of high at 1047 and 1035 cm^{-1} was

measured to quantity the order structure of potato starch of amount of ordered potato starch. Thus, the ratio of absorbance intensities of band at 1045 to 1037 cm^{-1} (1045/ 1037) was monitored for the data analysis in this study.

3.17 Differential scanning calorimetry

Differential scanning calorimetry (DSC) measurement was performed using Pyris Diamond DSC (Perkin Elmer, Connecticut, USA) equipped with an intercooler. An approximately 10 mg of sample was weighted into a 50 μL stainless steel pan and distilled water was added to obtain a starch-water suspension containing 75% water (w/w). The pan was hermetically sealed and left for overnight at room temperature before heating in the DSC. Indium was used as the standard. An empty stainless steel pan was used as the reference. The DSC run was performed from 1 to 200°C at a heating rate of 10°C/ min. The thermal transitions of starch sample were defined as onset temperature (T_o), peak of gelatinization temperature (T_p) and conclusion temperature (T_c) and the enthalpy of gelatinization (ΔH). Enthalpy was calculated on a starch dry weight basis. They were calculated automatically by Pyris Diamond software (Perkin Elmer, Connecticut, USA). The gelatinization temperature range was calculated as (T_c - T_o). DSC thermograms were determined as the points where the scan deviated from linearity before and after the peak. Peak transition temperature was defined as the temperature of peak maximum. The melting transition enthalpy, ΔH (J/g), was calculated from the area under peak transition.

3.18 Statistical Analysis

Analysis of variance (ANOVA) was conducted using SAS program (SAS Institute Inc, Carry, NC., USA). Triplicate determinations were performed for each test, and the results reported are average values. The differences among mean values were established using Duncan's multiple-range test (DMRT) at 95% significance level. The correlation coefficient was conducted between the molecular structure, physical, thermal parameters and RS content of DBS and RDBS.

The effect of starch concentration, pullulanase concentration and time on debranching process of cassava starch was analyzed using a factorial experiment in completely randomized design (CRD). The effects of debranching and retrogradation on resistant starch content and relative crystallinity were analyzed using a factorial experiment in CRD. The effects of temperature cycling on resistant starch content, relative crystallinity and total enthalpy (ΔH_T) were analyzed using a factorial experiment in CRD. The effects of nucleation temperature and propagation temperature on resistant starch content, relative crystallinity and ΔH_T were analyzed using a factorial experiment in Randomized complete block design (RCBD).

3.19 References

Association of Official Analytical Chemists (AOAC) (1990). **Official method of analysis** (15th eds.). Virginia: The Association of Official Agricultural Chemists.

Balagopalan, C, Padmaja, G., Nanda, S.K., and Moorthy, S.N. (1988). **Cassava starch in food, feed and animal industry**. Florida: CRC Press.

Bergmeyer, H.U., and Bernt, E. (1974). **Methods of Enzymatic Analysis**. New York: Academic Press.

Dubois, M., Gilles, K.A., Hamiltion, J.K., Rebers, P.A., and Smith, F. (1952). Colorimetric method for determination of sugars and related substances. **Analytical Chemistry** 28 (3): 350-356.

Govindasamy, S., Oates, C.G., and Wong, H.W. (1992). Characterisation of changes of sago starch components during hydrolysis by thermostable alpha-amylase. **Carbohydrate Polymers** 18: 89-100.

Hermans, P.H., and Weidinger, A. (1961). On the determination of the crystalline fraction of polyethylenes form X-ray diffraction. **Macromolecular Chemistry** 24: 24-36.

Hood, L.F., and Mercier, C. (1978). Molecular structure of unmodified and chemically modified manioc starch. **Carbohydrate Research** 61: 53-66.

Knutson, C.A. (1986). A simplified colorimetric procedure for determination of amylose in maize starch. **Cereal Chemistry** 63 (2): 89-92.

McCleary, B.V., and Monaghan, D.A. (2002). Measurement of resistant starch. **Journal of Association Official Analytical Chemistry** 85 (3): 665-667.

Novo industri A/S Enzyme Division. (1983). **Method for the determination of pullulanase activity**. Denmark: Novo Industri A/S.

Pulluzyme (1997). **Analytical method for Pulluzyme- amylo 1,6 glucosidase enzyme activity for use in laboratory conversion**. England: ABM Chemicals.

Schoch Y.J. (1964). Swelling power and solubility of starch granules. In R.L. Whistler, R.J. Smith and M.L. Wolfrom (eds.). **Methods in carbohydrates chemistry** (Vol .IV, pp. 106-108). New York: Academic Press.

Somogyi, M. (1952). Note on sugar determination. **The Journal of Biological Chemistry** 195: 19-23.

Van Soest, J.J.G., Tournois, H., Wit de, D., and Vliegenthart, J.F.G. (1995). Short-range structure in (partially) crystalline potato starch determined with attenuated total reflectance Fourier-transform IR spectroscopy. **Carbohydrate Research** 279: 201-214.

CHAPTER IV

RESULTS AND DISCUSSION

4.1 General properties of native cassava starch

4.1.1 Composition and structural properties of native cassava starch

Cassava starch used in this study is the commercial starch. Its chemical composition is presented in Table 4.1. It contained 99.82% starch and approximately 0.3% minor components, which were protein, fat, fiber and ash. These contents were usually considered as the purity index of starch extraction. The higher starch and the lower content of other components are highly desirable (Galliard and Bowler, 1987).

Table 4.1 Chemical composition of cassava starch

Composition	Content
Major components (% of total starch)	
Starch	99.82 $\pm$ 0.11
Amylose	17.25 $\pm$ 0.29
Amylopectin[1]	82.85
Moisture content (%)	11.55 $\pm$ 0.23
Minor components (% dry weight basis)	
Protein	0.12 $\pm$ 0.05
Fat	not detected
Fiber	0.04 $\pm$ 0.02
Ash	0.10 $\pm$ 0.00
Sulfur dioxide (ppm)	not detected

[1] Amylopectin content (%) = 100% – % amylose content

The high starch and low minor components and contamination of sulfur dioxide indicated that the cassava starch used in this study showed a high purity and a good quality.

Apparent amylose content of cassava starch was 17.25%. It was in a normal range of 16 to 18% amylose for cassava starch (Balagopalan, Padmaja, Nanda, and Moorthy, 1988). The molecular structure of amylose and amylopectin was studied after debranching with pullulanase and their characteristics are showed in Table 4.2.

Table 4.2 Structural characteristics of cassava amyloses and amylopectins

	Branch linkage (%)	β-Limit (%)	$\overline{NC}$[1]	$\overline{CL}_n$[2]	$\overline{ECL}$[3]	$\overline{ICL}$[4]
Amylose	0.48	77.2	23	64.6		
Amylopectin	5.79	58.0	173	17.2	12.1	4.0

[1] Average number of chain

[2] Number-average chain length

[3] External chain length = $\overline{CL}_n \times$ (β-Limit/100) + 2

[4] Internal chain length = $\overline{CL}_n - \overline{ECL} - 1$

For amylose, the percentage of branch linkage and β-amylolysis limit value was 0.48% and 77.2%, respectively. The β-amylolysis limit value is defined as the relative amount of maltose after hydolysis with β-amylase. β-Amylase hydrolyses every second α-D-glucosidic (1→4) linkage from the non-reducing ends, thereby producing maltose, but it is blocked by α-D-glucosidic (1→6) branch linkage. For this result, the amylose was not completely hydrolyzed into maltose. It suggested that cassava amylose contained slightly branched molecules. Hizukuri et al. (1997)

reported that the amount of branched amylose molecule was 42% by mole and the percentage of branch linkages was 0.49% for cassava amylose.

For amylopectin, the structure contained 5.61% of branch linkages which corresponded to a general value in the range of 4-6%. The β-amylolysis limit of cassava starch was 58% which was similar to the value of 57% reported by Hizukuri (1996). The average chain length ($\overline{CL}_n$) was 17.2, which was lower than that of 21 reported by Hizukuri (1996). The difference was possibly due to the reason that $\overline{CL}_n$ was determined using the cupric ion reduction (CIR) method. Gerard, Planchot, Colonna and Bertoft (2000) reported that $\overline{CL}_n$ value as determined with CIR method was lower than determined by size-exclusion chromatography. The external chain length ($\overline{ECL}$) and internal chain length ($\overline{ICL}$) were determined on the basis of the β-amylolysis limit and $\overline{CL}_n$ values. The $\overline{ECL}$ and $\overline{ICL}$ were 12.1 and 4.0, respectively. As compared with $\overline{ECL}$ and $\overline{ICL}$ of maize, waxy maize or potato amylopectin (Bertoft, 2004), those of cassava amylopectin were shorter, but similar to those of highly branched waxy rice amylopectin. This suggested that the cassava amylopectin had a highly branched structure.

4.1.2. Gelatinization properties of native cassava starch

Some physical properties of cassava starch were studied i.e. pasting properties using Rapid Visco Analyser (RVA) and thermal properties using Differential Scanning Calorimeter (DSC) and their characteristics are summarized in Table 4.3. Cassava starch had a gelatinization temperature range of 66 to 80°C and a high peak viscosity of 352.11 RVU. According to Sriroth et al. (1999), a temperature of gelatinization (T_p) of cassava starch in Thailand ranged from 69 to 71°C, depending on genetic variation and environmental condition impact on the structure-function of the

starch. Furthermore, pasting properties related with amylose content as changing on environmental conditions. From pasting characteristic, the pasting temperature indicates the minimum temperature required for cooking. The peak viscosity also indicates the water binding capacity of starch. Final viscosity is used to define the particular quality of starch and indicates the stability of the cooked paste in actual use. In addition, it also indicates the ability to form a various paste or gel after cooling and less stability of starch paste commonly accompanied with a high value of breakdown. Setback indicates the hardening or retrogradation of cooked starch during cooling. From setback value, this result showed a low value, indicating a slow rate of retrogradation occurring in cassava starch.

Table 4.3 Pasting and thermal properties of native cassava starch

Physical properties	Value		
Pasting properties			
Pasting temperature (°C)	74.42	±	0.34
Peak Viscosity (RVU)	352.11	±	9.32
Final viscosity (RVU)	234.83	±	6.60
Breakdown (RVU)	207.42	±	5.26
Setback (RVU)	90.37	±	8.36
Thermal properties			
Onset temperature (°C)	66.27	±	0.16
Peak temperature (°C)	72.30	±	0.00
Conclusion temperature (°C)	79.81	±	2.00
Enthalpy (J/ g)	12.78	±	0.77

For RS_3, the formation of RS_3 depends on the retrogradation of starch gel. Cassava starch showed a slow rate of retrogradation because it was mainly composed of amylopectin. However, the amylopectin rich starch cloud produced RS_3 by debranching

the starch to generate linear fragments (Lehmann, Jacobasch and Schmiedl, 2002). The length of chain greatly influences on RS_3 formation. The chain length of polyglucan with approximately 20 glucose units was optimal for high RS formation (Schmidl, Baurelein, Bengs and Jacobasch, 2000). The cassava amylopectin in this study had the $\overline{CL}_n$ of 17.2 glucose unit (Table 4.2). It was indicated that the α-1, 6-linked side chain was long enough. Thus, cassava starch is capable to produce RS_3 with pre-treatment by debranching with debranching enzyme, i.e. pullulanase.

4.2 Effect of starch concentration, pullulanase concentration and time on debranching process of cassava starch

At present, the information on debranching of cassava starch is limited and has not been investigated systematically. In this study, cassava starch was debranched by commercial pullulanase (Promozyme D2, Novozyme, Denmark) rather than highly purified pullulanase was used to investigate the feasibility on process development of the RS3 production for commercial application. The ability of pullulanase to debranch starch depends on various environmental factors. Some factors such as pH and incubation temperature were well studied (Jensen and Norman, 1984). However, other factors, i.e., starch concentration, pullulanase concentration and incubation times are varied, depending on starch source and needed a study for a selected starch. Therefore, these factors of debranching process of cassava starch were investigated in this study.

First, Promozyme D2 was evaluated the enzymatic activity. The enzyme had a pullulanase activity of 570 PUN/mL and also presented α-amylase activity of 23 AU/mL. This result indicated that commercial pullulanase was partially contaminated with α-amylase.

With respect to a study on the effect of starch concentration, enzyme concentration and debranching time on starch debranching, the extent of debranching was estimated from the degree of hydrolysis (D.H.) as evaluated from reducing sugar liberated after debranching and the data is showed in Table 4.4. The influence of starch concentrations and enzyme concentrations on D.H. as a function of debranching time are presented in Figure 4.1. The analysis of variance (ANOVA) indicated that the starch concentration, enzyme concentration and debranching time did affect D.H. of starch debranching were significantly (Appendix A, Table 1a).

Table 4.4 Degree of hydrolysis of debranched starch at various starch concentrations, enzyme concentrations and debranching times

time	5 % w/w Starch			8 % w/w Starch			10 % w/w Starch		
	5	15	30	5	15	30	5	15	30
0	0^c	0^d	0^d	0^c	0^e	0^c	0^c	0^d	0^d
1.5	2.37^b	2.87^c	4.76^c	2.97^b	3.91^d	4.65^b	2.20^b	2.87^c	4.79^c
3	2.84^b	4.18^b	5.34^{bc}	3.38^b	4.09^d	5.23^b	2.51^b	4.48^b	5.01^{bc}
6	2.91^b	4.27^b	6.10^a	3.60^b	5.11^c	6.44^a	2.77^b	4.74^a	5.56^{ab}
12	4.19^a	4.56^{ab}	5.98^{ab}	4.43^a	5.42^b	6.73^a	3.58^a	4.83^a	5.58^{ab}
24	4.21^a	4.81^{ab}	6.08^a	4.65^a	6.29^a	6.76^a	3.59^a	5.03^a	5.93^a
44	4.54^a	5.48^a	6.41^a	4.75^a	6.66^a	6.44^a	4.08^a	5.04^a	5.97^a

Degree of hydrolysis (%)

Mean values with different letters in each column are significantly different ($p<0.01$).

As the reaction time of debranching increased, the degree of hydrolysis was significant increased in all samples ($p < 0.01$) (Figure 4.1 and Table 4.4). The degree of hydrolysis increased dramatically during three hours of debranching and then increased gradually with longer debranching time (Figure 4.1). This result was similar to

the debranching of banana starch (Gonzalez-Soto, Agama-Acevedo, Solorza-Feria, Rendon-Villalobos and Bello-Perez, 2004) and rice starch (Guraya, Jame and Champagne, 2001b) in which the reducing sugar was released rapidly at the beginning and then approaching a relative constant on the prolonged incubation with a large amount of enzyme. Moreover, no further significantly increased D.H. was observed between 24 and 44 hours of debranching time ($p > 0.05$) (Table 4.4). This result indicated that the pullulanase digestion was not fully active after 24 h of incubation. In addition, the maximum D.H. value of debranched starch obtained at 44 h was 6.66%. It was higher than the amount of the branched linkages in amylopectin molecules which were reported to be approximately 4-6% of the total glucosidic linkages in cassava starch (Balagopalan et al., 1988). This result suggested that pullulanase was contaminated with α-amylase, resulting in a hydrolysis of α-1, 4 linkages was hydrolysis and subsequently increasing the liberated reducing sugar. This result was in accordance with a present of α-amylase activity in Promozyme D2 as mentioned previously.

The starch concentration did affect the action of Promozyme (Appendix A, Table 1a). The concentration of starch at 5% (3.90% D.H.), 8% (4.35% D.H.) and 10% (3.74% D.H.) were significantly different in D.H. ($p < 0.01$), where starch concentration of 8% was significantly different from 5% and 10% starch concentration while starch concentration of 5% and 10% did not showed a significant difference ($p > 0.05$). Figure 4.1 also showed that the D.H. of starch concentration of 8% was higher than that of 5% and 10% starch concentration at each enzyme concentration. This result demonstrated that the concentration of starch of 10% was not suitable for debranching with pullulanase enzyme. It might due to a high viscosity system in this

starch concentration, resulting in insufficient accessibility of enzyme on debranching reaction. The starch concentration of 8% was the highest level for debranching starch with Promozyme.

The D.H. of debranched starch at 5 PUN of enzyme concentration (3.03% D.H.) was significantly lower than that of 15 PUN enzyme (4.03% D.H.) and 30 PUN enzyme (4.94% D.H.), respectively ($p < 0.01$). Figure 4.1 was also showed that the higher enzyme concentration, the greater D.H. was observed. In general, the D.H. was increased with increasing enzyme/substrate ratio [E/S]. It demonstrated that these substrate concentrations needed a higher enzyme concentration to starch debranching. This result was similar to the study the effect of enzyme concentration on starch debranching of banana starch by Gonzalez-soto et al. (2004) and sago starch by Leong, Karim and Norziah (2007).

The enzyme concentration and debranching time was significantly interaction (Appendix A, Table 1a). In first period of starch debranching (1.5-3 h), the more enzyme was added, the higher debranched starch was produced as indicated from an increased D.H. (Figure 4.1). The rate and level of D.H. was constant after 12 h of debranching. However, the rate of D.H. was not constant after 12 h at 8% starch concentration with 15 PUN enzyme (Figure 4.1B). In addition, the D.H. at 8% starch with 15 PUN enzyme for 24 h was closed to that at 8% starch with 30 PUN enzymes for 12 h of debranching (Figure 4.1C). For this reason, the 15 PUN enzyme concentration and 8% starch concentration were selected for further debranching in this study. This result was similar to the study of Guraya et al. (2001b) who debranched rice starch with different enzyme level.
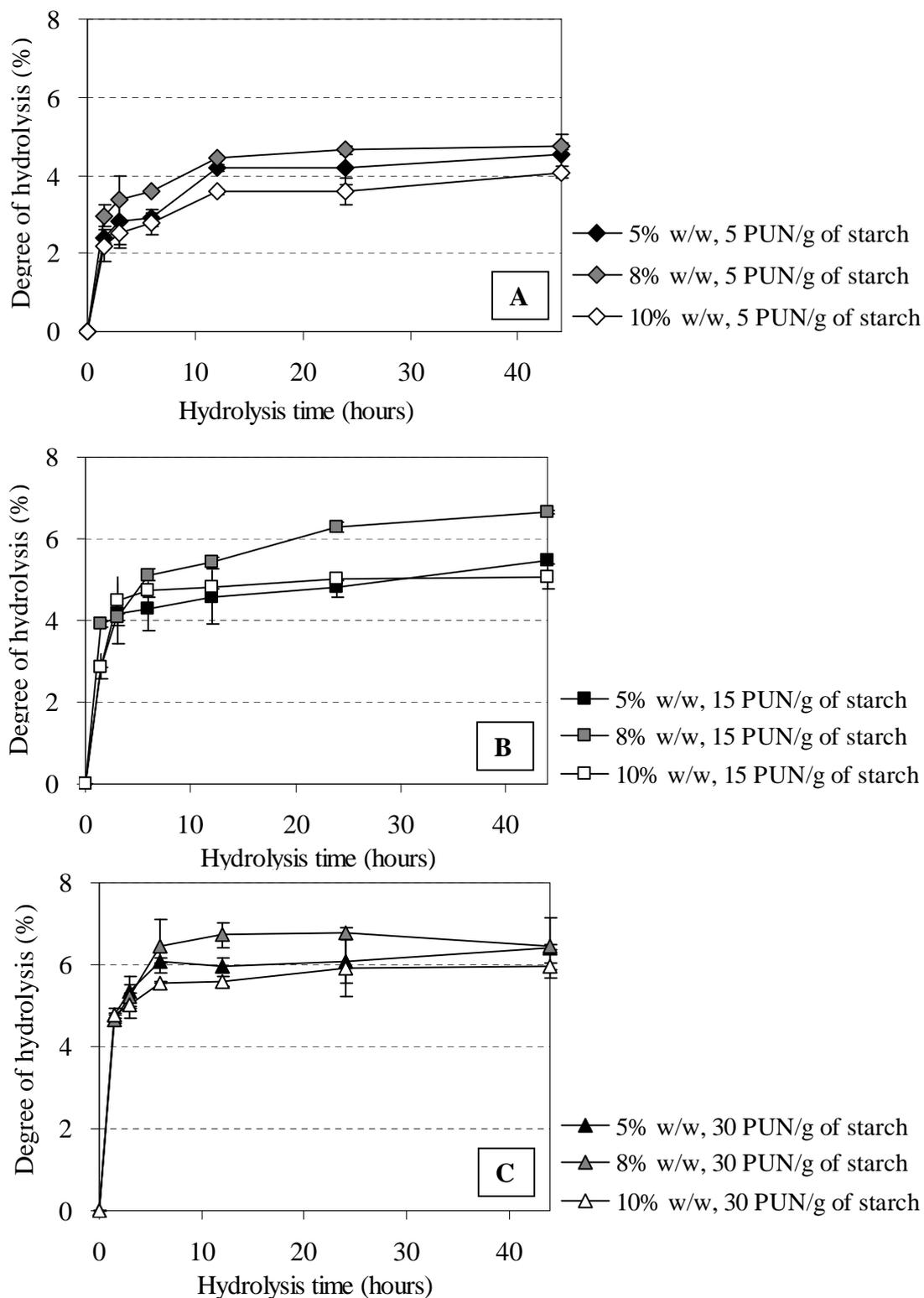
Figure 4.1 Effect of concentration of starch and enzyme as a function of debranching

time on degree of hydrolysis at levels of enzyme concentration of A: 5

PUN/g; B: 15 PUN/g; C: 30 PUN/g

They reported that the more enzymes did not ensure completed debranching due to the retrogradation of amylose during the incubation with enzyme. When the retrogradation was progressive, the debranching was extremely slow and independent of enzyme concentration.

4.3 Structural characteristics of debranched cassava starch

4.3.1 Number average of chain, degree of polymerization and iodine binding capacity properties of debranched starch

The 8% cassava starch hydrolyzed with 15 PUN pullulanase concentration for different incubation time was selected to studied on the structural characteristics. The liberated sugar produced by pullulanase action on the starch as a function of debranching time is shown in Figure 4.2. In first period (0-3 h), the longer debranching time, the more sugar was liberated. After 5 h of debranching, the liberated sugar content did not show a statistical difference ($p < 0.05$). An approximately 50% of debranching occurring in the first hour of treatment and the reaction rate slowed down afterward. This pattern was correlated with D.H. as described in the previous study.

The visible precipitate with cloud-like was observed in the starch suspensions after 5 h of debranching time and the more quantity of precipitate was noticed with longer debranching. This phenomenon demonstrated that the liberated short chain fragments produced by pullulanase hydrolysis re-associated and aggregated, resulting in retrogradation. Hizukuri, Takeda and Yasuda (1981) reported that the extent of debranching with pullulanase enzyme was not complete due to the retrogradation of amylose during incubation. Therefore, the total branched chain of starch may not be correctly quantified in the debranching system. In addition, the β-

amylolysis limit of debranched starch for 24 h was 84.80%, suggesting the incomplete debranching phenomenon. The re-associated of liberated short chain fragments might result in an inaccessibility of enzyme on the α-1, 6 linkages. Therefore, the degree of debranching was significantly unchanged after debranching for 5 h and the maximum degree of debranching was only 89.3%.
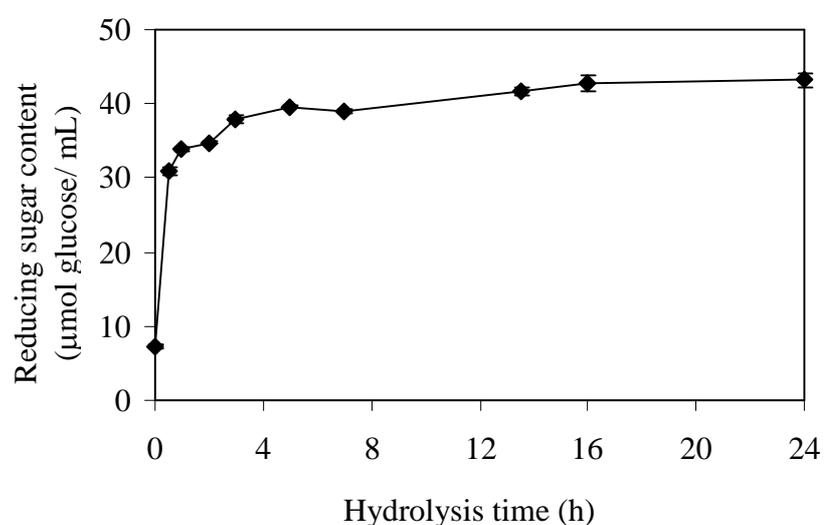
Figure 4.2 The reducing sugar content of cassava starch after debranching with pullulanase.

The structure of cassava starch after debranching is presented in Table 4.5. As increasing incubation time and degree of debranching (D.B.), the number-average degree of polymerization ($\overline{DP}_n$) decreased, whereas the average number of chain ($\overline{NC}$) increased. Iodine binding capacity (IBC) was another method to study the structure of debranched starch. The absorption spectra of debranched starch (DBS)-iodine complexes are presented in Figure 4.3 Theses spectra illustrated that the debranching of starch by pullulanase led to a shift of the second peak toward a lower wavelength with higher absorption intensity. The IBC and λ_{max} of DBS-iodine complex are presented in Table 4.5. As the D.B. was increased, the more IBC appeared,

Table 4.5 Structural characteristics of debranched cassava starch

Debranching time (h)	D.B. (%)	$\overline{NC}$	$\overline{DP}_n$	IBC at A_{620} nm	λ_{max}
0	0.0^a	9^a	263^a	0.224^a	619.4^a
0.5	58.9^b	22^b	117^b	0.481^b	591.2^b
1	66.2^c	26^{bc}	102^{bc}	0.536^c	588.6^{bc}
2	68.5^c	28^{cd}	93^{bc}	0.590^d	585.6^c
3	76.0^d	32^{de}	82^{bc}	0.604^{de}	584.3^d
5	80.6^f	35^e	73^c	0.617^e	583.9^{de}
7	79.1^e	38^{ef}	67^c	0.623^e	583.1^e
13	85.6^{ef}	37^{ef}	69^c	0.642^e	582.9^e
16	88.5^{fg}	40^{ef}	64^c	0.638^e	582.7^e
24	89.3^g	42^f	61^c	0.624^e	582.3^e

Mean values in each column with different letters are significantly different ($p<0.01$).
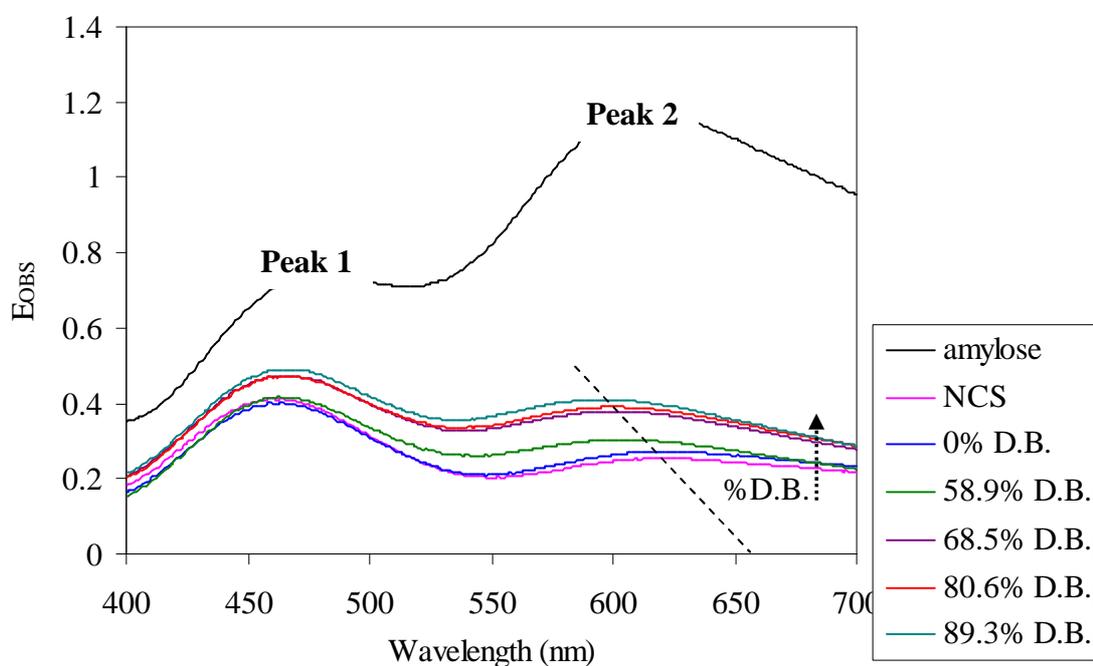
Figure 4.3 The absorption spectra of amylose-iodine and DBS-iodine complex at different degree of debranching.

but λ_{max} of DBS-iodine complex was lower. Since IBC was the measurement of absorbance at the maximum wavelength of amylose, 620 nm, the absorbance obtained at various D.B. is related to the amount of linear fragment liberated by pullulanase action on the starch. In addition, a positive correlation between IBC and $\overline{NC}$ was obtained from regression analysis with the high degree of correlation (r^2) of 0.92. This correlation suggested that the linear fragment was more released with longer debranching time.

Regarding λ_{max} of DBS-iodine complex, the absorption peak showed a shift from 619.4 to 582.3 nm (Figure 4.3 and Table 4.5). This shift of absorption peak was similar to that of a mixture of limited dextrins with different chain length, which was synthesized from polysaccharides. The limited dextrin with a few outer branches showed the shifts of absorption peak to shorter wavelengths (Swanson, 1947). Knutson (1999) mentioned that all α-1, 4-glucans formed helical inclusion complex with iodine to some degrees; the extent of iodine binding depended upon the degree of helix formation which could be attained. A single helix was required six glucose molecules per turn for supporting the complex formation. As the outer branch was partially released, the remained number of glucan chain per molecule of amylopectin was lower, and, hence, the number of helical turns decreased. The number of iodine molecules, which could be accommodated, also decreased; thus, the absorption of glucan-iodine complex was lower, resulting in shifting the absorbance to the shorter wavelength. In addition, it is probable that the branch point effectively limits the length of chain in the iodine complex formation and subsequently influencing the color formed. Linear regression analysis indicated a positive correlation between $\overline{DP}_n$ and λ_{max} with r^2 of

0.98. It indicated that the low molecular weight with a few outer branches was remained after debranching process.

The structure of DBS in this study was similar with the molecular weight distribution of debranched maize maltodextrin at different debranching time. When debranching was progressive, the amount of short linear chain with DP 24.1 was increased and the long linear chain with DP > 50 or branched molecules were decreased and still present after 48 h of debranching. This indicated that debranching was increased amylose fragment, short linear chain and decreased clusters structure to smaller branch molecules (Pohu, Planchot, Putaux, Colonna and Buleon, 2004).

4.3.2 Gel formation of debranched cassava starch

Gel formation of all debranched starch occurred during cooling in refrigerator. As the cooling progressed, an increase in turbidity was noticeable and the homogeneous white-gel was induced after cooling for 24 h. Miles, Morris and Ring (1985) showed that the low concentration of amylose solutions (2.4-7%) became turbid during the early stage of amylose gelation. An increase in turbidity was attributed to phase separation into polymer-rich region and polymer-deficient region, followed by network formation or the development of gel structure. The rate and extent of network formation depended on polymer concentration and polymer molecular sizes. Gidley and Bulpin (1989) described this phenomenon from cooling of aqueous synthetic amylose solutions. Short chain amyloses (DP < 110) were found to precipitate at all concentrations up to 5%. For intermediated chain length of DP 250 – 660 both gelation and precipitation were observed while long chain amylose (DP > 1100) were found to form gel upon cooling. This behavior was explained based on the chain alignment and cross-linking in the cooled aqueous solution. For long chain, the

extensive cross-linking occurred which resulted in the formation of macromolecular network and eventually gelation was formed. If the chain length over which these interactions occur was substantially shorter than the total chain length, then more than two regions within a single chain involved in separated interactions, thereby leading to a cross-linked network structure. In contrast, if the total chain length was not substantially longer than interacting chain length, then extensive cross-linking would not occur and chain alignment would predominate, followed by lateral aggregation, and eventually lead to precipitation. Lateral aggregations of shorter chains were due to the formation of double helices. These helices further aggregated, subsequently forming the ordered crystalline. In general, precipitation was favored by shorter chain length, lower concentration and slower cooling rate, but gelation was favored by longer chain length, high concentration and faster cooling rate (Guraya, Jame and Champagne, 2001a).

The characteristic of debranched starch in regard to gel structure was studied on water holding capacity. The ability of gel to held water indicating gel strength. The poor gel formation was observed after debranching process. Gelatinized starch without debranching held more water (99.63% WHC) than that of all debranched starch samples (Figure 4.4). This could be described from the basic of a gel formation into polymer-rich region and polymer-deficient region. The gel networks were formed as a result of the formation of covalent bonds between polymer molecules (Miles, Morris, Orford and Ring, 1985). For native cassava starch gel, which contained high molecular weight amylopectin, inter-chain associations can form more than one location of cross-link (junction zone), resulting in a network structure or gel. When

starch was debranched to 58.9% D.B., the WHC decreased to 49.52% and then increased from 49.52% to 71.43% with the higher D.B. of 58.9% - 89.3%.
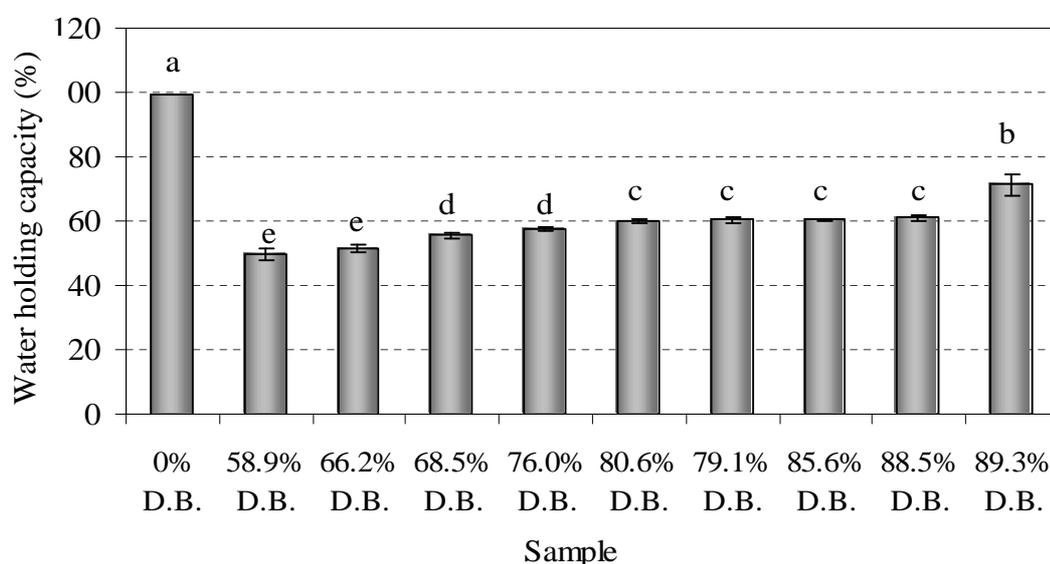
Figure 4.4 Effect of debranching degree on water holding capacity; 0%D.B.: non debranched starch; 58.9 - 89.3%D.B.: debranched starch at different degree of debranching of 58.9 - 89.3%, respectively. The different letters above solid graph are significantly different at confidence levels greater than 95%.

To observe the characteristic of debranched starch, the visible precipitate with cloud-like existing during debranching was separated from transparent gel by centrifugation at 1,500 g, 25°C for 10 min. The fractions of precipitate and supernatant were refrigerated at 4°C for 24 h for WHC investigation. As D.B. was increased, the WHC of precipitated fraction (fraction1) increased from 66.73% to 79.16% whereas the WHC of supernatant fraction (fraction 2) continuously decreased from 55.81% to 29.92% (Figure 4.5). The more WHC of fraction 1 was in accordance with increased of linear chain which was able to involve in double helix formation more than one location resulting in more cross-link to provide a strong network

structure (Gidley, 1989). However, WHC of fraction 1 was lower than that of gelatinized starch without debranching, due to greater abundance of smaller chains aggregation resulting in precipitation. It could lead to formation of weak gel or precipitates as observed for all debranched starch. For fraction 2, a decreased in WHC was similar to the lowering of λ_{max} of DBS-iodine complex behavior. This probably due to low molecular weight molecules with a few outer branches was remained. Since amylopectin was continuously debranched, resulting in smaller branched molecules, this could bring up a weak gel formation at a high D.B. Obviously, the structural characteristic of debranched starch as indicated from WHC was agreed with IBC properties in the previous study.
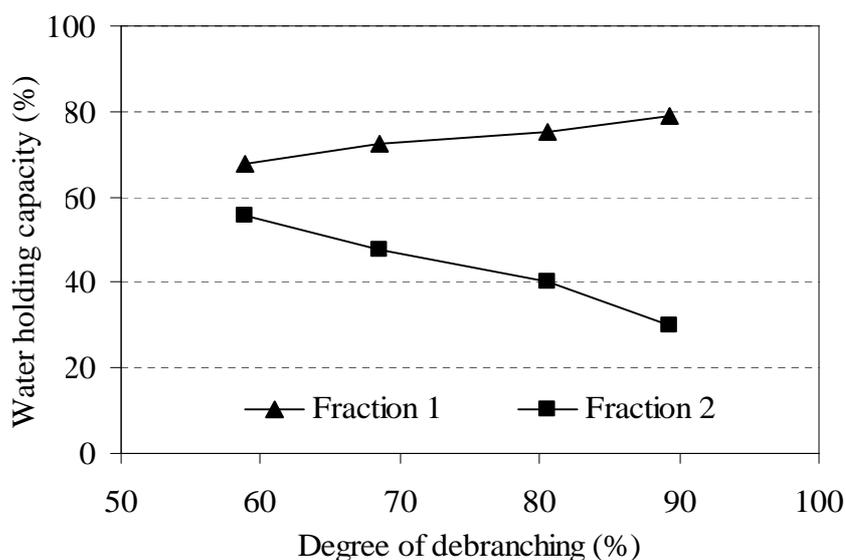
Figure 4.5 Water holding capacity of precipitated fraction (Fraction 1) and supernatant fraction (Fraction 2) of debranched cassava starch

From all results, the D.B. of debranched cassava starch by pullulanase debranching for 0.5, 2, 5 and 24 h did show statistical differences ($p < 0.01$). Furthermore, the structural characteristics i.e. $\overline{NC}$, $\overline{DP}_n$, IBC and WHC did show

statistical differences ($p < 0.01$) at D.B. of 58.9, 68.5, 80.6 and 89.3%, respectively. For this reason, the debranching time of 0.5, 2, 5 and 24 hour was selected for further study the on the RS_3 formation.

4.4 Resistant starch type III formation from debranched cassava starch

4.4.1 Effect of debranching and retrogradation on resistant starch content

The debranching degree and time dependence on RS_3 formation were investigated. The RS content of debranched cassava starch with and without aging was determined according to McCleary and Monaghan (2002). As mentioned previously, RS was produced by three steps: gelatinization, debranching and retrogradation. Gelatinized sample was debranched by pullulanase enzyme at 50°C. The sample resulted from enzyme digestion was referred to DBS (debranched starch). Another part of debranched samples was retrograded at 5°C for 4 days. The latter sample was referred to RDBS (retrograded-debranched cassava starch).

The RS content of DBS and RDBS are shown in Table 4.6. The more degree of debranching, the greater RS content obtained for both DBS and RDBS. Starch debranching yielded the high RS content of 18.25% for DBS. Furthermore, after it was aged at 5°C for 4 days, the RS content was raised up to 27.56% for RDBS at 89.3%D.B. Thus, retrogradation was a possible factor to improve RS content. This was similar to the result of waxy sorghum starch studied by Shin et al. (2004) in that the RS content was the highest in the sample debranching for 24 h with storage at 1°C for 6 days.

Table 4.6 Resistant starch content of modified cassava starch

Debranching time (h)	D.B. (%)	Resistant starch content (g/100 g starch)		RS ratio of RDBS/DBS
		DBS	RDBS	
0	0	$1.06 \pm 0.0^{a, A}$	$1.86 \pm 0.7^{a, A}$	1.20^{a}
0.5	58.9	$9.29 \pm 0.4^{b, B}$	$12.02 \pm 1.5^{b, CD}$	1.29^{a}
2	68.5	$11.20 \pm 0.2^{c, C}$	$17.08 \pm 1.9^{c, E}$	1.52^{b}
5	80.6	$12.90 \pm 0.1^{d, D}$	$21.42 \pm 0.8^{d, F}$	1.66^{b}
24	89.3	$18.25 \pm 0.1^{e, E}$	$27.56 \pm 0.6^{e, G}$	1.51^{b}
Native cassava starch		27.68 ± 0.4		

Mean values with different small letters in each column are significantly different ($p<0.01$).

Mean values with different capital letters in two columns are significantly different ($p<0.01$).

The RS content of DBS and RDBS had a significantly negative relationship ($r^2 = 0.953$, $p < 0.01$ for DBS; $r^2 = 0.964$, $p < 0.01$ for RDBS) with the logarithmic value of $\overline{DP}_n$ (Figure 4.6). This result indicated that the RS formation from amylopectin is strongly dependent on its molecular size. Branched amylopectin with large molecular size gave a lower RS content, whereas its small molecular size gave a higher RS content. This indicated that the low molecular weight of branched polymer promoted the retrogradation leading to a greater of RS formation. It can be concluded that the debranching process release medium to small molecules which were able to form RS. This result is similar to that of debranched banana starch with DP of 6-30 where RS content of 51% was induced (Lehmann et al., 2002). Based on retrogradation phenomenon, the rate and extend of retrogradation of amylopectin is markedly influenced by fine structure of branched molecule. According to Ring et al. (1987), amylopectin chain with less than 15 units did not take part in the

recrystallization process. The amylopectin chains with DP 14-24 and 16-30 increased the retrogradation. Therefore, the retrograded amylopectin may contain different level of RS when incubation conditions were optimized to favor amylopectin retrogradation.

Besides molecular size affecting the RS formation, the aggregation of linear fragment molecules during incubation with enzyme at 50°C was also considered to affect RS formation as observed from RS in all DBS sample. This temperature was lower than melting temperature (T_m), but higher than glass transition temperature (T_g) that cloud promote the retrogradation. The aggregation of linear fragment molecules was confirmed from the results of X-ray diffraction and DSC where the crystal and the ordered structure were performed.
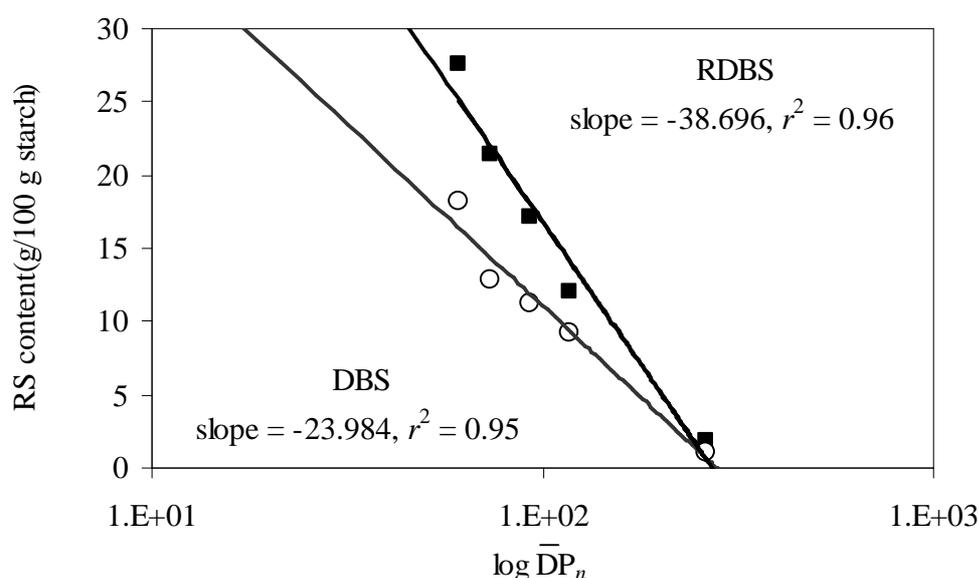
Figure 4.6 Effect of number-average degree of polymerization ($\overline{\text{DP}}_n$) on RS content formation in DBS (O) and RDBS (■).

The increment of RS content of RDBS to the decrement of log $\overline{\text{DP}}_n$ (slope = -38.696) was profoundly higher than that of DBS (slope = -23.984) (Figure 4.6). However, the RS ratio of RDBS/DBS did not correlate with log $\overline{\text{DP}}_n$ (Table 4.6). It

indicated that the RS formation of RDBS not only depends on the molecular weight of amylopectin but also on the arrangement of molecular structure during retrogradation. In DBS, the formation of RS would occur from the aggregation of low molecular weight and linear fragment molecules during incubation. For RDBS, these molecules were able to re-associate slowly under the storage temperature of 5°C. The more RS content of RDBS over DBS showed that the storage at 5°C for 4 days could increase RS content up to 1.2-1.7 times (Table 4.6). Consequently, an increase in RS content of RDBS with different debranching degree was a result of an aggregation of molecules in DBS and their molecular arrangement during retrogradation.

Furthermore, RS ratio of RDBS/DBS at 58.9% D.B. was lower than that of 68.5-89.3% D.B. while RS ratio of RDBS/DBS at 68.5-89.3% D.B. did not show a statistical difference. It indicated that molecular size had two groups effects on RS formation in retrogradation process i.e. 1) a number of branched molecules with high molecular weight ($\overline{DP}_n > 100$) and 2) linear fragment and lower branched molecules with low molecular weight ($\overline{DP}_n < 100$). Eerlingen, Deceuninck and Delcour (1993) found that amylose with longer chain contributed slightly lower RS content. The amyloses with high $\overline{DP}_n$ was not sufficient to diffusion of the amylose molecules to crystallization nuclei. As also reported by Gidley et al. (1995), gelation and aggregation based on inter chain junction zones of double helices occurred over the chain lengths of DP > 10 to about 100 with limiting the aggregation into B-type arrays. The minimum chain length required for double helix formation is 10 with B-type crystallization being favored for DP 13 and above. The upper limit of uninterrupted helix lengths was DP 100 as most helix interruptions were expected to be enzyme-sensitive. This is a reasonable explanation for two groups of molecular size

that affected the increased RS content of debranched starch after retrogradation in this study. At 58.9% D.B., the debranched starch had $\overline{\text{DP}}_n$ 117 where the double helix interruption, resulting the lower RS formation than that of 68.5%-89.3% D.B. with $\overline{\text{DP}}_n$ 93-61. This indicated that debranched starch at 58.9% D.B. contained mostly partial debranched amylopectin with larger branch molecules. For debranched starch at 68.5%-89.3% D.B., the abundance of linear fragment and low molecular weight molecules with a few branches were present and their chain length were sufficient to RS formation.

From Table 4.6, the RS content of DBS at 68.5% and 80.6%D.B. was not statistically different from that of RDBS at 58.9%D.B. Similarly, the RS content of DBS at 89.3%D.B. and RDBS at 68.5%D.B. did not show a statistical difference. Obviously, longer incubation time of enzymatic digestion can improved RS content similar to retrogradation of DBS at lower D.B. It indicated that the enzymatic digestion temperature of 50°C far from the T_m and T_g of the system was combined factor to accelerate the RS formation.

4.4.2 Crystallinity of DBS and RDBS

X-ray diffraction was used to investigate the structural changes and a long-range order structure of starch into RS formation. The X-ray diffraction patterns of native cassava starch, freeze-dried DBS and freeze-dried RDBS are presented in Figure 4.7 and 4.8. The X-ray diffraction parameters and crystalline type are given in Table 4.7. The relative crystallinity was calculated from a ratio of diffraction peak area to total diffraction area according to Hermans and Weidinger (1961) and the d-spacing was use to discriminate the planes of different sites, these parameters are summarized in Table 4.8. Native cassava starch showed an A-type pattern, which is generally found

in cassava starch (Figure 4.7), as indicated from the typical peaks at 2θ of 15°, 17°, 18°, 20° and 23° (Table 4.7). No distinct peak cloud be observed in freshly gelatinized starch (DBS at 0% D.B.) and in gelatinized starch stored at 5°C for 4 days (RDBS at 0% D.B.) due to the fact that they are mainly composed of amorphous structure. In Figure 4.8, the diffraction pattern of DBS and RDBS at 58.9%-89.3%D.B. was different from that of the native cassava starch, as the peak at 15° disappeared. The diffraction parameter of DBS sample was differed from RDBS one in that a small peak at 5° and weak shoulder peak at 22° appeared in RDBS where they were the characteristics for B-type (Figure 4.8 and Table 4.7). Thus, all RDBS was classified as C_B-type. On the other hand, the polymorphic of DBS altered with different D.B. With higher D.B., the peak at 17° and 23° became progressively larger and broader. The broad peak at 23° and the absence of peak at 5° indicated that A-type crystalline is predominant in DBS at high degree of debranching. The transition of crystalline type of debranched concentrated maltodextrin was studied by Pohu et al. (2004). They reported that gradual transition from almost B-type to A-type structure occurred simultaneously during debranching between 12 and 48 h. Furthermore, Cheetham and Tao (1998) also report that average chain length of amylopectin has a significant effect on crystal form and crystallinity. It was concluded that the long chains favored formation of B-type crystalline and short chains benefited A-type. The transition of crystal type $A \rightarrow C \rightarrow B$ was accompanied with an increased average chain length. The result of this study was in accordance with Cheetham and Tao's conclusions.
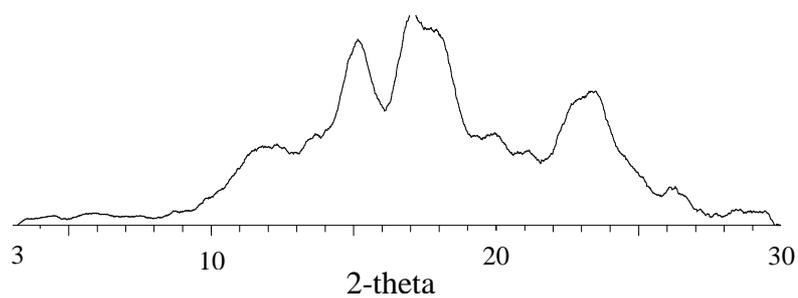
Figure 4.7 X-ray diffraction spectra of native cassava starch
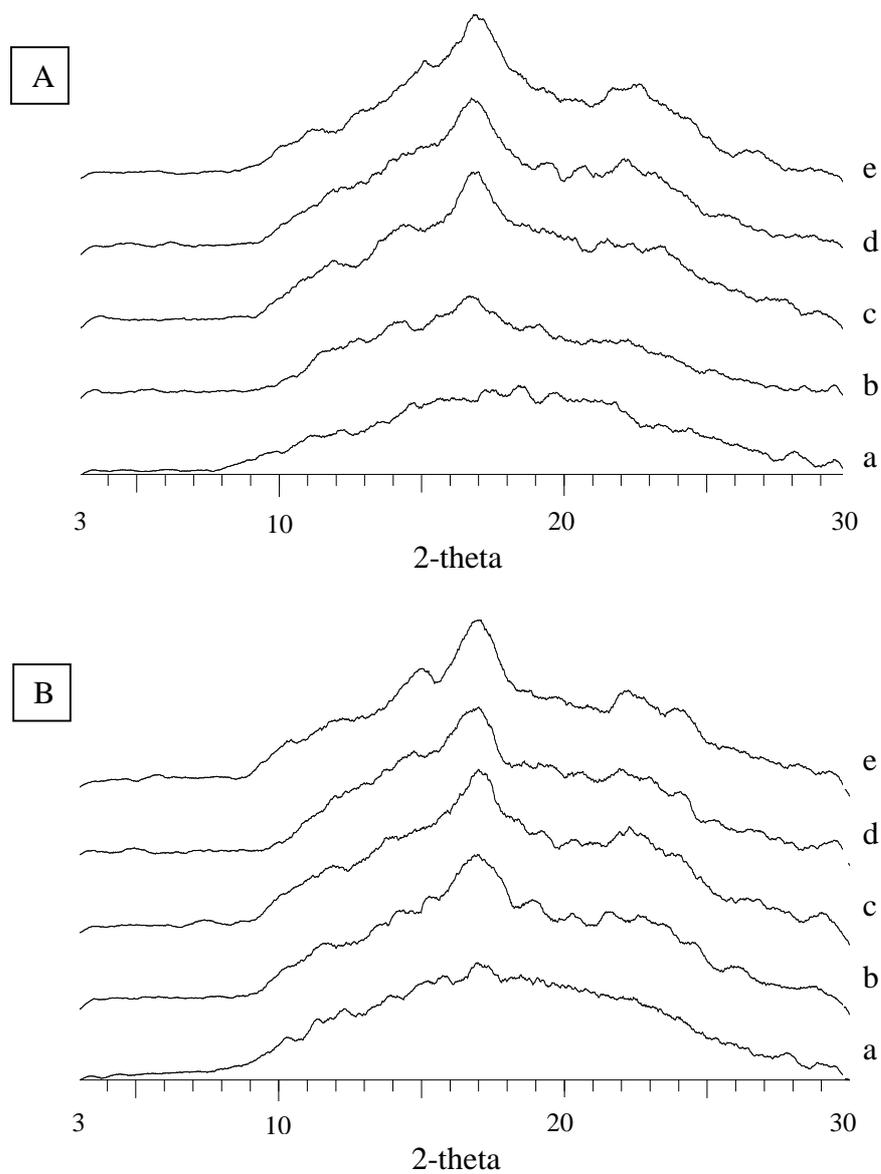
Figure 4.8 X-ray diffraction spectra of (A) DBS and (B) RDBS with degree of debranching of a: 0%D.B., b: 58.9%D.B., c: 68.5%D.B., d: 80.6%D.B., e: 89.3%D.B.

Table 4.7 X-ray diffraction data of native starch, debranched starch (DBS) and retrograded-debranched starch (RDBS) with different degree of debranching

Sample	Diffraction peak at 2θ value (°angle)								Crystal pattern
	5°	15°	17°	18°	20°	22°	23°	30°	
Potato[a]	5.5 (16.2 Å)[c]	14.8 (5.99 Å)	17.0 5.21 Å	-	19.3 (4.60 Å)	22.1 (4.03 Å)	23.8 (3.74 Å)	30.1 (2.90 Å)	B
Potato[b]	5.6 (15.8 Å)	14.4 (6.2 Å)	17.2 (5.2 Å)	-	19.5 (4.60 Å)	22.2 (4.00 Å)	24.0 (3.7 Å)	-	B
Waxy corn[a]	-	14.8 (6.00 Å)	16.6 (5.35 Å)	17.7 (5.01 Å)	-	-	22.6 (3.92 Å)	30.1 (2.96 Å)	A
Wheat starch[b]	-	14.9 (5.94 Å)	16.9 (5.24 Å)	18.1 (4.90 Å)	19.9 (4.45 Å)	-	23.2 (3.83 Å)	-	A
Native cassava starch	-	15.1 (5.87 Å)	17.0 (5.20 Å)	17.8 (4.98 Å)	20.0 (4.44 Å)	-	23.0 (3.86 Å)	29.3 (3.05 Å)	A
DBS-58.9	-	-	17.1 (5.22 Å)	-	-	-	-	-	C
DBS-68.5	-	-	16.9 (5.24 Å)	-	-	-	-	29.2 (3.05 Å)	C
DBS-80.6	-	-	16.8 (5.27 Å)	-	-	-	23.2 (3.92 Å)	29.1 (3.07 Å)	C$_A$

Table 4.7 X-ray diffraction data of native starch, debranched starch (DBS) and retrograded-debranched starch (RDBS) with different

degree of debranching (continued)

Sample	Diffraction peak at 2θ value (°angle)								Crystal pattern
	5°	15°	17°	18°	20°	22°	23°	30°	
DBS-89.3	-	-	16.7 (5.30 Å)	-	-	-	23.5 (3.87 Å)	29.6 (3.02 Å)	C_A
RDBS-58.9	4.7 (23.85 Å)	-	17.0 (5.18 Å)	-	-	-	-	29.4 (3.03 Å)	C_B
RDBS-68.5	5.3 (16.72 Å)	-	17.1 (5.17 Å)	-	-	-	23.0 (3.78 Å)	29.2 (3.06 Å)	C_B
RDBS-80.6	4.0 (22.42 Å)	-	16.9 (5.25 Å)	-	-	-	23.7 (3.76 Å)	29.4 (3.04 Å)	C_B
RDBS-89.3	4.6 (24.38 Å)	14.7 (6.01 Å)	17.0 (5.22 Å)	-	-	22.3 (3.99 Å)	23.8 (3.74 Å)	29.3 (3.05 Å)	C_B

[a] Source: Jeroen, Van Soest, Hulleman, Wit de and Vliegenthart (1996).

[b] Source: Hoover and Vansanthan (1994).

[c] The figures in parentheses represent interplanar spacing.

The relative crystallinity of DBS increased with the increased in degree of debranching (Table 4.8) and log $\overline{\text{DP}}_n$ was shown a high negative correlation (r^2 of 0.995, $p < 0.01$) with relative crystallinity (Figure 4.9). This suggested that short chain fraction played an important role in the formation of crystallinity. Although, the relative crystallinity of RDBS increased with a higher D.B. (Table 4.8) as well as the smaller in molecular size (Figure 4.9), the crystalline type did not change. It indicated that various molecular sizes (average chain length) did not affect the transition of polymorphic form of crystallite under the experiment retrogradation conditions. The explanation cloud be made based on the storage temperature affecting an alteration in long-range ordering. The retrogradation at low temperature brought up the formation of B-type crystalline due to the fact that low temperature favored double helices ordered in a hexagonal structure requiring the least activation energy (Eerlingen, Crombez and Delcour, 1993). On the other hand, the retrogradation at high temperature led to the formation of A-type crystalline (Shamai, Bianco-Peled and Shimoni, 2003; Bello-Perez, Ottenhof, Agama-Acevedo and Farhat, 2005). This result suggested that low storage temperature at 5°C induced of the crystalline structure of RS to be B-type.

On the comparison between DBS and RDBS, the peak at 2θ of 17° of RDBS was narrower than that of DBS indicating a decrease in the d-spacing of 17° (Table 4.8). In addition, d-spacing of 22° and 23° was appeared in RDBS, which was closed to that in potato starch and narrower than DBS. It was probably due to the fact that the aging of debranched starch suspensions at low temperature was able to increase the crystal perfection and content. The crystallization of debranched starch was explained through three sequential steps. Crystallization stages were classified

into nucleation, propagation and maturation (Roos, 1995b). The rate of crystal nucleation approached zero at T_m and was maximum near T_g, while the rate of crystal growth approached zero at T_g and was maximum near T_m. Thus, the storage temperature at 5°C promoted crystal nucleation resulting in raising crystal formation.

Table 4.8 X-ray diffraction data of modified cassava starch[1]

Debranching time (h)	D.B. (%)	Relative crystallinity (%)		Crystallinity ratio of RDBS/DBS
		DBS	RDBS	
0	0	$0.91 \pm 0.1^{a, A}$	$0.94 \pm 0.0^{a, A}$	1.04^a
0.5	58.9	$5.23 \pm 0.2^{b, B}$ (5.22 Å)[2]	$6.84 \pm 0.7^{b, C}$ (5.18 Å)	1.31^a
2	68.5	$6.26 \pm 0.9^{c, BC}$ (5.24 Å)	$12.82 \pm 0.5^{c, E}$ (5.17 Å)	2.05^b
5	80.6	$7.10 \pm 0.2^{c, C}$ (5.29 Å)	$15.33 \pm 1.0^{d, F}$ (5.24 Å)	2.16^b
24	89.3	$8.51 \pm 0.9^{d, D}$ (5.30 Å)	$18.99 \pm 1.3^{e, G}$ (5.22 Å)	2.23^b
Native cassava starch		28.76 ± 0.1		

[1]Mean values with different small letters in each column are significantly different ($p<0.01$).

 Mean values with different capital letters in two columns are significantly different ($p<0.01$).

[2] The figure in parentheses represents Interplanar spacings at 2-Theta of 17°.

From the crystallinity ratio of RDBS/DBS in Table 4.8, an increment of relative crystallinity ratio of RDBS over DBS during retrogradation appeared to increase up to 2.23 times. The behavior of this ratio was similar to that in RS content which resulted from the molecular size of branched amylopectin as described in a previous section 4.4.1.
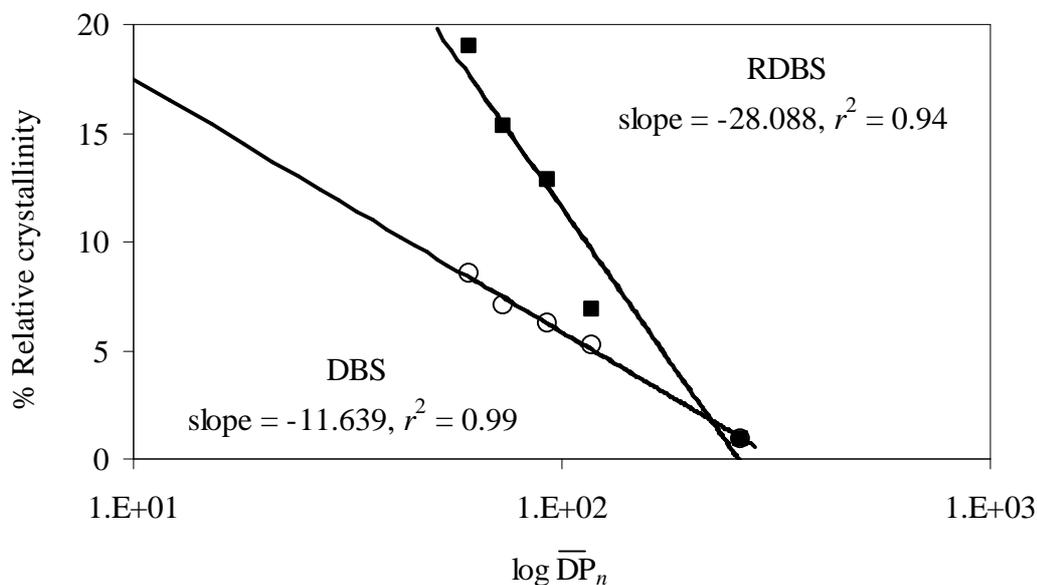
Figure 4.9 Relative crystallinity and number-average degree of polymerization ($\overline{DP}_n$) relationship in DBS (O) and RDBS (■).

To confirm the ordered structure formation of DBS and RDBS samples, the short-range order structure was investigated with attenuated total reflectance Fourier Transform Infrared spectroscopy (ATR-FTIR). The differences in polysaccharide conformation in solution as well as in the solid state cloud be distinguished in the region between 1200 and 800 cm^{-1} in FTIR spectra (Rindlav, Hullernan and Gatenholm, 1997). The deconvoluted spectra in range 800-1200 cm^{-1} of DBS and RDBS with different in D.B. are shown in Figure 4.10 and 4.11. This spectra region comprised series of band, mostly the result of C–O and C–C stretching. The bands at 1045 and 1022 cm^{-1} were sensitive to the amount of ordered and amorphous region respectively (Van Soest, Tournois, Wit de and Vliegenthart, 1995). In the ATR-FTIR spectrum, the band intensity at 1045 cm^{-1} increased with increasing D.B. (Figure 4.10-4.11). Thus, the amount of short-range ordering of DBS and RDBS at various D.B. could be expressed as the intensity ratio of bands at 1045 and 1037 cm^{-1}. The

absorbance ratio of DBS and RDBS as a function of relative crystallinity is shown in Figure 4.12. The absorbance ratio increased with increasing relative crystallinity and this result was in accordance with Van Soest et al., (1995) who studied on retrograded potato starch gels. It suggested that an increase in D.B. induced a greater proportion of available chains to participate in ordered structure by increasing molecular order in the short-range (double helix formation) and long-range ordering (crystallite formation).
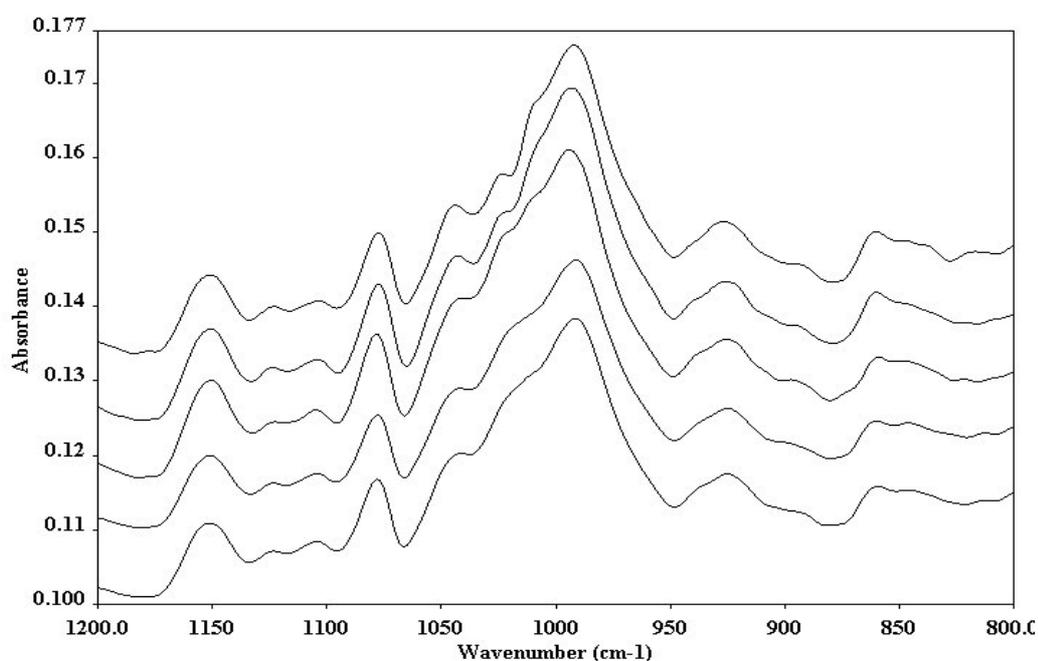
Figure 4.10 Deconvoluted ATR-FTIR spectra of DBS at different degree of debranching. From bottom upward, the degree of debranching are 0%, 58.9%, 68.5%, 80.6% and 89.3%, respectively
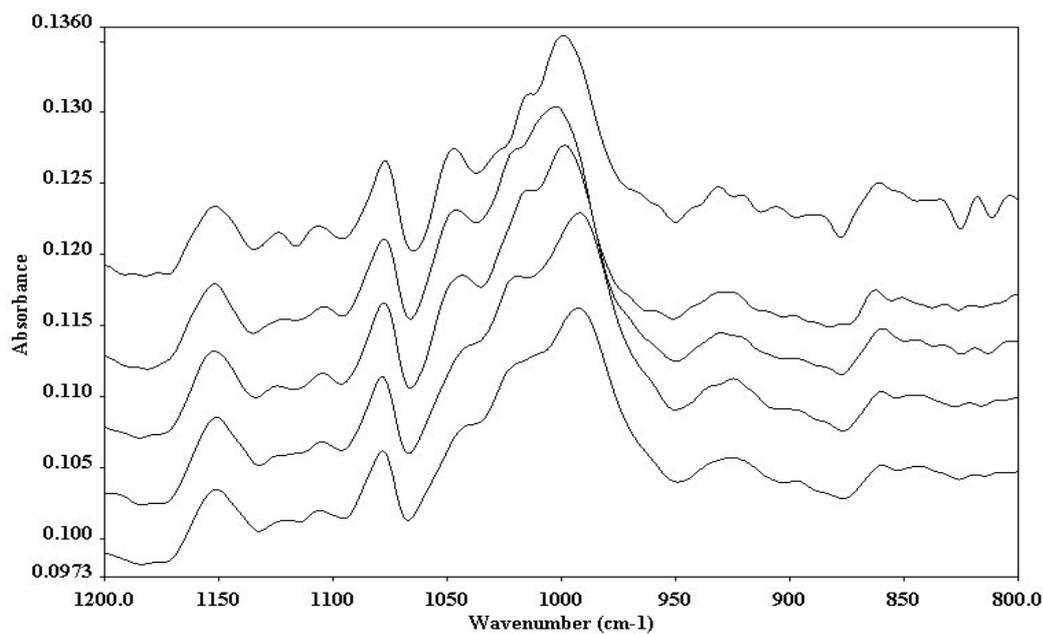
Figure 4.11 Deconvoluted ATR-FTIR spectra of RDBS at different degree of debranching. From bottom upward, the degree of debranching are 0%, 58.9%, 68.5%, 80.6% and 89.3%, respectively.
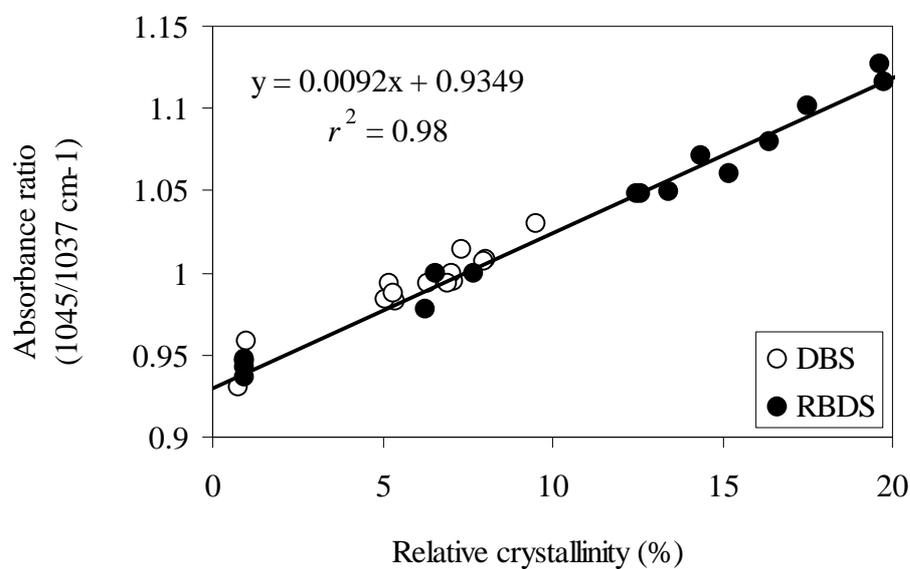
Figure 4.12 Absorbance ratio of peaks at 1045 and 1037 cm^{-1} of ATR-FTIR spectra of DBS (○) and RDBS (●) as a function of relative crystallinity.

4.4.3 Thermal properties of DBS and RDBS

DSC measures heat absorbed or given off from a sample in a controlled atmosphere at specified temperatures. This provides information about sample's specific heat and latent heat which indicate changes in the amorphous and crystalline structures. DSC measurements made on granular starch and starch polymer in excess water usually produce endotherms with distinct peaks. These endothermic peaks are characterized by the parameters of onset temperature (T_o), peak temperature (T_p), conclusion temperature (T_c) and enthalpy (ΔH). The T_o indicates the start of thermal conversion. The value for T_p shows the temperature at which maximum thermal conversion of the crystalline material takes place, whereas T_c represents the temperature at which the conversion process is complete. The conversion enthalpy, ΔH, is determined by calculating the peak area. It presents the total energy needed for the transformation. Results from DSC measurement were used to characterize the thermal characteristic of DBS and RDBS.

As a mean of comparison, the gelatinization temperature of native cassava starch was measured (data not shown). Native cassava starch showed a characteristic gelatinization curve with endothermic transition at temperature of $T_o = 66.3$°C, $T_p = 72.3$°C, $T_c = 79.8$°C and enthalpy of $\Delta H = 12.78$ J/g dry sample. These observations are in good agreement with others (Gunaratne and Hoover, 2002; Lewandowicz and Soral-Smietana, 2004). The transition temperatures and the corresponding enthalpies of DBS and RDBS are summarized in Table 4.9 and 4.10. The thermal transition values of DBS and RDBS were greater than those of native cassava starch due to the production of linear chain and small molecules during pullulanase digestion. In general, the T_m of amylopectin crystallites is lower than that

of amylose crystallites. Thus, branch crystallites are less stable than linear crystallites (Shin et al., 2004). In addition, DBS exhibited three endothermic transitions over the T_m range of 50-120°C, 140-170°C and 170-197°C, respectively (Table 4.9). A wide range of T_c - T_o may be due to the present of crystallites, which were composed of small crystallites, and each one had slightly different crystal strength (Vasanthan and Bhatty, 1996). Therefore, DBS probably produced several different types of crystallites formation during incubation. Based on the thermal stability of amylose and amylopectin, it was possible that the first endothermic transition was probably come from a few branched crystallites and some linear crystallites. The second and third endothermic transition was probably come from linear crystallites due to double helical segments of retrograded amylose unwind at temperature of 160°C in water (Gidley et al., 1995). As the degree of debranching increased, the T_p and ΔH of the first transition was higher. This was similar to those of HCl-treated waxy rice starch observed by Chang and Lin (2007). It indicated that the few branch molecules were easier to aggregate into a dense structure.

With regarded to RDBS, when the debranched cassava starch sample were stored at 5°C for 4 days. The thermal properties showed two endothermic transitions over the T_m range of 48-80°C and 130-150°C (Table 4.10). The first endothermic transition was probably of highly branched crystallites because this range of was closed to the T_m of retrograded amylopectin which was 45-70°C (Eerlingen and Delcour, 1995). The second transition was likely to be the thermal transition of crystallites from linear fragments and low molecular weight with a few branched molecules. As the degree of debranching increased, the ΔH of first transition decreased, illustrating that amylopectin was hydrolyzed into lower branched molecules. Moreover,

Table 4.9 Thermal properties of debranched tapioca starch (DBS) [1,2]

D.B.	First transition					Second transition					Third transition				
	T_o	T_p	T_c	T_c-T_o	ΔH	T_o	T_p	T_c	T_c-T_o	ΔH	T_o	T_p	T_c	T_c-T_o	ΔH
0	n.d.	n.d.	n.d.	n.d.	n.d.	n.d.	n.d.	n.d.	n.d.	n.d.	n.d.	n.d.	n.d.	n.d.	n.d.
58.9	54.6	78.7	113.5	58.9	4.9	140.8	153.7	171.5	30.7	1.0	180.0	188.2	196.3	16.3	0.6
68.5	54.1	88.2	121.9	62.8	8.2	126.5	148.5	157.7	31.2	1.6	173.1	184.4	196.9	23.8	1.3
80.6	56.4	100.1	120.9	64.5	10.4	136.1	147.8	161.3	25.2	0.6	170.1	182.0	196.8	26.7	2.0
89.3	55.5	105.1	119.5	64.0	11.8	n.d.	n.d.	n.d.	n.d.	n.d.	172.1	184.1	193.2	21.1	1.6

[1] T_o, T_p, T_c = onset, peak and completion temperature in °C, respectively; ΔH = enthalpy in J/g of dry matter; n.d.: not detected.

[2] All values are average of 3-4 measures.

Table 4.10 Thermal properties of debranched tapioca starch with retrogradation (RDBS) [1,2]

D.B.	First transition					Second transition				
	T_o	T_p	T_c	T_c-T_o	ΔH	T_o	T_p	T_c	T_c-T_o	ΔH
0	n.d.	n.d.	n.d.	n.d.	n.d.	n.d.	n.d.	n.d.	n.d.	n.d.
58.9	50.4	60.5	80.6	30.2	5.1	128.5	130.2	133.9	5.4	12.1
68.5	48.9	75.2	79.9	31.0	3.6	127.5	130.5	134.3	6.8	14.3
80.6	47.5	58.1	68.1	20.5	1.2	131.0	132.2	136.4	5.4	15.8
89.3	n.d.	n.d.	n.d.	n.d.	n.d.	146.3	148.1	155.2	9.0	16.4

[1] T_o, T_p, T_c = onset, peak and completion temperature in °C, respectively; ΔH = enthalpy in J/g of dry matter; n.d.: not detected.

[2] All values are average and standard deviations of 3-4 measures.

as the degree of debranching increased, ΔH at the second transition increased, presumably that the linear fragment and low molecular weight molecules were greater re-associated after retrogradation. Obviously, the ΔH of RDBS was higher than native cassava starch. The ΔH could refer to the amount of double helix. For highly ordered starch, the enthalpy of amylomaized V and VII was 17.5 and 27.5 J/g, respectively.

4.4.4 Correlation between structural, physical properties and resistant starch content

The correlations between molecular sized ($\overline{\text{DP}}_n$), relative crystallinity, melting parameters and RS content are presented in Table 4.11. The RS content was high negatively correlated ($r = -0.98$, $p < 0.01$; $r = -0.98$, $p < 0.01$) with the molecular size and positively correlated ($r = 0.98$, $p < 0.01$; $r = 0.99$, $p < 0.01$) with the relative crystallinity for both DBS and RDBS, respectively. In addition, the relative crystallinity was also negatively correlated ($r = -0.99$, $p < 0.01$; $r = -0.97$, $p < 0.01$) with the molecular size of DBS and RDBS, respectively. This illustrated that RS content depended on the number of crystal where crystal formation was dependent on the crystallization of different molecular sizes. In this study, the small molecular size of branched polymer ($\overline{\text{DP}}_n < 100$) promoted the double helices formation from re-association of polymer. These helices further aggregated leading to the formation of ordered structure (and crystalline arrays), where the more ordered structure would resist to the enzymatic digestion.

Regarding the melting parameters from DSC, the RS content of DBS was well positively correlated ($r = 0.97$, $p < 0.01$; $r = 0.91$, $p < 0.01$) with the ΔH and T_p of the first transition. Therefore, it probably indicated that RS of DBS was generated from the aggregation of small molecule size with a few branched molecules

into a crystalline structure during debranching process. For RDBS, the RS content was positively correlated ($r = 0.91$, $p < 0.05$) with ΔH of the second transition. It was probably that RS content of RDBS occurred from reassociation and rearrangement of linear fragment and low molecular weight molecules into an ordered structure, resulting in improving the crystal perfection as seen from endothermic peak temperature around 130°C (Table 4.10).

Table 4.11 Correlation coefficient (r) between the structural, physical properties and RS content of modified cassava starch.

Properties		DBS		RDBS	
		RS^1	$CRYS^2$	RS	CRYS
CRYS		0.984**	1	0.995***	1
Log $\overline{DP}_n$		-0.977**	-0.997***	-0.982**	-0.972**
Thermal first transition	To	0.374	0.365^{ns}	-0.899*	-0.978^{ns}
	Tp	0.905**	0.968*	-0.086^{ns}	
	Tc	0.403^{ns}		-0.869^{ns}	
	ΔH	0.970**	0.935*	-0.109^{ns}	-0.141^{ns}
Thermal second transition	To	-0.353^{ns}		0.868^{ns}	
	Tp	-0.928^{ns}		0.863^{ns}	0.771^{ns}
	Tc	-0.734^{ns}		0.865^{ns}	
	ΔH	0.027^{ns}		0.913*	0.896*

Correlation significance at confident levels of 99.9% (***), 99.0% (**), 95% (*) and ns = not significant.

[1] RS, Resistant starch content (g/100 g starch)

[2] CRYS, Relative crystallinity (%)

The RS formation from debranching and retrogradation might be attributed to two reasons: (1) more free linear chains were produced after debranching.

A similar to amylose, it could participate in crystal formation by chain elongation and folding (Eerlingen, Deceuninck and Delcour, 1993). These newly formed crystals could become more perfect during retrogradation (2) low molecular weight molecules with a few branch chains could disentangle. As similar to amylopectin, the double helices and crystallites were formed by reassociation of amylopectin A-chain during retrogradation. The storage at particular temperature would promote the association of these molecules and their close packing (Vasanthan and Bhatty, 1998). Consequently, the number of perfect starch crystals would became greater with increasing D.B., resulting in the more order structure and, hence, the more resistance on enzyme digestion.

In general, endothermic transition temperature of retrograded RS is > 140°C (Shin et al., 2004). In this study, the thermal property of RS from DBS was 100°C whereas that of RDBS was 130°C. Although, RS yield is dependent on the number of crystal and RS in DBS was greater with higher degree of debranching, but the thermal properties of DBS was inferior to that of RDBS and RS from other research. Therefore, the production of the thermally stable RS from cassava starch should be debranched with pullulanase and then following by retrogradation process. These would facilitate the association of low molecular weight molecule into an order structure, resulting in higher crystal and thermal properties.

4.5 Effect of temperature cycling on resistant starch type III formation from debranched cassava starch

4.5.1 Effect of temperature cycling on resistant starch content

Debranched cassava starch suspensions were subjected to different temperature treatments aiming to produce extensive amount of RS content.

Accordingly, the current theory of RS formation can be summarized under the term of starch retrogradation or starch crystallization. The RS formation could be interpreted in terms of crystallization of a partially crystalline polymer system. In general, crystallization consists of three steps of nucleation, propagation and maturation mechanism (Roos, 1995b). Nucleation and propagation is a liquid state event which requires the orientation mobility of polymer chains. The crystallization process can occur within the temperature range between T_g of the system and T_m of the crystals. The overall crystallization depends mainly on the nucleation and propagation rate (Eerlingen, Crombez and Delcour, 1993). It is logical that the amount of RS formed is dependent on the overall crystallization, which is a function of nucleation and propagation rate. Nucleation rate increases exponentially with decreasing temperature down to T_g, while the propagation rate increases exponentially with increasing temperature up to T_m. Slade and Levine (1995) reported that the T'_g of B-type starch gels was -5°C. Therefore, the temperatures favoring nucleation at low and high level of 5 and 55°C were studied. In this study, the thermal properties of debranched starch as presented in the previous section 4.4.3 in Table 4.10 show that the T_m of retrograded debranched starch was observed at 130°C. Thus, the temperatures for promoting propagation at low and high level of 80 and 120°C were selected in this study. The debranched starch samples were stored at 5°C and subsequent storage at 80°C for four cycles, referred to "5/80°C". A storage temperature at 5°C and subsequent storage at 120°C was referred to "5/120°C" or at 55°C and subsequent storage at 80°C was referred to "55/80°C" or at 55°C and subsequent storage at 120°C was referred to "55/120°C".

The RS content of the debranched cassava starch samples with four different time-temperature cycles, as well as freshly gelatinized cassava starch, gelatinized cassava starch retrograded for 54 h at 5°C, native cassava starch and commercial RS, i.e., novelose330 were present in Table 4.12. The RS content of temperature cycle starch gels (0% D.B.) was more than that of non-cycle sample (retrograded 54 h at 5°C) and gelatinized cassava starch, except the temperature treatment of "55/120°C". This result was in accordance with the autoclaving-cooling cycle method (Sievert and Pomeranz, 1989; Skrabanja and Kreft, 1998), time/temperature treatment (Eerlingen, Crombez and Delcour, 1993; Eerlingen, Jacobs and Delcour, 1994), and temperature cycling (Fredriksson et al., 2000; Leeman, Karlsson, Eliasson and Bjorck, 2006; Leong et al., 2007). This suggested that temperature cycling was done in order to obtain a growth of crystalline regions, a perfection of crystallites and possibly a change to more stable crystal structure.

The RS content was positively with increasing D.B. at all temperature treatments. The RS content was significantly higher in DBS of 80.6 and 89.3% D.B. ($p < 0.01$). It was due to a difference in molecular size as described previously. However, RS content of DBS at 80.6% D.B. was higher than that of 89.3% D.B. with the temperature cycling of "5/80°C" and there was no difference in DBS from 58.9 to 80.6% D.B. at the temperature cycling of "55/120°C".

With respect to different temperature treatments, DBS with "55/120°C" at 0% D.B. contained the lowest RS content as compared to "5/80°C", "55/80°C" and "5/120°C" ($p < 0.01$). For DBS at 58.9% D.B., no different RS content was observed among the temperature cycling of "55/80°C", "5/120°C" and "55/120°C" ($p > 0.05$). For 68.5% D.B., DBS with "5/80°C" contained a higher RS content as compared to the

other temperature treatments. The DBS with "5/80°C" at 80.6% and at 89.3% D.B. was

also contained a higher amount of RS as compared with "55/80°C", "5/120°C, and

"55/120°C", respectively ($p < 0.01$). For overall statistical result, the RS content of

DBS with the temperature cycling treatment of "5/80°C", "55/80°C", "5/120°C, and

Table 4.12 Resistant starch content of debranched cassava starch after subjecting to
different temperature cycle treatments

D.B. (%)	Resistant starch content (g/100 g starch)			
	5/80°C	55/80°C	5/120°C	55/120°C
0	$2.33 \pm 0.5^{a,B}$	$1.68 \pm 0.7^{a,B}$	$2.58 \pm 0.4^{a,B}$	$0.71 \pm 0.0^{a,A}$
58.9	$10.11 \pm 0.8^{b,B}$	$9.12 \pm 0.3^{b,A}$	$9.31 \pm 0.3^{b,A}$	$8.82 \pm 1.8^{b,A}$
68.5	$22.94 \pm 1.6^{c,C}$	$14.44 \pm 0.4^{c,B}$	$13.21 \pm 1.9^{c,B}$	$7.03 \pm 1.7^{b,A}$
80.6	$37.83 \pm 1.8^{e,D}$	$28.07 \pm 2.6^{d,C}$	$22.03 \pm 2.1^{d,B}$	$6.54 \pm 2.1^{b,A}$
89.3	$34.36 \pm 2.0^{d,D}$	$27.98 \pm 0.5^{d,C}$	$23.11 \pm 1.7^{d,B}$	$19.65 \pm 1.9^{c,A}$
Gelatinized cassava starch	1.06 ± 0.0			
Retrograded 54 h at 5°C	1.64 ± 0.0			
Native cassava starch	27.68 ± 1.4			
Novelose 330	39.30 ± 1.8			

Mean values with different small letters in each column are significantly different ($p<0.01$).

Mean values with different capital letters in each row are significantly different ($p<0.01$).

"55/120°C" shows the following trends:

$RS_{5/80} > RS_{55/80} > RS_{5/120} > RS_{55/120}$ (22.37 > 16.99 > 14.96 > 8.55 g/100 g starch)

These result demonstrated that the incubation with low temperature

cycling of "5/80°C" was the best method to gain a high RS content. Furthermore, DBS

of 80.6% D.B. with the temperature cycling of "5/80°C" could increase RS up to 38%

which was comparable to novelose 330. It showed that it is possible to produce modified starch with high amount of RS from cassava starch.

The nucleation temperature and propagation temperature had an influence on RS content (Appendix A, Table 2a). The RS content of nucleation temperature of 5°C (18.67 g/100 g starch) was greater than that of 55°C (12.77 g/100 g starch) ($p < 0.01$). A similar result was also observed between the propagation temperature of 80°C (19.68 g/100 g starch) and 120°C (11.75 g/100 g starch) ($p < 0.01$). There was no interaction between nucleation temperature and propagation temperature ($p > 0.05$). The relationship between nucleation temperature and propagation temperature on RS content was present in Figure 4.13. The highest nucleation and propagation temperature had a negative effect on RS formation, showing the lower RS content. The formation of RS under these temperatures could be described according to a polymer crystallization theory. When DBS suspension was stored at low temperature at 5°C, the extent of undercooling (T_m-T) for the formation of amylose crystal was relatively high (130-5°C). Thus, the nucleation rate was very high, resulting in forming many nuclei. On the other hand, the different between T_g and 5°C was very small, where a molecular mobility was insufficient because of the high viscosity system, inducing the rearrangement of molecules into crystalline state (Roos, 1995a). For 55°C, the nucleation rate was slower than that of 5°C because the viscosity of suspension was lower and the material was in a rubbery state, resulting in slow molecular reorganization and limit number of nuclei formed. When DSB was subsequently stored at 80°C and 120°C, the nucleation was limited but propagation was favored. At the temperature of 80°C, the storage temperature was lower than T_m. In this situation, the viscosity reduced; thereby increasing molecular mobility and

improving the molecular diffusion. The diffusion of molecules onto the surface of nuclei resulted in growing nuclei and growing further into crystal (Roos, 1995b; Eerlingen, Crombez and Delcour, 1993). On the other hand, at the temperature of 120°C, the storage temperature was near T_m. It was possible that the propagation rate was approach to zero at this temperature. The result of high propagation temperature of 120°C in this study was similar to the autoclaving-cooling cycles of amylomaize VII starch at autoclaving temperature of 121°C, 134°C and 148°C in that the higher temperature, the lower yield of RS was obtained, especially at temperature of 148°C (Sievert and Pomeranz, 1989).
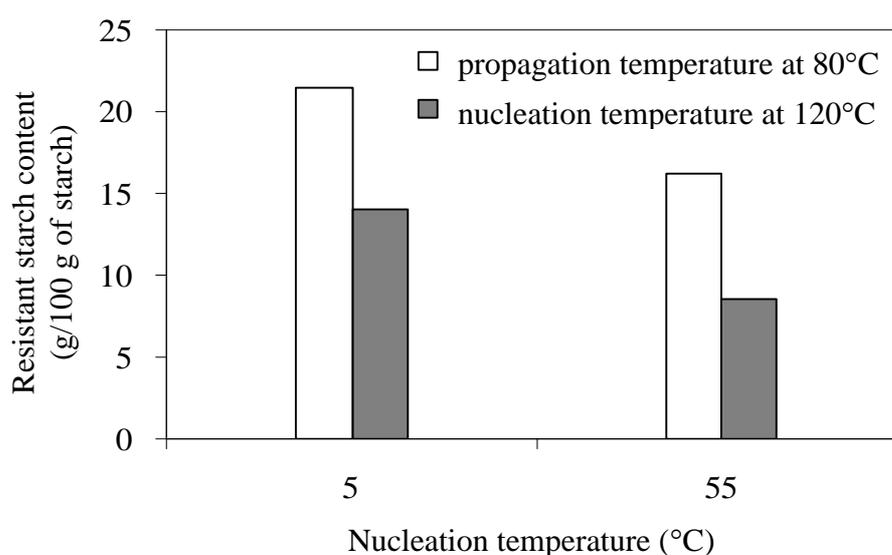
Figure 4.13 The relation between nucleation temperature and propagation temperature affected on resistant content.

The RS formation from temperature cycling cloud be explanted that the substantial amount of high-melting linear chain and high-melting low molecular weight molecule a few branched chains would nucleate at 5°C and 55°C within 3 h,

follow by the propagating step at 80°C to promote the growth of these crystals for the formation of RS. Although some of the crystallized starch chains were re-dispersed by reheating in the second to fourth cycle, leading to restoration of digestibility, the other which was retrograded-molecules remained resistant. During cooling and reheating cycle, slightly more RS_3 was formed (Sievert and Pomeranz, 1989). Therefore, the amount of RS was increased by successive heating and cooling cycles. This result was similar to the autoclaving-cooling (Sievert and Pomeranz, 1989; Skrabanja and Kreft, 1998) and temperature cycling (Fredriksson et al, 2000) in that the repeated cycles of heating and cooling improved starch molecular order and increased crystalline perfection. This, in turn, enhanced the resistance of starch to enzymatic digestion.

4.5.2 Effect of temperature cycling on crystallinity

The X-ray diffraction pattern of debranched starch at 0%, 58.9%, 68.5%, 80.6% and 89.3% D.B. with different time-temperature cycles are showed in Figure 4.14- 4.18, respectively. The X-ray diffraction pattern of Novelose330 is also showed in Figure 4.19. The corresponding X-ray diffraction parameters and crystalline type are given in Table 4.13. At 0% D.B., DBS with the temperature cycling of "5/80°C" and "55/80°C" showed a small peak at the 2θ of 17°, whereas that with the temperature cycling of "5/120°C" and "55/120°C" did not show any peaks (Figure 4.14). For DBS at 58.9% and 68.5% D.B., the diffraction pattern at the temperature treatment of "5/80°C" and "55/80°C" was observed to resemble the C_B type pattern (Figure 4.15, 4.16 and Table 4.13). A 80.6% and 89.3% D.B., the DBS with the temperature cycling of "5/80°C" and "55/80°C" show a distinct diffraction peak at 17° and two small peaks at 22° and 23°. An additional peak appeared at about 5° with d

spacing of 16-17 Å (Figure 4.17, 4.18 and Table 4.13). These spectra are basically similar to that of potato starch, which is characterized to be B-type (Table 4.7). In addition, the novelose330 also showed a B-type pattern (Figure 4.19). This result was similar to the X-ray diffraction pattern of RS formed at temperature combinations of 0°C followed by 68°C or 100°C, exhibiting B-type pattern (Eerlingen, Crombez and Delcour, 1993). In general, the B-type nuclei or crystal formed at 5°C had not changed into A-type. However, a C_A-type polymorph was observed in the DBS at 89.3% D.B. with the temperature cycling of "55/120°C". Gidley (1987) and Shamai et al. (2003) demonstrated that a higher crystallization temperature favored the formation of the more stable A-type, rather than B-type, starch polymorph. Lower temperatures were expected to favor the polymorphic form requiring the least entropy change (thus, the least activation energy) from solution (B-type), i.e., the kinetic product. At higher temperature, crystallization tended to favor more stable polymorph (A-type) requiring a higher activation energy, i.e. the thermodynamic product (Gidley, 1987).

The relative crystallinity of the debranched cassava starch with the four different time-temperature cycles and novelose330 was present in Table 4.14. As the D.B. was increased, the relative crystallinity of DSB with the temperature cycling of "5/80°C" and "55/80°C" were higher ($p < 0.01$), but it did not show the same trend for the treatment of "5/120°C" and "55/120C" with increasing D.B. from 58.9% to 89.3%.

In the aspect of temperature treatment, the relative crystallinity of all DBS was the highest at the temperature cycling of "5/80°C" and the lowest at treatment of "55/120°C" ($p < 0.01$). For DBS at 58.9% and 68.5% D.B., the relative crystallinity was not different between the temperature cycling of "55/80°C" and "5/120°C" ($p > 0.01$).
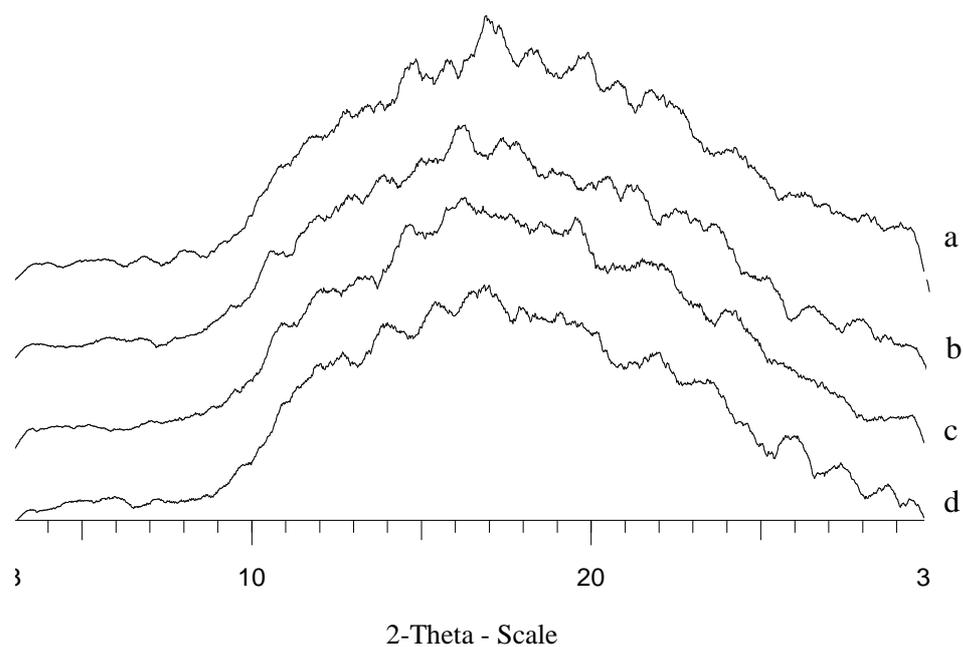
Figure 4.14 X-ray diffraction spectra of gelatinized starch (0% D.B.) with different

temperature cycles of a: 5/80°C, b: 55/80°C, c: 5/120°C and d: 55/120°C.
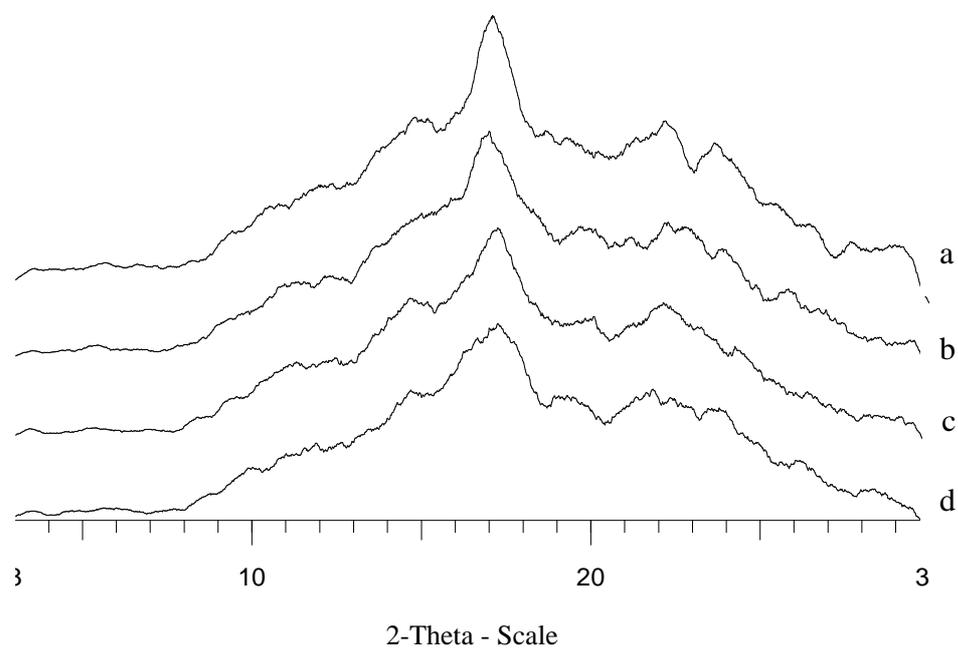
Figure 4.15 X-ray diffraction spectra of debranched starch at degree of debranching

58.9% with different temperature cycles of a: 5/80°C, b: 55/80°C, c:

5/120°C and d: 55/120°C.

2-Theta - Scale
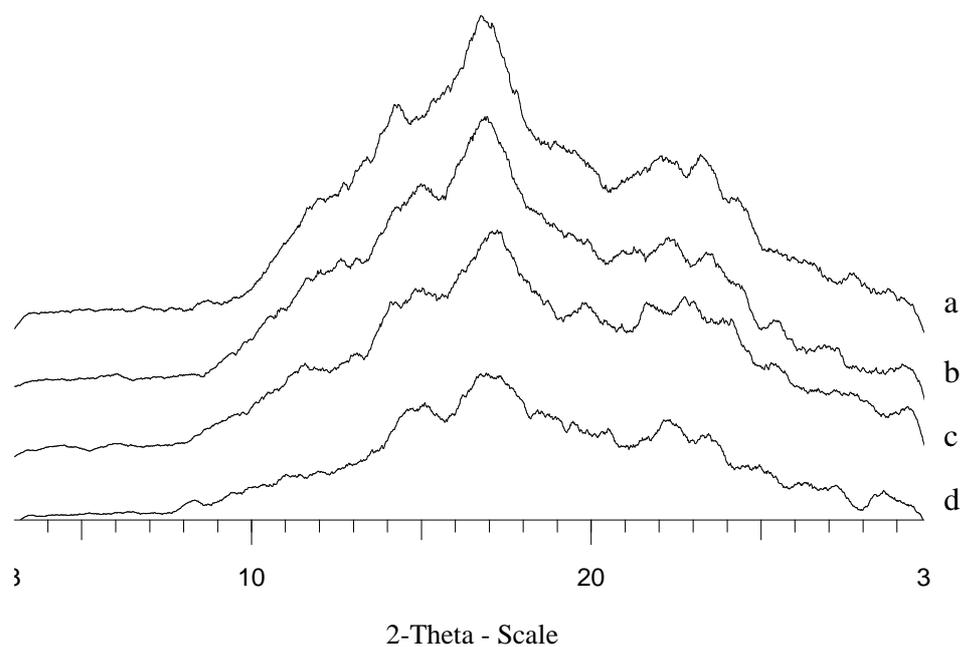
Figure 4.16 X-ray diffraction spectra of debranched starch at degree of debranching 68.5% with different temperature cycles of a: 5/80°C, b: 55/80°C, c: 5/120°C and d: 55/120°C.

2-Theta - Scale
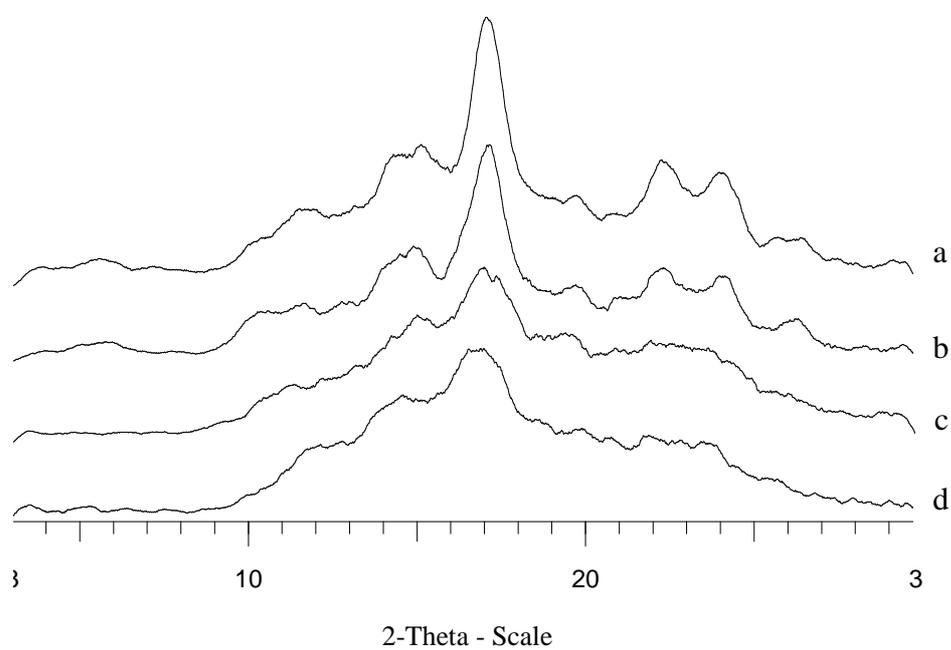
Figure 4.17 X-ray diffraction spectra of debranched starch at degree of debranching 80.6% with different temperature cycles of a: 5/80°C, b: 55/80°C, c: 5/120°C and d: 55/120°C.
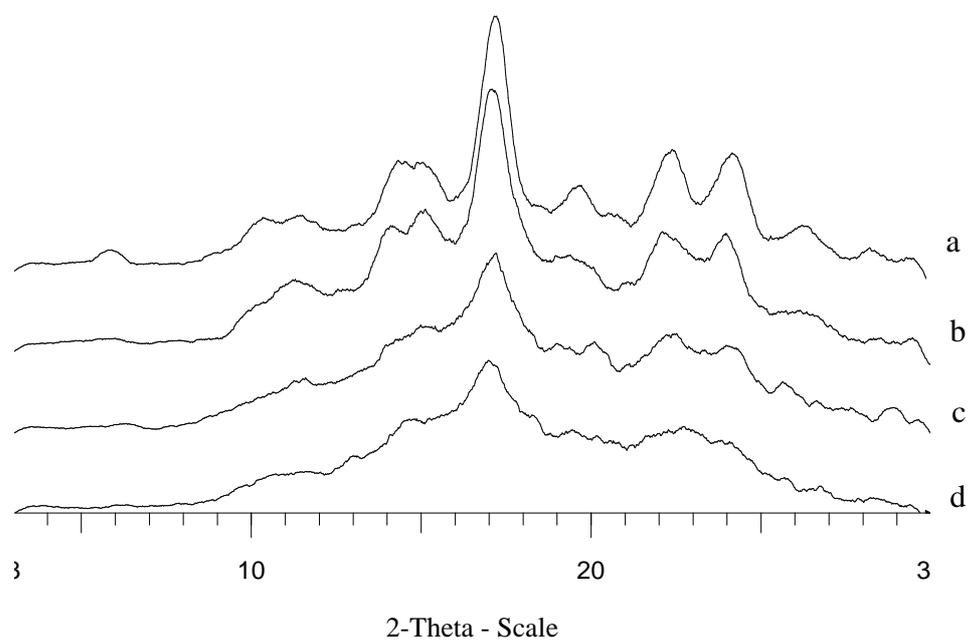
Figure 4.18 X-ray diffraction spectra of debranched starch at degree of debranching 89.3% with different temperature cycles of a: 5/80°C, b: 55/80°C, c: 5/120°C and d: 55/120°C.
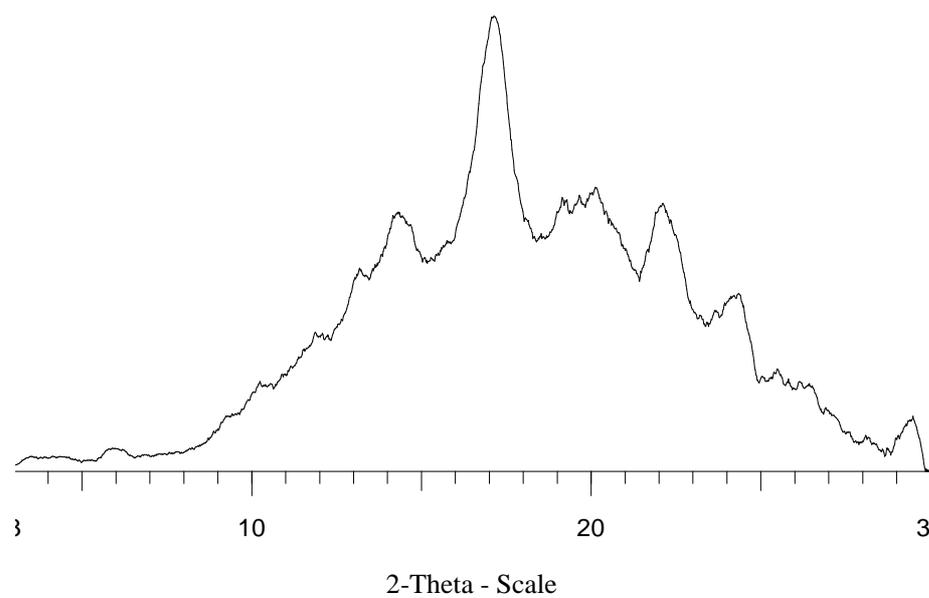
Figure 4.19 X-ray diffraction spectra of novelose 330

Table 4.13 X-ray diffraction data of debranched starch after subjecting to different temperature cycle treatments

Sample		Diffraction peak at 2θ value (°angle)								Crystal pattern
D.B. (%)	Temperature treatment	5°	15°	17°	18°	20°	22°	23°	30°	
0	5/80°C	-	14.4 (6.14 Å)[a]	16.8 (5.29 Å)	-	-	-	-	29.3 (3.04 Å)	C
	55/80°C	-	-	17.0 (5.20 Å)	-	-	-	-	29.3 (3.05 Å)	C
58.9	5/80°C	-	15.0 (5.90 Å)	17.1 (5.18 Å)	-	-	22.1 (4.02 Å)	23.7 (3.75 Å)	29.2 (3.05 Å)	C_B
	55/80°C	-	14.9 (5.96 Å)	17.1 (5.19 Å)	-	-	-	-	29.5 (3.03 Å)	C
	5/120°C	-	14.5 (6.10 Å)	17.0 (5.20 Å)	-	-	-	23.7 (3.80 Å)	29.5 (3.00 Å)	C
	55/120°C	-	-	17.2 (5.10 Å)	-	-	-	-	29.5 (3.00 Å)	C
68.5	5/80°C	-	15.1 (5.88 Å)	17.1 (5.20 Å)	-	-	22.77 (4.07 Å)	24.0 (3.70 Å)	29.3 (3.04 Å)	C_B
	55/80°C	-	14.8 (5.99 Å)	16.8 (5.26 Å)	-	-	22.86 (4.05 Å)	23.9 (3.72 Å)	29.2 (3.06 Å)	C_B
	5/120°C	-	-	16.9 (5.25 Å)	-	-	-	24.0 (3.71 Å)	29.4 (3.03 Å)	C
	55/120°C	-	-	16.9 (5.23 Å)	-	-	-	-	29.3 (3.05 Å)	C

Table 4.13 X-ray diffraction data of debranched starch after subjecting to different temperature cycle treatments (Continued)

| Sample | | Diffraction peak at 2θ value (°angle) | | | | | | | | Crystal pattern |
D.B. (%)	Temperature treatment	5°	15°	17°	18°	20°	22°	23°	30°	
80.6	5/80°C	5.6 (15.82 Å)	14.7 6.03 Å)	17.1 (5.18 Å)	-	-	22.3 (3.98 Å)	24.1 (3.70 Å)	29.3 3.04 Å)	B
	55/80°C	4.4 (17.86 Å)	-	17.0 (5.22 Å)	-	-	22.3 (3.98 Å)	24.0 (3.70 Å)	29.1 (3.07 Å)	B
	5/120°C	-	-	17.2 (5.16 Å)	-	-	-	-	29.3 (3.05 Å)	C
	55/120°C	-	-	17.1 (5.17 Å)	-	-	-	-	29.3 (3.04 Å)	C
89.3	5/80°C	5.7 (15.38 Å)	15.0 (5.92 Å)	17.1 (5.17 Å)	-	19.6 (4.52 Å)	22.2 (3.99 Å)	24.1 (3.69 Å)	29.4 (3.04 Å)	B
	55/80°C	4.6 (15.55 Å)	14.6 (6.06 Å)	17.1 (5.17 Å)	-	19.4 (4.56 Å)	22.2 (4.00 Å)	24.0 (3.71 Å)	29.2 (3.05 Å)	B
	5/120°C	-	14.5 (6.10 Å)	17.1 (5.18 Å)	-	20.1 (4.42 Å)	22.0 (4.04 Å)	24.0 (3.71 Å)	29.1 (3.06 Å)	C_B
	55/120°C	-	-	17.1 (5.19 Å)	-	-	-	23.9 (3.73 Å)	29.3 (3.04 Å)	C_A
Novelose330		5.6 (15.56 Å)	13.7 (6.47 Å)	17.1 (5.17 Å)	-	19.8 (4.47 Å)	22.1 (4.02 Å)	24.1 (3.68 Å)	29.4 (3.04 Å)	B

[a] The figures in parentheses represent interplanar spacing.

For overall result, the relative crystallinity of DBS with temperature cycling treatment showed the following trends:

$CRYS_{5/80} > CRYS_{55/80} > CRYS_{5/120} > CRYS_{55/120}$ (16.48% > 11.12% > 6.83% >4.50%)

This trend was highly correlated with that of RS content of DBS after temperature treatment process.

Table 4.14 Relative crystallinity of debranched starch after subjecting to different temperature cycle treatments

D.B. (%)	Relative crystallinity (%)			
	5/80°C	55/80°C	5/120°C	55/120°C
0	$1.89 \pm 0.6^{a,B}$	$1.68 \pm 0.1^{a,B}$	$1.04 \pm 0.1^{a,A}$	$0.75 \pm 0.3^{a,A}$
58.9	$10.93 \pm 0.8^{b,C}$	$6.14 \pm 0.1^{b,BC}$	$7.09 \pm 0.7^{b,B}$	$5.02 \pm 0.7^{b,A}$
68.5	12.92 ± 0.8^{cC}	$6.96 \pm 0.2^{b,B}$	$7.85 \pm 0.8^{b,B}$	$5.31 \pm 0.9^{b,A}$
80.6	$26.76 \pm 0.7^{d,D}$	$11.05 \pm 0.5^{c,C}$	$7.73 \pm 0.7^{b,B}$	$5.76 \pm 1.0^{b,A}$
89.3	$37.62 \pm 0.1^{e,D}$	$29.77 \pm 0.6^{d,C}$	$10.91 \pm 1.2^{c,B}$	$6.20 \pm 0.8^{b,A}$
Novelose 330	12.77 ± 1.2			

Mean values with different small letters in each column are significantly different ($p<0.01$).

Mean values with different capital letters in each row are significantly different ($p<0.01$).

The nucleation temperature and propagation temperature also affected crystallization (Appendix A, Table 3a). There was a different relative crystallinity in nucleation temperature of 5°C (11.65%) and 55°C (7.9%) ($p < 0.01$), as well as propagation temperature at 80°C (13.73%) and 120°C (5.66%) ($p < 0.01$). The interaction between nucleation temperature and propagation temperature did not show statistic different ($p > 0.05$). The relationship between nucleation temperature and

propagation temperature on the relative crystallinity is presented in Figure 4.20. The highest nucleation and propagation temperature had a negative effect on crystallization, showing the lower relative crystallinity. This trend was correlated with RS formation as previously described on partially polymer crystallization.
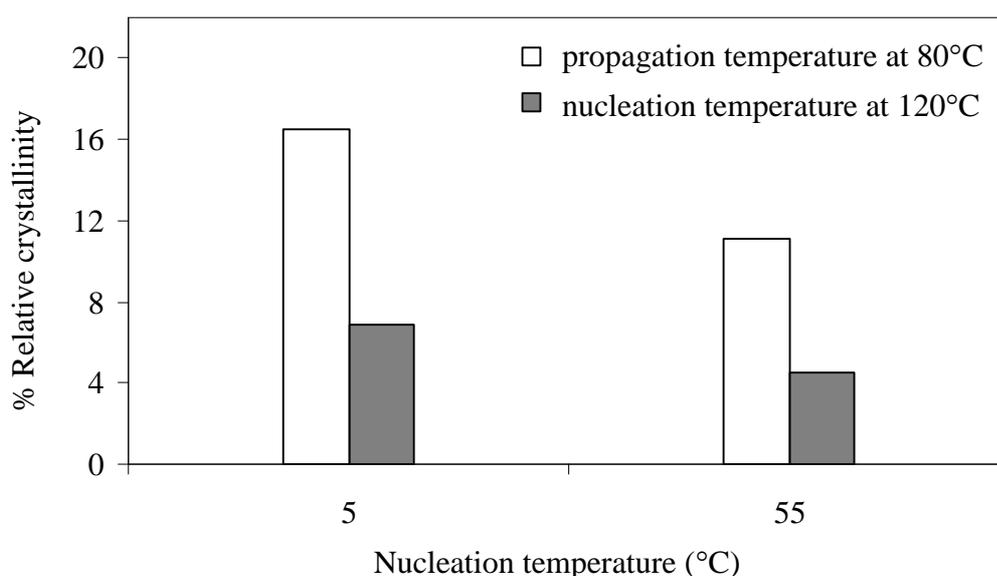
Figure 4.20 The relation between nucleation temperature and propagation temperature affected on relative crystallinity.

The RS content and relative crystallization were higher at the temperature cycling of "5/80°C" because the nucleation rate was favored and then propagation rate was promoted under these temperatures, resulting that more nuclei and large crystals was formed. It indicated that the storage of debranched starch at 5°C followed by 80°C could accelerate crystal formation and generated more crystal perfection.

4.5.3 Effect of temperature cycling on thermal stability

The thermal property of debranched cassava starch after treatment with different four time-temperature cycles was investigated using DSC. The transition temperature and enthalpy are summarized in Table 4.15. The debranched cassava starch with different time-temperature cycling treatment exhibited two major endothermic transitions over the T_m range of 87-130°C and 134-177°C, respectively. The temperature cycling caused a general increase in the T_m of crystallites. Compared to native starch and RDBS (retrograded at 6°C for 4 days) (Table 4.9-4.10), the T_m of debranched starch with time-temperature cycling in all treatments was higher. It indicated that the time-temperature cycling treatment could improve the crystal perfection. This result was similarly to time-temperature cycling which reported by Silverio, Fredrisson, Andersson, Eliasson and Aman (2000) and autoclave-cooling cycles of Sievert and Pomeranz (1989).

The effect of temperature cycling at different D.B. on the total enthalpy (ΔH_T) of debranched starch is showed in Table 4.16. As D.B. was increased, an increase in ΔH_T was observed for the temperature cycling of "5/80°C", "55/80°C" and "5/120°C". For overall result of temperature cycling treatment, the increased ΔH_T of different temperature cycling treatment was similar to RS content and relative crystallinity, as follows:

$$\Delta H_{T\ 5/80} > \Delta H_{T\ 55/80} > \Delta H_{T\ 5/120} > \Delta H_{T\ 55/120}\ (23.3\ \text{J/g} > 15.2\ \text{J/g} > 10.4\ \text{J/g} > 6.3\ \text{J/g})$$

The ΔH_T of nucleation temperature at 5°C (16.9 J/g) was greater than that of 55°C (10.8 J/g) ($p < 0.01$). A similar result was observed in the propagation temperature of 80°C (19.3 J/g) and 120°C (8.4 J/g) ($p < 0.01$). The negative

relationship between nucleation or propagation temperature and ΔH_T is showed in Figure 4.21. Cooke and Gidley (1992) mentioned that the ΔH represented the amount of double helices that unraveled or melted during gelatinization. In this study, ΔH_T was positively correlated ($r = 0.95$, $p < 0.01$) with the relative crystallinity. Thus, ΔH_T referred to the amount of ordered material formed in the debranched starch during storage. It suggested that the lower nucleation and propagation temperature determined the formation of ordered structure (crystalline structure) in the starch/water dispersion.

The effect of temperature cycling on the melting temperature of debranched starch is present in Table 4.15. The temperature cycling of "5/80°C" and "5/120°C" exhibited three endothermic transitions over the T_m range of 50-80°C, 90-117°C and 135-160°C, while the temperature cycling of "55/80°C" and "55/120°C" exhibited two endothermic transitions over the T_m range of 110-140°C and 141-177°C. The first endothermic transition of the temperature cycling of "5/80°C" and "5/120°C" was in the same region as that of RDBS (Table 4.10). This indicated that the recrystallization of branched molecules occurred during cooling at 5°C. For the temperature cycling of "55/80°C" and "55/120°C, the crystallization of branched molecules disappeared because the temperature of 55°C was higher than its T_o of melting (about 50°C, Table 4.10).

Table 4.15 Thermal properties of debranched starch after subjecting to different temperature cycle treatments

D.B. (%)		First transition					Second transition					Third transition				
		T_o	T_p	T_c	T_c-T_o	ΔH	T_o	T_p	T_c	T_c-T_o	ΔH	T_o	T_p	T_c	T_c-T_o	ΔH
0	5/80	n.d.	n.d.	n.d.	n.d.	n.d.	n.d.	n.d.	n.d.	n.d.	n.d.	n.d.	n.d.	n.d.	n.d.	n.d.
	55/80	n.d.	n.d.	n.d.	n.d.	n.d.	n.d.	n.d.	n.d.	n.d.	n.d.	n.d.	n.d.	n.d.	n.d.	n.d.
	5/120	n.d.	n.d.	n.d.	n.d.	n.d.	n.d.	n.d.	n.d.	n.d.	n.d.	n.d.	n.d.	n.d.	n.d.	n.d.
	55/120	n.d.	n.d.	n.d.	n.d.	n.d.	n.d.	n.d.	n.d.	n.d.	n.d.	n.d.	n.d.	n.d.	n.d.	n.d.
58.9	5/80	50.0	59.6	74.2	24.1	3.4	89.4	98.6	104.2	14.7	2.9	134.3	138.5	147.3	13.0	6.2
	55/80	n.d.	n.d.	n.d.	n.d.	n.d.	112.8	124.9	129.1	16.3	3.4	134.8	144.9	159.7	24.9	3.3
	5/120	49.8	61.5	78.0	28.2	1.3	93.3	105.8	112.1	18.8	4.2	135.6	142.2	144.7	9.1	2.1
	55/120	n.d.	n.d.	n.d.	n.d.	n.d.	112.2	124.5	128.7	16.4	3.5	145.9	156.0	178.1	32.3	2.9
68.5	5/80	57.1	66.0	77.1	20.0	3.2	87.6	100.2	105.5	17.9	4.7	138.8	144.3	148.1	9.2	11.6
	55/80	n.d.	n.d.	n.d.	n.d.	n.d.	124.2	131.8	134.9	10.8	8.6	141.2	151.6	168.6	27.4	4.0
	5/120	51.6	60.2	66.9	15.3	1.4	97.2	107.9	111.4	14.2	4.7	148.4	162.2	166.7	18.3	3.3
	55/120	n.d.	n.d.	n.d.	n.d.	n.d.	128.3	141.1	144.9	16.7	3.2	147.7	157.8	163.3	15.6	2.2
80.6	5/80	56.5	66.3	73.9	17.3	2.1	89.0	102.1	108.2	19.2	8.2	148.4	151.6	153.9	5.5	17.8
	55/80	n.d.	n.d.	n.d.	n.d.	n.d.	108.4	117.9	127.6	19.2	7.7	147.4	156.9	162.1	14.7	8.5
	5/120	54.5	60.4	72.7	18.2	1.4	87.4	104.4	110.3	23.0	4.9	147.4	156.9	162.1	14.7	6.5
	55/120	n.d.	n.d.	n.d.	n.d.	n.d.	117.9	125.3	131.2	13.4	2.5	147.2	157.6	164.7	17.5	3.8

Table 4.15 Thermal properties of debranched starch after subjecting to different temperature cycle treatments (continued)

D.B. (%)		First transition					Second transition					Third transition				
		T_o	T_p	T_c	T_c-T_o	ΔH	T_o	T_p	T_c	T_c-T_o	ΔH	T_o	T_p	T_c	T_c-T_o	ΔH
89.3	5/80	n.d.	n.d.	n.d.	n.d.	n.d.	96.3	107.3	117.1	20.8	14.3	155.6	159.0	161.5	5.9	18.9
	55/80	88.4	97.8	109.7	21.3	4.6	118.7	128.1	131.6	12.9	7.7	155.7	163.5	177.4	21.8	13.0
	5/120	n.d.	n.d.	n.d.	n.d.	n.d.	103.4	109.5	114.4	11.0	5.8	140.7	149.1	161.4	20.7	6.0
	55/120	n.d.	n.d.	n.d.	n.d.	n.d.	122.2	126.5	131.3	9.1	3.0	144.5	153.6	157.7	13.2	4.2

[1]To, Tp, Tc = onset, peak and completion temperature in °C, respectively; ΔH = enthalpy in J/g of dry matter; n.d.: not detected.

[2]All values are the average of 3-4 measures.

Table 4.16 The total enthalpy of debranched starch after subjecting to different

temperature cycle treatments

D.B. (%)	Total enthalpy (ΔH_T, J/ g)			
	5/80°C	55/80°C	5/120°C	55/120°C
0	nil	nil	nil	nil
58.9	12.6[a,B]	6.7[a,A]	7.6[a,A]	6.4[ab,A]
68.5	19.5[b,D]	12.6[ab,C]	9.5[b,B]	5.4[a,A]
80.6	28.0[c,D]	16.3[b,C]	12.8[c,B]	6.3[ab,A]
89.3	33.2[d,D]	25.3[c,C]	11.8[c,B]	7.2[b,A]

Mean values with different small letters in each column are significantly different ($p<0.01$).

Mean values with different capital letters in each row are significantly different ($p<0.01$).
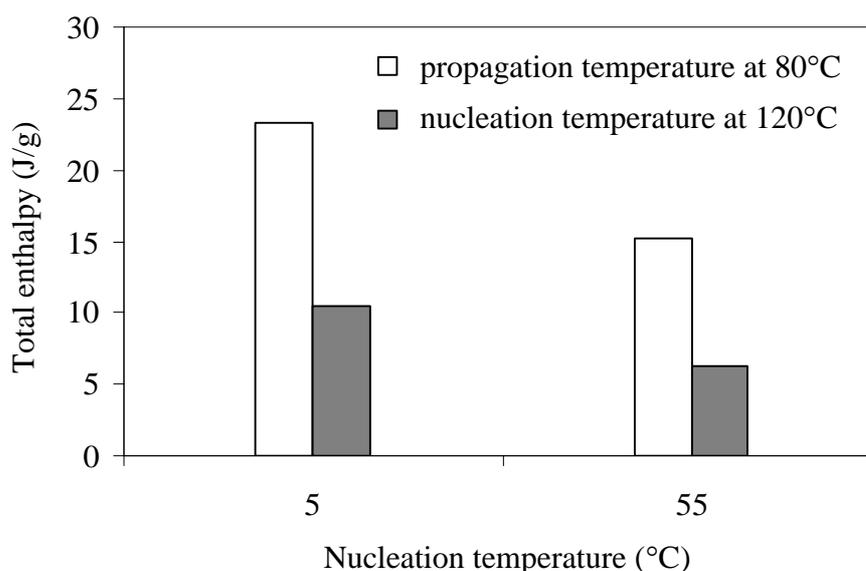
Figure 4.21 The relationship between nucleation temperature and propagation
temperature affected on the total enthalpy.

The phenomenon of molecular reorganization at different temperature
cycling might be described in terms of annealing (Tester and Debon, 2000). At the first
cycle of low nucleation temperature of 5°C, unstable and imperfect crystallites were

formed, while nucleation temperature of 55°C, the unstable crystallites of DBS (T_o < 55°C) were melted and more stable crystallites were nucleated, resulting in a higher T_o at the second transition. When the crystallite nuclei were already formed, annealing at higher temperature of 80°C and 120°C performed. The annealing at high temperature but below gelatinization temperature led to a physical reorganization of the crystallites (Tester and Debon, 2000). At 80°C and 120°C, the less thermally stable crystallites melted and then followed by reformation and growth of more perfect or ordered structures. From second to fourth cycles, the crystallites reformed, reorganized and grew into the more thermally stable form, resulting in a high T_m. With increased in the number of cycle, the higher T_m and the more ΔH appeared (Silverio et al., 2000). This suggested the high T_m of crystallites after treatment with four temperature cycles in this study.

Although aging at the low nucleation and propagation temperature (5/80°C) could bring up to the highest RS formation, the low nucleation and the high propagation temperature (5/120°C) did not accelerated RS formation as compared with the high nucleation temperature and the low propagation temperature (55/80°C). It was probable due to the fact that the temperature cycling of "55/80°C" could organize an ordered structure into a high thermal stability structure, which in turn, enhanced the resistance of starch to enzymatic digestion. For temperature cycling of "5/120°C", the perfect crystallite was also present, but at low level (low ΔH_T and relative crystallinity) due to the fact that the temperature of 120°C limited growth of crystal from the high diffusion of molecule. It resulted in low RS content.

The overall result demonstrated that the temperature cycling with subsequent incubation at 5°C or 55°C and higher temperature at 80°C for 4 cycles was

the condition to achieve a high RS yield with very thermally stable in a relatively short time.

4.5.4 Effect of temperature cycling on water absorption index (WAI) and water solubility index (WSI)

Water absorption index (WAI) and water solubility index (WSI) depend on several factors such as starch origin, amylose and amylopectin content, isolation procedure and thermal history (Singh and Smith, 1997). WSI and WAI were important properties to be considered when RS was applied into new products. As the debranching was performed, WAI and WSI were decreased (Table 4.17 and 4.18). This behavior agreed with the RS content in that the higher RS content, the lower WSI and WAI because the crystallization during time-temperature cycles reduced the water absorption capacity of starch. In Table 4.18, the WSI decreased with increasing D.B. and the lowest WSI was found at the temperature treatment of "5/80°C" and "55/80°C", which agreed with the RS content. As RS content was higher, the lower WSI was present. It indicated that RS was not well solubilized at 30°C. In addition, RS had a lower water holding ability.

Table 4.17 Water absorption index of debranched starch after subjecting to different

temperature cycle treatments

D.B. (%)	Water absorption index (WAI, g/g dry sample)			
	5/80°C	55/80°C	5/120°C	55/120°C
0	13.76 ± 0.7	10.73 ± 0.7	11.32 ± 1.3	8.05 ± 0.5
58.9	4.30 ± 0.3	4.50 ± 0.3	4.37 ± 0.4	4.23 ± 0.2
68.5	4.40 ± 0.9	4.13 ± 0.5	3.95 ± 0.1	3.76 ± 0.2
80.6	3.52 ± 0.3	4.28 ± 0.4	3.73 ± 0.1	3.73 ± 0.5
89.3	3.09 ± 0.0	3.16 ± 0.0	3.75 ± 0.2	3.38 ± 0.4

Table 4.18 Water solubility index of debranched starch after subjecting to different

temperature cycle treatments

D.B. (%)	Water solubility index (WSI, %)			
	5/80°C	55/80°C	5/120°C	55/120°C
0	25.71 ± 3.1	25.82 ± 1.5	24.36 ± 2.0	29.07 ± 4.9
58.9	20.20 ± 4.0	16.21 ± 5.0	17.37 ± 4.5	22.52 ± 6.1
68.5	13.34 ± 1.4	17.95 ± 3.3	18.16 ± 2.2	20.48 ± 1.0
80.6	11.30 ± 1.6	11.42 ± 2.9	15.86 ± 1.6	24.54 ± 4.8
89.3	11.84 ± 0.0	10.76 ± 1.0	13.18 ± 0.2	17.57 ± 3.8

Water holding capacity was an important property for low and intermediate moisture food. From the physical property of RS produced from cassava starch, particularly its low-water-holding capacity, it can be a functional ingredient that provides good handling in processing and crispness, expansion, and improved texture in the final product. Thus, it was suitable for food applications, especially appropriate for grain-based low- and moderate-moisture foods (particularly extruded foods) such as RTE cereals, snacks, pasta/noodles, some baked goods, and fried foods. It will not only make it possible to obtain a good source of nutritional fiber in the product, but also will impart excellent textures for these products without compromising quality.

4.6 References

Balagopalan, C, Padmaja, G., Nanda, S.K., and Moorthy, S.N. (1988). **Cassava starch in food, feed and animal industry**. Florida: CRC Press.

Bello-Perez, L.A., Ottenhof, M.A., Agama-Avcevedo, E., and Farhat, I.A. (2005). Effect of Storage time on the retrogradation of banana starch extrudate. **Journal of Agricultural and Food Chemistry** 53: 1081-1086.

Bertoft, E. (2004). Analysing starch structure. In: A.C. Eliasson (eds.). **Starch in food Structure, function and application** (p. 57-96) Cambridge, England: Woodhead.

Chang, Y.H., and Lin, J.H. (2007). Effect of molecular size and structure of amylopectin on retrogradation thermal properties of waxy rice corn starches. **Food Hydrocolloids** 21: 645-653.

Cheetham, N.W.H., and Tao, L. (1998). Variation in crystalline type with amylose content in maize starch granules: an X-ray powder diffraction study. **Carbohydrate Polymers** 36: 277-284.

Cooke, D., and Gidley, M.J. (1992). Loss of crystalline and molecular order during starch gelatinization: origin of the enthalpic transition. **Carbohydrate Research** 227: 103-112.

Eerlingen, R.C., and Delcour, J.A. (1995). Formation, analysis, structure and properties of typeIII enzyme resistant starch. **Journal of Cereal Science** 22: 129-138.

Eerlingen, R.C., Crombez, M., and Delcour, J.A. (1993). Enzyme-resistant starch. I. Quantitative and qualitative influence of incubation time and temperature of autoclave starch on resistant starch formation. **Cereal Chemistry** 70 (3): 339-344.

Eerlingen, R.C., Deceuninck, M., and Delcour, J.A. (1993). Enzyme-resistant starch. II. Influence of amylose chain length on resistant starch formation. **Cereal Chemistry** 70 (3): 345-350.

Eerlingen, R.C., Jacobs, H., and Delcour, J.A. (1994). Enzyme-resistant starch V. effect of retrogradation of waxy maize starch on enzyme susceptibility. **Cereal chemistry** 71 (4): 351-355.

Fredriksson, H., et al. (2000). Studies on α-amylase degradation of retrograded starch gels from waxy maize and high-amylopectin potato. **Carbohydrate Polymers** 43: 51-87.

Gerard, C., Planchot, V., Colonna, P., and Bertoft, E. (2000). Relationship between branching density and crystalline structure of A- and B-type maize mutant starches. **Carbohydrate Research** 326: 130–144.

Gidley, M.J. (1989). Molecular mechanisms underlying amylose aggregation and gelation. **Macromoleclues** 22: 351-358.

Gidley, M.J., and Bulpin, P.V. (1989). Aggregation of amylose in aqueous systems: the effect of chain length on the phase behavior and aggregation kinetics. **Macromoleclues** 22: 341-346.

Gidley, M.J., et al. (1995). Molecular order and structure in enzyme-resistant retrograded starch. **Carbohydrate Polymers** 28: 23-31.

Gilliard, T., and Bowler (1987). Morphology and composition of starch. In: T. Galliard (eds.). **Starch: properties and potential** (Vol. 13) New York: Wiley and Sons.

Gonzalez-Soto, R.A., Agama-Acevedo, E., Solorza-Feria, J., Rendon-Villalobos, R., and Bello-Perez L.A. (2004). Resistant starch made from banana starch by autoclave and debranching. **Starch/Stärke** 56: 495-499.

Gunaratne, A., and Hoover, R. (2002). Effect of heat-moisture treatment on structure and physicochemical properties of tuber and root starches. **Carbohydrate Polymers** 49: 425-437.

Guraya, H.S., James, C., and Champagne, E.T. (2001a). Effect of cooling, freezing on the digestibility of debranched rice starch and physical properties of resulting material. **Starch/Stärke** 53: 64-74.

Guraya, H.S., James, C., and Champagne, E.T. (2001b). Effect of enzyme concentration and storage temperature on the formation of slowly digestible starch from cooked debranched rice starch. **Starch/Stärke** 53: 131-139.

Hermans, P.H., and Weidinger, A. (1961). On the determination of the crystalline fraction of polyethylenes form X-ray diffraction. **Macromolecular Chemistry** 24: 24-36.

Hizkuri, S. (1996). Starch: analytical aspects. In: A.C. Eliasson (eds.). **Carbohydrates in Food** (pp 376-377). New York: Marcel Dekker.

Hizukuri, S., Takeda, Y., and Yasuda, M. (1981). Multi-branched nature of amylose and the action of debranching enzymes. **Carbohydrate Research** 94: 205-213.

Hizkuri, S., et al. (1997). Analytical development: molecular and microstructural charecterization. In: P.J. Farazier, Donald A.M. and P. Richmoand (eds.). **Starch: structure and functionality** (pp 121-127). UK: Thomas Graham House.

Hoover, R. and Vasanthan, T. (1994). Effect of heat-moisture treatment o the structure and physicochemical properties of cereal, legume, and tuber starch. **Carbohydrate Research** 252: 33-53.

Jensen, B.F. and Norman, B.E. (1984). *Bacillus acidopulluticus* Pullulanase: application and regulatory aspects for use in food. **Process Biochemistry** 19 (4): 129-134.

Jeroen, J.G., Van Soest, J.J.G., Hulleman, S.H.D., Wit de, D., and Vliegenthart, J.F.G. (1996). Crystallinity in starch bioplastic. **Industrial Crops and Products** 11-22.

Knutson, C.A. (1999). Evaluation of variations in amylose-iodine absorbance spectra. **Carbohydrate Polymers** 42: 65-72.

Leeman A.M., Karlsson M.E, Eliasson A.C., and Bjorck I.M.E. (2006). Resistant starch formation in temperature treated potato starches varying in amylose/ amylopectin ratio. **Carbohydrate Polymers** 65: 306–313.

Lehmann, U., Jacobasch, G., and Schmidiedl, D. (2002). Characterization of resistant starch typeIII from banana (*Musa acuminata*). **Journal of Agricultural and Food Chemistry** 50: 5236-5240.

Leong, Y.H., Karim, A.A., and Norziah, M.H. (2007). Effect of pullulanase debranching of sago (*Metroxylon* sagu) starch at subgelatinization temperature on yield of resistant starch. **Starch/Stärke** 59: 21-32.

Lewandowicz, G., and Soral-Smietana, M. (2004). Starch modification by iterated syneresis. **Carbohydrate Polymers** 56: 403-413.

McCleary, B.V., and Monaghan, D.A. (2002). Measurement of resistant starch. **Journal of Association Official Analytical Chemistry** 85 (3): 665-667.

Miles, M.J., Morris, V.J., and Ring, S.G. (1985). Gelation of amylose. **Carbohydrate Research** 135:257-269.

Miles, M.J., Morris, V.J., Orford, P.D., and Ring, S.G. (1985). The roles of amylose and amylopectin in gelation and retrogradation of starch **Carbohydrate Research** 135: 271-281.

Pohu, A., Planchot, V., Putaux, J. L., Colonna, P., and Buleon, A. (2004). Split Crystallization during Debranching of Maltodextrins at High Concentration by Isoamylase. **Biomacromolecules** 5: 1792-1798.

Rindlav, A., Hullernan, S.H.D., and Gatenholm, P. (1997). Formation of starch films with varying crystallinity **Carbohydrate Polymers** 34: 25-30.

Ring, S.G., et al. (1987). The gelation and crystallization of amylopectin. **Carbohydrate Research** 162: 277-293.

Roos Y.H. (1995a). Characterization of food polymers using state diagrams. **Journal of Food Engineering** 24: 339-360.

Roos, Y.H.. (1995b). **Phase transition in foods**. New York: Academic Press.

Schmidl, D., Baurelein, M., Bengs, H., and Jacobasch, G. (2000). Production of heat-stable, butyrogenic resistant starch. **Carbohydrate Polymers** 43: 183-193.

Shamai, K., Bianco-Peled, H., and Shimoni, E. (2003). Polymorphism of resistant starch type III. **Carbohydrate Polymers** 54: 363-369.

Shin, S.I., et al. (2004). Slowly digestible starch from debranched waxy sorghum starch: preparation and properties. **Cereal Chemistry** 81 (3): 404-408.

Sievert, D., and Pomeranz, Y. (1989). Enzyme-resistant starch. I. characterization and evaluation by enzymatic, thermoanalytical and microscopic method. **Cereal Chemistry** 66 (4): 342-347.

Silverio, J., Fredrisson, H., Andersson, R., Eliasson, A.C., and Aman, P. (2000). The effect of temperature cycling on the amylopectin retrogradation of starches with different amylopectin unit-chain length distribution. **Carbohydrate Polymers** 42: 175-184.

Singh, N., and Smith, A. C. (1997). A comparison of wheat starch, whole wheat meal and oat flour in the extrusion cooking process. **Journal of Food Engineering** 34: 15–32.

Skrabanja, V., and Kreft, I. (1998). Resistant starch formation following autoclaving of buckwheat (*Fagopyrum esculentum* Moench) Groats. An In Vitro Study. **Journal of Agricultural and Food Chemistry** 46: 2020-2023.

Slade, L., and Levine, H. (1995). Water and the glass transition - dependence of the glass transition on composition and chemical structure: special implications for flour functionality in cookie baking. **Journal of Food Engineering** 24: 431-509.

Sriroth, K., et al. (1999). Cassava starch granule structure–function properties: influence of time and conditions at harvest on four cultivars of cassava starch. **Carbohydrate Polymers** 38: 161–170.

Swanson, M.A. (1947). Studies on the structure of polysaccharides IV. Relation of the iodine color to the structure. **The Journal of Biological Chemistry** 825-837.

Tester, R.F., and Debon, S.J.J. (2000). Annealing of starch — a review. **International Journal of Biological Macromolecules** 27: 1–12.

Van Soest, J.J.G., Tournois, H., Wit de, D., and Vliegenthart, J.F.G. (1995). Short-range structure in (partially) crystalline potato starch determined with attenuated total reflectance Fourier-transform IR spectroscopy. **Carbohydrate Research** 279: 201-214.

Vasanthan, T., and Bhatty, R.S. (1996). Physicochemical properties of small- and large-granule starches of waxy, regular and high-amylose barleys. **Cereal Chemistry** 73: 199-207.

Vasanthan, T., and Bhatty, R.S. (1998). Enhancement of resistant starch (RS3) in amylomaize, barley, field pea and lentil starches. **Starch/Stärke** 50: 286-291.

CHAPTER V

SUMMARY

The formation of resistant starch (RS) type III depended on the structure of the starch. The fine structure of cassava starch was composed of 17.25% amylose with branch linkage of 0.48% and 82.85% amylopectin with branch linkage of 5.79% and $\overline{CL}_n$ of 17.2. The chain length of cassava amylopectin was long enough to induce the RS formation. A debranching process with pullulanase was an appropriate technique to make the chains in clusters become available. The ability of pullulanase to debranch starch depended on starch concentration, enzyme concentration and debranching time. The higher enzyme concentration and longer incubation time, the degree of hydrolysis was increased, but the high starch concentration limited the accessibility of enzyme.

The low molecular weight molecules and linear fragment molecules were liberated after debranching with pullulanase. An increase in degree of debranching resulted in the greater amount of low molecular weight molecules and linear fragment molecules. The RS formation would occur during debranching with the reason of the aggregation of debranched molecules over debranching condition. The retrogradation of debranched starch could increase RS content and improved thermal properties.

The RS formation from debranching and retrogradation might be attributed to two reasons: (1) more free linear chains could participate in crystal formation by chain elongation and folding. These newly formed crystals could become more perfect during retrogradation (2) low molecular weight molecules with a few branch chains

could disentangle. The double helices and crystallites were formed by reassociation of their outer branch chains in an ordered structure during retrogradation. The number of perfect starch crystals became greater with increasing D.B., resulting in the more ordered structure.

The temperature cycling promoted the crystallization through nucleation and propagation, thus enhanced the greater formation of RS. The lowest temperature of nucleation and propagation at 5 and 80°C could promote the RS formation in order to obtain the growth and perfection of crystallites as well as the more stable crystal structure. Therefore, after debranching and time-temperature cycling, the RS product was the very thermally stable and, hence, more resistant to enzyme digestion.

The debranching and time-temperature cycling treatment reduced WSI and WAI of debranched starch. It indicated that the RS had a low water holding ability. Therefore, it is able to apply in low- and intermediate-moisture food, provide good handing in processing and be a good source of nutritional fiber.

APPENDIX

APPENDIX A

Table 1a The analysis of variance for the influence of starch concentration, enzyme

concentration and debranching time on degree of hydrolysis

Source	DF	Sum Square	Mean Square	F Value
Starch	2	8.596	4.298	34.29**
Enzyme	2	79.977	38.489	307.04**
Time	6	387.313	64.552	514.95**
Starch × Enzyme	4	1.378	0.344	2.75*
Starch × Time	12	3.125	0.260	2.08*
Enzyme × Time	12	16.605	1.384	11.04**
Starch × Enzyme × Time	24	3.263	0.136	1.08^{ns}

Comparisons significant at confidence levels greater than **99 % and *95%.

ns = not significant

Table 2a The analysis of variance for the influence of degree of debranching,

nucleation temperature and propagation temperature on RS content

Source	DF	Sum Square	Mean Square	F Value
D.B.	4	7961.66	1990.42	520.40**
Nucleation	1	1043.95	1043.95	272.95**
Propagation	1	1886.23	1886.23	493.16**
D.B. × Nucleation	4	473.42	118.35	30.94**
D.B. × Propagation	4	1247.94	311.98	81.52**
Nucleation × Propagation	1	7.99	7.99	2.09^{ns}
D.B. × Nucleation × Propagation	4	102.17	25.54	6.68**

Comparisons significant at confidence levels greater than **99% and *95%.

ns = not significant

Table 3a The analysis of variance for the influence of degree of debranching, nucleation temperature and propagation temperature on relative crystallinity

Source	DF	Sum Square	Mean Square	F Value
D.B.	4	3049.88	762.47	1453.05**
Nucleation	1	256.92	256.92	489.62**
Propagation	1	1186.77	1186.95	2261.99**
D.B. × Nucleation	4	198.23	49.55	94.45**
D.B. × Propagation	4	1516.67	379.16	722.59**
Nucleation × Propagation	1	56.77	56.77	1.94^{ns}
D.B. × Nucleation × Propagation	4	157.70	39.42	75.13**

Comparisons significant at confidence levels greater than **99% and *95%.

ns = not significant

APPENDIX B

1b Reducing sugar determination

The reducing sugar content was determined using Somogyi method (Somogyi, 1952).

1.1 Reagents

1.1.1 Copper reagent

Na_2CO_3	24 g
$Na_2HPO_4.12H_2O$	12 g
$NaHCO_3$	16 g
Na_2SO_4	180 g
$CuSO_4.5H_2O$	10 %

Mixture A: Dissolve 24 g of Na_2CO_3 and 12 g of $Na_2HPO_4.12H_2O$ in about 250 mL of distilled water, add 40 mL of 10% $CuSO_4.5H_2O$, mix and then add 16 g of $NaHCO_3$.

Mixture B: Dissolve 180 g of Na_2SO_4 in 500 mL of distilled water with boiling and cool to room temperature.

Mix the mixture A and B and adjust to 1 L.

1.1.2 Arsenomolybdate color reagent

$(NH_4)_6Mo_7O_{24}.4H_2O$ 25 g

Concentrated H_2SO_4 21 mL

$Na_2HAsO_4.7H_2O$ 3 g

Dissolve 25 g of $(NH_4)_6Mo_7O_{24}.4H_2O$ in 450 mL of distilled water, add 21 mL of concentrated H_2SO_4, mix, add 3 g of $Na_2HAsO_4.7H_2O$ dissolved in 25 mL of H_2O, mix, and place in an incubator at 37°C for 24 to 48 h or 55°C for 25 min.

1.2 Procedure

1 mL of sample is pipette into screw cap test tube and 1 mL of copper reagent is added. The solution is mixed and heated for 15 min in a boiling water bath. At the end of 15 min, the tube is cooled to room temperature. 1 mL of the arsenomolybdate color reagent is added and stand at room temperature for 30 min. After that, 5 mL of water is added and mixed. The mixture is measured the absorbance against reagent blank at 520 nm (as glucose standard) or 540 nm (as maltose standard).

2b Total sugar determination

The total sugar content was determined using phenol-sulfuric acid assay (Dubois, 1956).

2.1 Reagents

5% Phenol

Concentrated H_2SO_4

2.2 Procedure

0.5 mL of sample is pipette into test tube. 1 mL of 5% phenol is added, mix, and then 2.5 mL of concentrated H_2SO_4 is added into sample tube. The mixture is cooled to room temperature and stand for 30 min. The mixture is measured the absorbance against reagent blank at 520 nm (as glucose standard).

3b Glucose assay

The glucose content was determined by glucose oxidase assay (Bergmeyer and Bernt, 1974).

3.1 Reagents

3.1.1 Assay reagent

glucose oxiadase/ Peroxidase 1 capsule

(1 capsule contains 500 unit of glucose oxidase (*Aspergillus niger*), 100 purpurogallin unit of peroxidase (horseradish) and buffer salts)

o-dianisidine   5 mg

Dissolve the contents of the capsule in 39.2 mL of deionized water into an amber bottle. Add 0.8 mL of 0.5% o-dianisidine reagent to the amber bottle containing Glucose oxiadase/ Peroxidase reagent. Invert bottle several time to mix.

3.1.2 12 N H_2SO_4

3.2 Procedure

1 mL of sample is pipette into test tube. The sample is treated with 2 mL of assay reagent. The mixture is incubated at 37°C for 30 min and the reaction is stopped by adding 2 mL of 12 N H_2SO_4. Carefully mix the tube thoroughly. The mixture was measured the absorbance against reagent blank at 540 nm.

CURRICULUM VITAE

Worawikunya Kiatponglarp was born in October 15, 1981 at Suphan Buri, Thailand. She studied for her high school diploma at Rachiniebourana School (1994-1997) and Satrirachinutit School (1998-1999). In 2003, she received the degree of Bachelor of Science (Food Technology) from Suranaree University of Technology.

In 2003, she studied the degree of Master at Suranaree University of Technology and also worked as a research assistant. She has co-published the article entitled "Effect of aging temperature on retrogradation of concentrated cassava starch gel" in Starch: Progress in Structural Studied, Modifications and Applications, Poland. During graduated study (2004-2006), she received scholarship from Thailand Research Fund (TRF) through TRF-MAG to financially support for thesis research. She also presented poster presentation and published a research articles including:

- **Worawikunya Kiatponglarp** and Sunanta Tongta. Effect of Debranching on Enzyme-Resistant Starch Formation in Tapioca Starch. The 8th Agro-Industrial Conference. June 15-16, 2006. BITEC, Thailand.

- **Worawikunya Kiatponglarp** and Sunanta Tongta. 2007. Structural and Physical Properties of Debranched Tapioca Starch. Suranaree J. Sci. Technol. 14 (2): 195-204.

- **Worawikunya Kiatponglarp** and Sunanta Tongta. Structural and Physical Properties of Enzyme-Resistant Starch Produced from Debranching and Retrogradation of Cassava Starch. Starch update 2007: The 4th Conference on Starch Technology. November 6-7, 2007. The Queen Sirikit National Convention Center, Thailand.